Rapport annuel
Jaarverslag
Annual report

2019

Observatoire royal de Belgique
Koninklijke Sterrenwacht van België
Royal Observatory of Belgium

ORB - KSB

Cover illustration: Astronomy Day 2019 at the Royal Observatory of Belgium. (Credit: Hans Coeckelberghs/Planetarium of the Royal Observatory of Belgium)

Foreword

Dear readers,

I am happy to present you with the annual summary report of the Royal Observatory of Belgium. As in the previous years, we have decided to only present the highlights of our scientific activities and public services, rather than providing a full, detailed and lengthy overview of all of our work during the year. We hope to provide you, in doing so, with a report that is more interesting to read and gives a taste of life at the Observatory. If you need more or other information on the Royal Observatory of the Belgium and/or its activities, contact rob_info@oma.be or visit our website http://www.observatory.be.

A list of publications and staff statistics are included at the end. To also suit our international readers & collaborators and to give it an as wide visibility as possible, the report is written in English.

Ronald Van der Linden

Director General

Table of Contents

Foreword ... 3

Life at the Royal Observatory of Belgium ... 6

Anniversary: 10 years of PROBA2 ... 7

Launch of the citizen science project Val-u-Sun ... 7

Prizes, awards and grants ... 8

Preparation of space missions ... 10

ExoMars: LaRa integrated on the platform Kazachok ... 11

EUI and Solar Orbiter ready for launch! ... 12

Service and expertise ... 13

Seismic activity in Belgium in 2019 ... 14

Man-induced earthquakes in Belgium ... 16

A European approach to Space Weather ... 17

Research at the Royal Observatory of Belgium ... 19

Seismology ... 20

How could seismic activity knowledge reflect future activity? ... 20

Extracting Microseismic Ground Motion to Validate Ocean-Climate Models ... 22

Gravimetry ... 24

The sensitivity of superconducting gravimeter is so large that it can also serve as a pluviometer ... 24

Global Navigation Satellite Systems ... 26

Impact of GSM signals on GNSS high precision applications ... 26

GNSS interferometric reflectometry to measure snow melting in Antarctica ... 28

Planetary Science ... 30

Mercury's crustal thickness controlled by mantle melt production ... 30

Mars surface-atmosphere interactions: Methane ... 32

Solar Physics ... 35

PROBA2: 10 Years of Observations ... 35

Long-term evolution of the solar corona in PROBA2 data ... 38

Astronomy and Astrophysics ... 40

First Results with the NASA Space Mission TESS ... 40

STARLAB ... 42

POEMS: Physics Of Extreme Massive Stars ... 45

How yellow hypergiant stars repeatedly cool and heat up ... 47

The project RUSTICCA: revalorising the Ukkel Schmidt Telescope ... 49

Outreach and communication 55
Astronomy Day on September 21, 2019 56
Exhibition at the Royal Palace in 2019 56
Asgard IX – Meet and Greet 57
Information to the public 57
Website, news, press releases and social media 58
The Planetarium 59
Daily Activities 60
Special Events 60
Annex 1: Publications 63
Publications with peer review 64
Non-refereed publications 77
Other publications 84
Annex 2: Workforce 85

Life at the Royal Observatory of Belgium

Anniversary: 10 years of PROBA2

On November 2, the ESA satellite PROBA2 celebrated its 10th anniversary. Since 2009, PROBA2 has observed the Sun with the telescope SWAP and the radiometer LYRA. Both instruments were conceived and operated by researchers of the Royal Observatory of Belgium. Over ten years, SWAP and LYRA have provided data from flares, coronal mass ejections and other manifestations of solar activity with a very high cadence and an unprecedented, large field-of-view, and they have helped forecasting their effects on the Earth environment.

Figure 1: The PROBA2 team around the model show ten fingers to illustrate the 10th anniversary of the satellite

On the occasion of the 10th anniversary of PROBA2, a press release was sent out and the news was shared to different Belgian media. While PROBA2 was initially intended to last two years, the mission is still ongoing. Today, PROBA2 remains in excellent shape and is one of the few satellites that can be used by European space weather forecasters to detect solar eruptions.

More information on PROBA2 can be found at https://proba2.sidc.be.

Launch of the citizen science project Val-u-Sun

Solar scientists from the Royal Observatory of Belgium launched the citizen science project Val-u-Sun. This project, open to everyone, allows citizens to help research by counting sunspots on archived drawings.

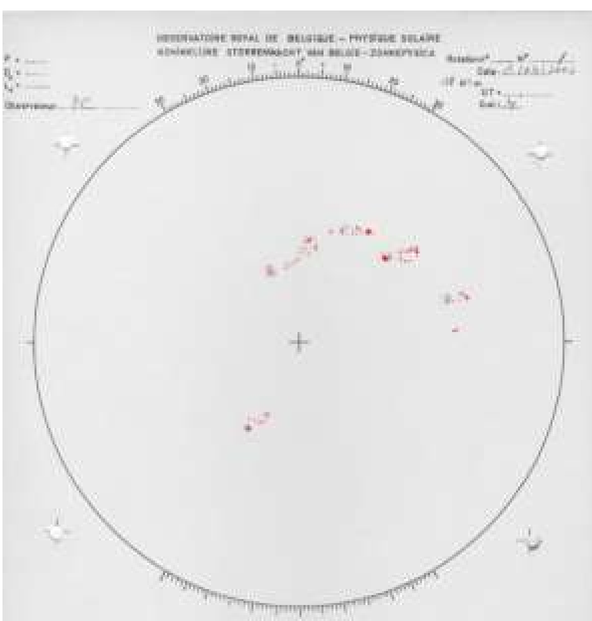

Figure 2: An example of a typical sunspot drawing

Observers around the globe have counted and drawn sunspots by hand for more than 400 years and still continue to do so. The reason they still do it in the old fashioned-way, with a pencil and a paper sheet, is to keep the continuity between past and modern observations. By applying the same method, scientists can compare the sunspots from the past with present-day sunspots. This gives one of the longest scientific data archives in the history of science, dating back from Galileo's observations and drawings from more than 400 years ago.

Citizens can help the solar scientists of the Royal Observatory of Belgium by counting sunspots on the original drawings from the SIDC archive. To participate to this project and for more information, see the Val-u-Sun website:

http://sidc.be/valusun/citizenscience/index.php

Prizes, awards and grants

The 2019 EGU Runcorn-Florensky Medal is awarded to Tim Van Hoolst

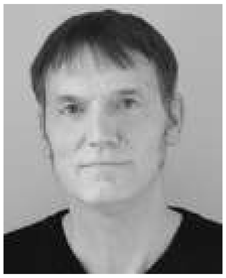

Tim van Hoolst, project leader in planetary science at the Royal Observatory of Belgium won the 2019 Runcorn-Florensky Medal of the European Geosciences Union for his seminal contributions to the field of geodesy and geophysics of the terrestrial planets and satellites and for leadership in planetary geodesy. His field of research is the rotation and tides of planets and satellites and how these can be used to explore the planets' interior structures. He participates in numerous spatial missions such as BepiColombo to Mercury and JUICE (JUpiter ICy moons Explorer) to the Galilean moons of Jupiter, in which he is the chair of the working group on the interior and geophysics of the moons. He is also Co-Investigator of ExoMars 2020 in which LaRa, a radio-science instrument of which the Observatory is responsible, will be integrated.

One of Van Hoolst's most important contributions is related to the understanding of the rotational dynamics of Mercury and of icy satellites, whose sub-surface oceans decouple their interior from the solid but deformable ice shells. Van Hoolst and his team have also worked on determining the interior structure of Mars.

The Vanderlinden Prize is awarded to Sebastien Le Maistre

Sébastien Le Maistre, researcher at the Royal Observatory of Belgium, received on December 14, 2019 the Georges Vanderlinden Prize from the Royal Academy of Belgium (Science Class) for his research in data processing for Martian missions.

Sébastien Le Maistre is an aeronautical and aerospace engineer and holds a doctorate in science. Since his PhD thesis, he specializes in the analysis of radio communications between Earth and Martian landers. He is part of the LaRa project (Lander Radioscience), of which he has been project manager and deputy principle investigator (Deputy PI) since 2018. He became principal investigator (PI) in July 2020. Sébastien Le Maistre has published a large number of scientific papers and has acquired an international reputation in the processing and interpretation of radioscience data.

New grant from the European Research Council for the study of the Earth's interior

On Friday October 11, 2019, the European Research Council (ERC) announced the award of new grants to European researchers (ERC Synergy Grants). Among the laureates is Dr. **Véronique Dehant**, researcher at the Royal Observatory of Belgium for the project GRACEFUL: GRavimetry, mAgnetism and CorE Flow. She shares this grant with Anny Casenave and Mioara Mandea (both from France).

This is the second ERC grant awarded to Véronique Dehant. Her first grant (ERC Advanced Grant) was obtained in 2015 for the project "RotaNut" (Rotation and Nutation of a wobbly Earth). The aim of GRACEFUL is to probe the deep Earth's interior by using observations of the magnetic and gravity fields, and of the rotation of the Earth, A. Cazenave being expert in gravity field, M. Mandea in geomagnetism, and V. Dehant in Earth's rotation. By using in synergy these three global observables, they intend to provide new insights about processes occurring inside the Earth's liquid core and at the core-mantle boundary. See the announcement on the ERC website: http://erc.europa.eu/news/erc-2019-synergy-grants-results

Preparation of space missions

ExoMars: LaRa integrated on the platform Kazachok

On November 2019, the Belgian instrument LaRa (Lander Radioscience) was accepted for integration on the Kazachok platform of the second ESA ExoMars mission (launch postponed to 2022).

The final inspection of LaRa was performed end of July 2019 at the Space Research Institute of the Russian Academy of Sciences (IKI). Representatives of various international organisations attended to this event. In particular, Véronique Dehant, LaRa's Project Manager (PI), and her Deputy PI Sébastien Le Maistre (who became PI in the meantime) of the Royal Observatory of Belgium, along with Lieven Thomassen, design engineer and representative of Antwerp Space, the Belgian instrument Prime Contractor, were present at this crucial moment. They were accompanied by Vaclav Valenta, ESA's Technical Officer in the PRODEX programme (Scientific Experiment Development Programme), Russian mission experts, as well as staff members of IKI (Russian Space Research Institute) and TsNIIMash (Russian Company responsible for ExoMars).

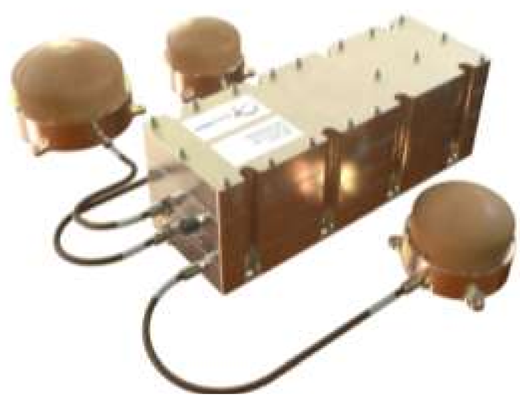

Figure 3 Model of the LaRa instrument.

This inspection included electrical and mechanical compatibility tests with the Russian platform. The tests were realised in a sterile environment to prevent contamination of Mars' surface with biological traces from Earth. On November 7, the acceptance was pronounced, based on the test results during the Test Review Board (TRB). A graduation, in a way. "This is a wonderful achievement, because LaRa is the result of many years of dedicated work!", says Véronique Dehant.

The LaRa instrument

The second ExoMars mission (launch planned in 2022) consists of a rover and a surface platform that will land on Mars on 2023. Belgium develops LaRa (Lander Radioscience), one of the platform instruments.

LaRa is made of an electronic box (a coherent transponder) and three antennas: a receiving antenna and two transmitting antennas. Its purpose is to measure the rotation and orientation of Mars. This measurement will allow extracting the physical properties of the interior of the red planet, in particular the physical state, composition, and dimension of its core.

The transponder part of the instrument was developed, produced and tested by Antwerp Space and the antennas by UCLouvain. Belgium, through the Belgian Federal Science Policy (BELSPO), is funding the LaRa mission with the support of the ESA PRODEX programme.

Link: https://lara.oma.be/

EUI and Solar Orbiter ready for launch!

On October 2019, the instrument EUI (Extreme Ultraviolet Imager) was integrated into the Solar Orbiter satellite launched towards the Sun in February 2020.

The ESA Solar Orbiter mission will perform close-up studies of the Sun, at a distance of only 42 million km. That is less than one third of the distance from the Earth to the Sun, and also well within Mercury's orbit. The EUI telescope will take pictures of the solar atmosphere in non-visible light, i.e. in extreme ultraviolet.

EUI will offer scientists a unique opportunity to have a close look at the dynamic processes in the solar atmosphere. In particular, EUI will image the solar poles for the first time and will provide the sharpest movies ever of the solar atmosphere. This will help us to better understand solar eruptions, which can have severe consequences on our technology such as GNSS (Global Navigation Satellite System) and radio communication, power grids, and pipelines.

The EUI project started in 2008 under the scientific lead of the Royal Observatory of Belgium and the engineering lead of the Centre Spatial de Liège (Belgium). The Institut d'Astrophysique Spatiale (France) and Max Planck Institute for Solar System Research (Germany) contributed to the telescopes of EUI. The computer of EUI was developed by the Mullard Space Science Laboratory, UK. The Physikalisch-Meteorologisches Observatorium Davos/World Radiation Center (Switzerland) developed the telescope enclosure. During operation, the EUI instrument will be managed by the Royal Observatory of Belgium.

EUI website: http://sidc.be/EUI/

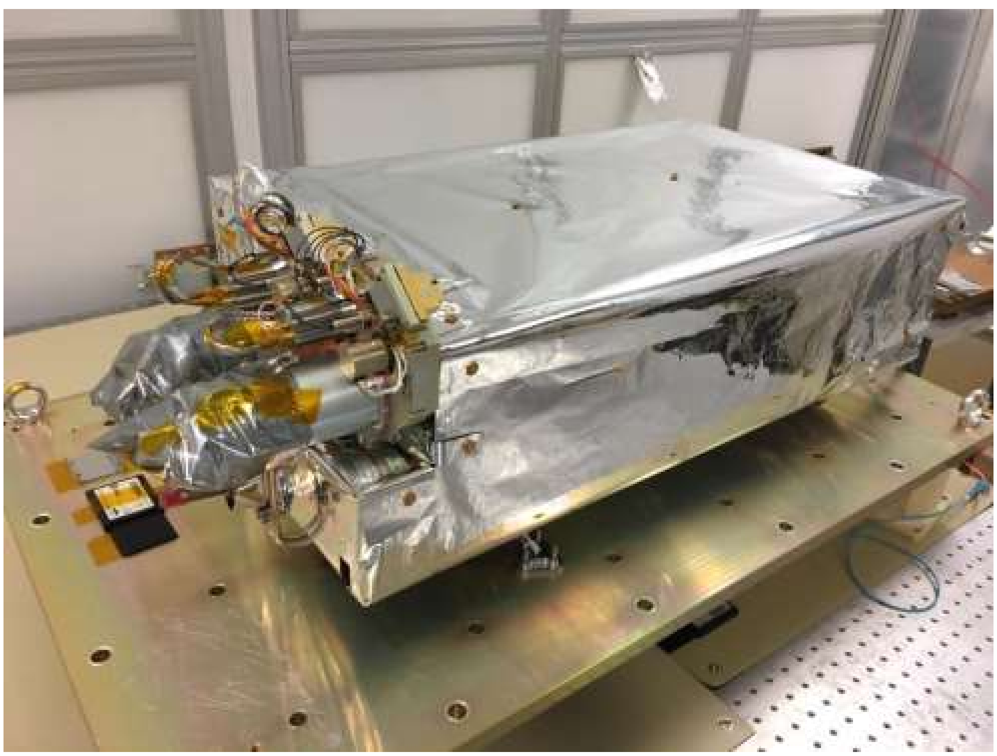

Figure 4. Flight model of EUI (Credit: Jean-Philippe Halain).

Service and expertise

Seismic activity in Belgium in 2019

In 2019, 45 natural earthquakes, 14 induced earthquakes and 199 quarry blasts and explosions occurred in and around Belgium (Figure 5). This catalogue is complete for natural earthquakes and contains a selection of quarry blasts and earthquakes induced by human activities, e.g. linked to (rock) mass removal in mines or geothermal exploitation. The largest event recorded in Belgium in 2019 was the induced earthquake on 23 June 2019 in Dessel (Belgium, M_L=2.1; M_L for local magnitude, commonly referred to as "Richter magnitude"). In 2019, there were at least 16 measurable explosions at sea, performed by the Belgian, Dutch or French Army to destroy old ammunition.

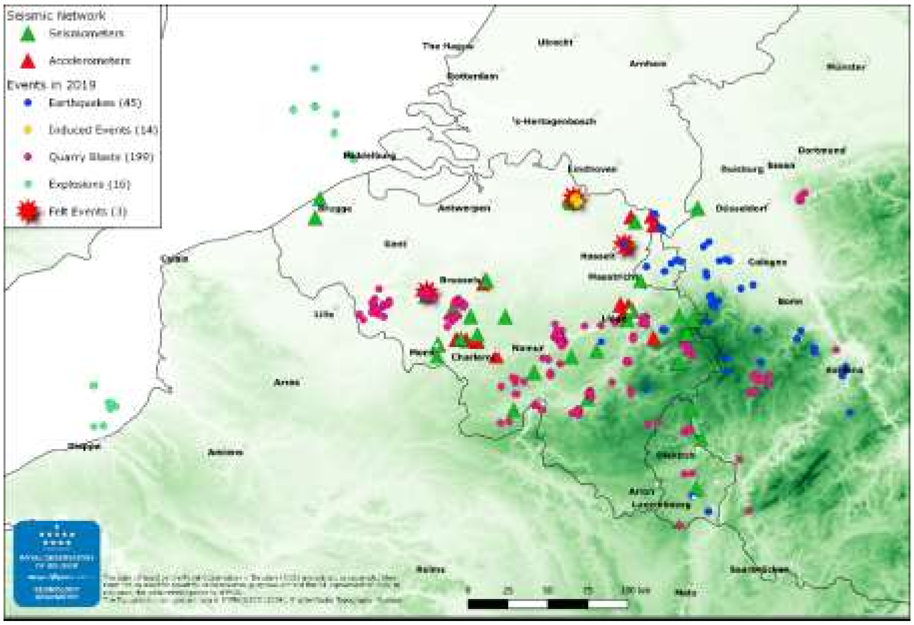

Figure 5: Events recorded in 2019 by the Belgian Seismic Network of the Royal Observatory of Belgium.

In 2019, one earthquake (5 December 2019 near Genk, ML=1.6), one induced event (23 June 2019 near Dessel, ML=2.1; Figure 6) and one quarry blast (20 May 2019 at Lessines, ML=1.8) were felt in Belgium. We know that these events were felt because the local population spontaneously answered the 'Did You Feel It questionnaire' on the ROB macroseismic inquiry website http://seismologie.be/en.

Date and Time	Latitude	Longitude	Depth	Mag.	Name	Inquiries	Type
05/12/2019 01:07	*50.987*	*5.5388*	*6.1*	1.6	Genk (BE)	47	Earthquake
23/06/2019 19:30	*51.240*	*5.109*	*4.0*	2.1	Dessel (BE)	44	Induced
20/05/2019 14:31	*50.732*	*3.852*	*0.0*	1.8	Lessines (BE)	7	Quarry Blast

Table 1: Felt events in the region in 2019.

In comparison, in 2018, 65 natural earthquakes occurred in and around Belgium. The largest was located in Kinrooi 25 May 2018 (magnitude ML=3.1) and was largely felt.

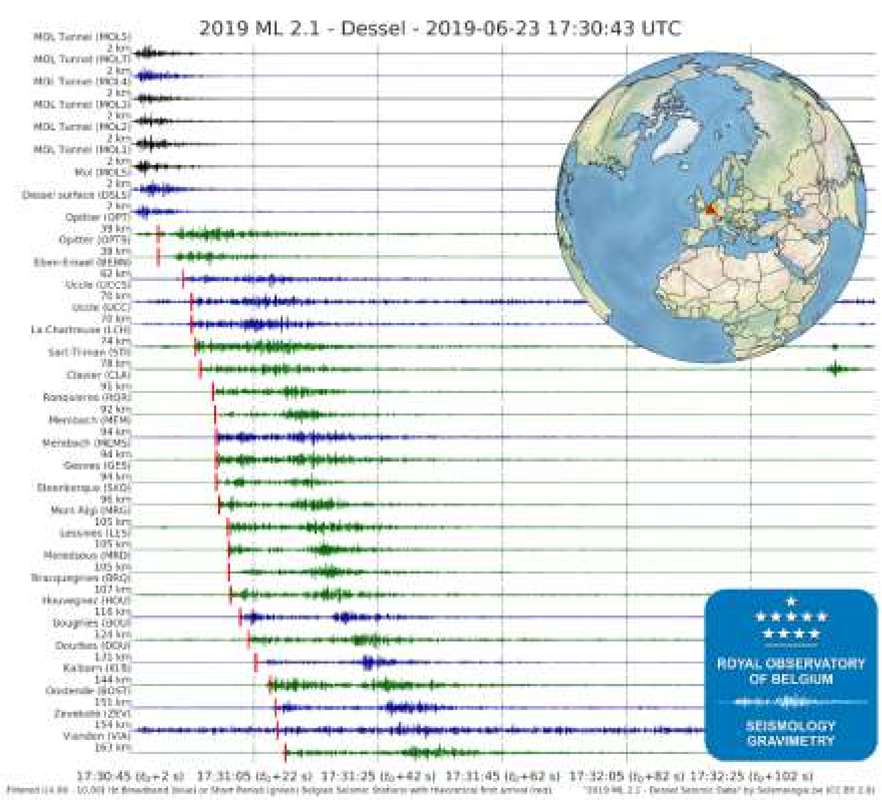

Figure 6: Seismic records of the induced seismic event in Dessel on 23 June 2019 (ML=2.1), the largest event that occurred in Belgium in 2019.

Man-induced earthquakes in Belgium

Earthquakes triggered by industrial activity associated to the filling of artificial water reservoirs in many regions worldwide, or injection of waste water from oil and gas extraction are known since the mid of the 20th century. These events include several earthquakes of magnitude larger or equal to 5.0 that caused significant damage. (Here we refer to moment magnitude, measuring the size of an earthquake based on the area of fault rupture and average amount of slip, and on the force that was required to overcome the friction sticking the rocks together that were offset by faulting.)

Therefore, even if many injection processes are apparently aseismic, industry has to monitor and reduce hazard during injection activities, for example by installing “traffic-light” systems monitoring seismic activity and establishing thresholds for reducing injection rates or stopping injection when necessary. Nevertheless, monitoring and controlling industrial processes may not be sufficient in some specific cases, as indicated by the large events of magnitude $M_W = 5.8$ in Oklahoma in 2016 or $M_W = 5.4$ in 2017 in South Korea.

Man-induced or triggered earthquake activity is currently a significant contribution to seismic hazard in a few stable continental regions (SCR). More generally, we assume that it could be a hazard at least equally important as natural seismicity in some SCR, particularly where there is a lack of previous seismic activity.

This seems to be the case in Belgium, around Mol-Dessel in the province of Limburg, where fluid injection tests have been carried out since 2016. The different tests have induced hundreds of earthquakes. The Seismology and Gravimetry Service monitored the seismic activity locally thanks to the seismometers installed in the Mol-Dessel area, in collaboration with ONDRAF/NIRAS. An induced event occurred on 23 June 2019 close to the injection borehole, the local magnitude has reached $M_L=2.1$ and was felt locally.

In 2019, the Seismology and Gravimetry Service provided expertise services to VITO, SCK•CEN, ONDRAF/NIRAS, the Walloon and Flemish Regions concerning natural and man-made seismic hazards. This consisted in specific studies at some sites (e.g., in depth analysis of the induced activity at Mol-Dessel), reports (e.g., the seismic hazard evaluation at different SEVESO sites in Wallonia), and participation to workshops.

Natural processes explain the occurrence of the SCR seismicity before and in parallel to the advent of industrial processes, and continue to be at the origin of a part, often significant, of the current activity in many SCR. Nevertheless, since 1960, about 10% of moderate earthquakes with $M_W \geq 5.5$ that occurred in SCR worldwide are related to human activities.

Progressing in the understanding of SCR earthquakes needs to address the question of how the different natural and man-induced processes are modifying stresses in the crust and/or fault strength favouring slippage on faults. The Royal Observatory of Belgium is working in particular on inferring man-induced seismic activity rates, estimating the possible maximum magnitude values that can be reached with such events.

The monitoring of induced events in SCR are really challenging, as such moderate shallow earthquakes could be very destructive and deadly. Evaluating the possible consequences of industrial activities in terms of induced or triggered seismicity and associated vulnerabilities should be the rule. This includes not only evaluation of the earthquake resistance of the industrial infrastructures, but also of the different existing types of buildings in the concerned areas.

Reference: Camelbeeck, T., Vanneste, K., Lecocq, T., 2019, Natural and man-induced destructive earthquakes in stable continental regions. Bulletin of the Royal Academy for Overseas Sciences.

A European approach to Space Weather

Researchers at the Royal Observatory of Belgium contributed to a report written by international experts on space weather. This report, released on October 10, 2019, explains the challenges of space weather and provides a set of recommendations against radiation hazards in space.

Space weather refers to the environmental conditions in space as influenced by solar activity. To prevent radiation hazards on satellites and spacecraft and to limit the health risks for astronauts, a thorough knowledge of space weather is of high importance.

The report, spearheaded by European Space Science Committee (ESSC) of the European Science Foundation is directed to the European Space Agency (ESA), the European Union (EU) and their respective member states. It highlights the need of strong coordination between member states and European bodies and organisation.

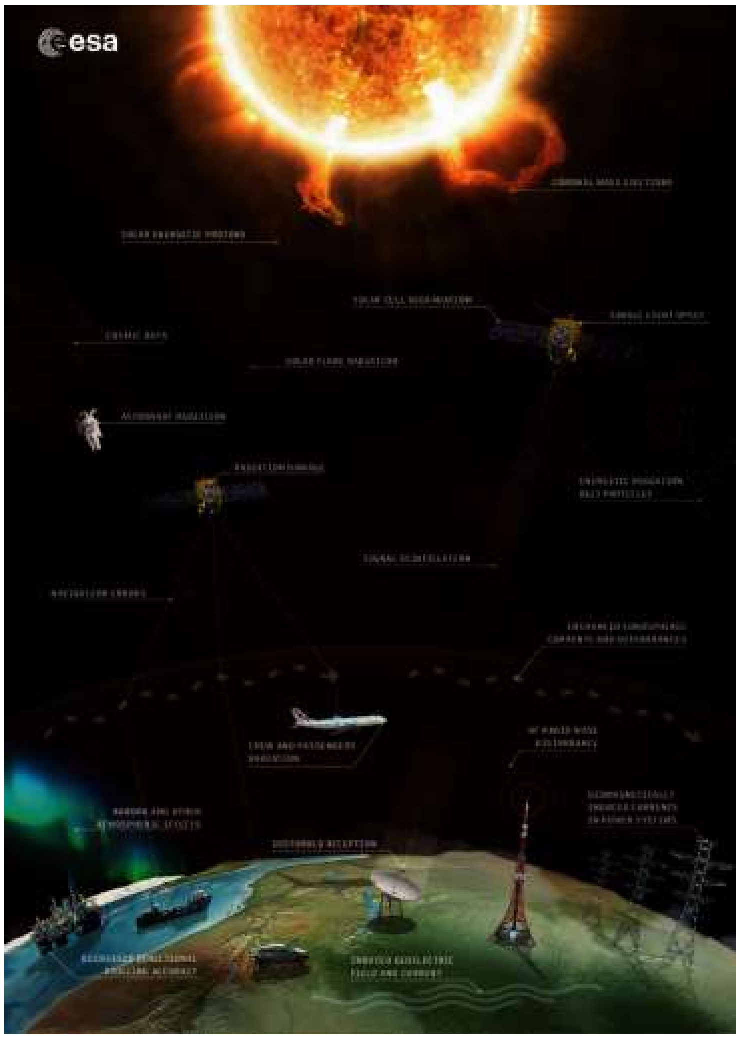

Figure 7: Space weather effects. Image credit: European Space Agency / Science Office, CC BY-SA 3.0 IGO.

The ESSC experts have identified six activities that urgently require coordination at European level:

- Enabling critical science to improve our scientific understanding of space weather. Support must be provided for launching the next generation of space missions and for the maintenance and augmentation of ground-based infrastructure.

- Development and coupling of advanced models by applying a system-science approach that utilises physics-based modelling.
- Assessment of risks at national, regional and European levels. This requires close cooperation between decision makers, space weather scientists, service providers, and end-users.
- Consolidation of European User Requirement on a regular basis, considering regional and societal differences and needs.
- Supporting continuous iteration and feedback between space weather scientists and candidate organisations for space weather services (transition from Research to Operations).
- Definition and implementation of an operational network for future space weather observations, leading to predictions that will allow us to protect the society's infrastructure.

Given that many countries are developing increasingly sophisticated infrastructure, which at this point can still be better prepared against space weather risks, this is a crucial step towards making our modern and technology-reliant society sustainable and resilient.

The report: https://www.swsc-journal.org/articles/swsc/abs/2019/01/swsc190036/swsc190036.html (free access, *under a Creative Commons CC BY 4.0 licence*)

Original press release of the European Science Foundation: http://www.esf.org/news-media/news-press-releases/article/how-can-europe-explore-further-understand-more-and-prepare-better-for-adverse-space-weather-effects/

Research at the Royal Observatory of Belgium

Seismology

How could seismic activity knowledge reflect future activity?

During the last 20 years, the Royal Observatory of Belgium studied past seismicity and large earthquakes evidenced in the geological and geomorphological records in the region between the Lower Rhine Graben (LRG) and southern North Sea. A synthesis of the main results of these investigations is published, including an analysis discussing whether this past and present earthquake activity could reflect future seismic activity. In that area, since the 14th century, there has been a moderate seismic activity with 14 earthquakes of magnitude M_W larger or equal to 5.0 (see Figure 8).

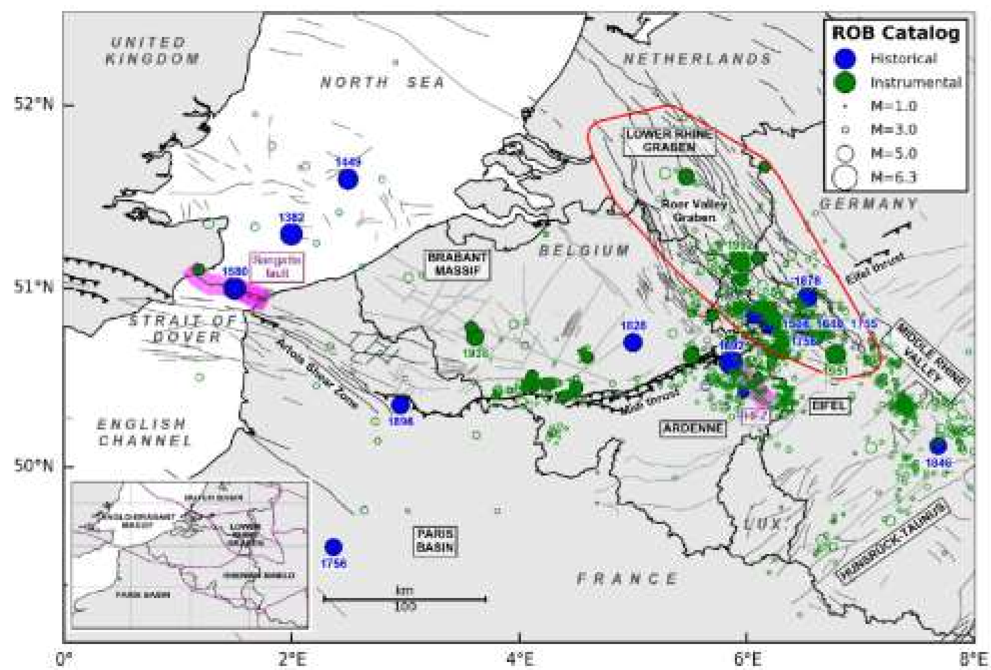

Figure 8: Seismic activity in the region from the Lower Rhine Graben (LRG) to the southern North Sea between 1350 and 2018 (Catalogue of the Royal Observatory of Belgium). The red contour shows the limit of the LRG. The magenta zones represent the Sangatte fault and the Hockai Fault zone (northern Ardennes).

More generally, in Western Europe, north of the Pyrenees and the Alpine arc, such moderate and large earthquakes are sparsely located (Figure 8). They occurred clustered in patches of activity separated from regions where seismicity is absent. This could indicate that some regions would be more susceptible to generate moderate to large earthquakes. However, recent studies of plate interior seismic activity suggest that such apparent concentrations and gaps in seismicity likely reflect the short earthquake record compared to the long and variable recurrence interval of large earthquakes.

Is this persistent or absent seismicity simply a consequence of the short duration of the observations, or is it more permanent? This is an important question for seismic hazard assessment. This requires identifying and collecting information on large earthquakes that occurred before the Middle Age, i.e., when there was no historical reports. For that purpose, we performed paleoseismological investigations during the last 20 years and retrieved traces of past large earthquakes in the geomorphology and the recent geologic record.

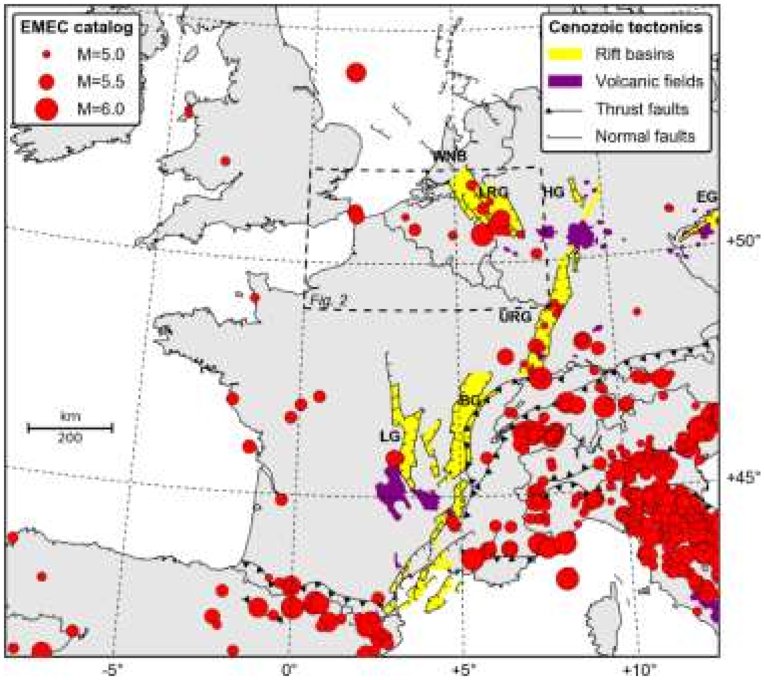

Figure 9: Seismic activity in Western Europe. Epicenters of earthquakes with estimated M_W≥5.0 as reported in the European Mediterranean Earthquake Catalogue (EMEC) (Grünthal and Wahlström, 2012). WNB: West Netherlands Basin, LRG: Lower Rhine Graben, EG: Eger Graben, HG: Hessian Graben, URG: Upper Rhine Graben, BG: Bresse Graben and LG: Limagne Graben. The rectangle with dotted line shows the limits of Figure 8.

Outside the LRG, earthquake activity appears as typical of stable continental regions. Large and moderate earthquakes occur on inherited fault zones presenting little activity for the last 2 millions of years at best. Three of the largest historical earthquakes with M_W ≥ 5.5 occurred outside the LRG, but the activity along the fault zones suspected to be the source of two of these earthquakes, i.e. the 1580 Strait of Dover and 1692 northern Belgian Ardennes earthquakes, is very elusive, if it exists (Figure 8).

This leads to the suggestion that the large earthquakes to the west of the LRG between 1350 and 1700 would give an overestimated perspective of the real long-term seismicity in this region. On average, there should be less large events in the area and the actual activity is likely closer to that observed since the 18th century. Hence, the seismicity outside the LRG is episodic and clustered on some faults during periods of a few hundreds of years, interrupted by long periods of inactivity typically lasting for some tens to hundreds of thousand years.

The LRG is the only area in the region between the LRG and the southern North Sea where the earthquake activity is continuous in the recent geological periods and concentrates on the faults delimiting the Graben. Those faults are the source of large surface rupturing earthquakes that have occurred for the last 130,000 years. The estimated magnitudes range from 6.3±0.3 to 7.0±0.3 while their average recurrence on individual faults varies from ten thousand to a few ten thousand years. Hence, we can infer activity rates, estimate the possible maximum magnitude values, and use this information for probabilistic seismic hazard assessment to the long term.

Reference: Camelbeeck, T., Vanneste, K., Verbeeck, K., Garcia-Moreno, D., Van Noten, K. & Lecocq, T., 2020, How well does known seismicity between the Lower Rhine Graben and southern North Sea reflect future earthquake activity? Proceedings of Historical Earthquakes, Paleoseismology, Neotectonics and Seismic Hazard: New Insights and Suggested Procedures, 53-72, DOI: 10.23689/fidgeo-3866.

Extracting Microseismic Ground Motion to Validate Ocean-Climate Models

Seismologists observed and recorded the Earth's continuous ground motions long before the onset of digital seismography, as early as 1855. For more than a century, analogue seismic data were recorded on smoked paper, with ink, or on photographic paper. For ocean waves, visual observations from ships make up nearly all the available data until 1946 with only a few instrumented records, which became more common in the 1980s with the deployment of buoys.

Global measurements of major ocean storms using wave heights became ubiquitous as of 1993 with satellite measurements, but coverage is usually not sufficient to record the peak of storms. Therefore, our general knowledge of ocean wave climate heavily relies on numerical models based on wind parameters obtained from atmospheric reanalyses.

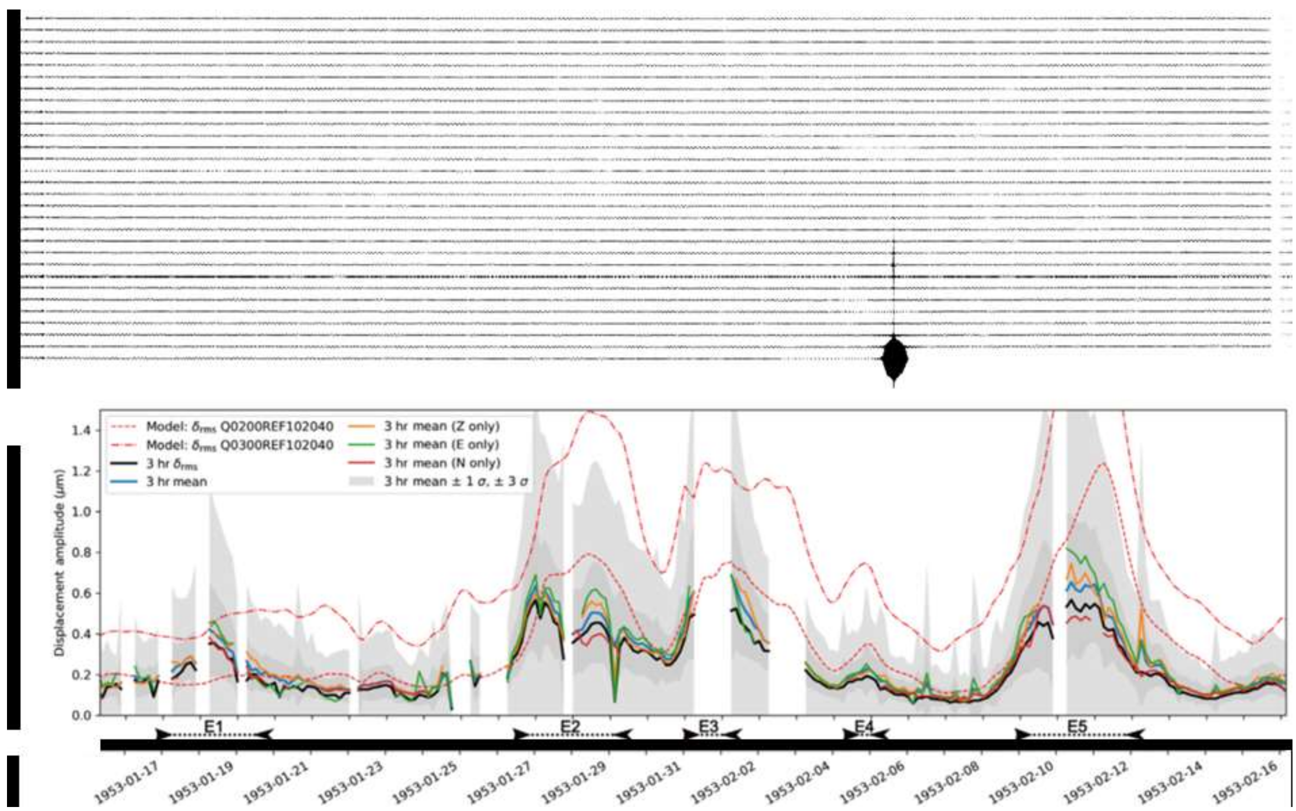

Figure 10: 1953 Scanned analogue photographic seismic record (above) and analysis (below). Comparison of the observed and modelled ground displacement amplitude. Two ocean generated ground-motion models with different anelastic attenuation models are presented. The arrows indicate the five periods of significant microseismic activity seemingly higher than a background level that could be estimated at 0:25 µm: 17–21 January, 26–30 January, 31 January–2 February, 4–5 February, and finally 8–12 February.

Before 1994, there were only a few measurements of wind speed and direction at sea level. Hence, their estimates and climate trends are prone to artificial biases. Another source of quantitative data comes from the microseisms recorded by seismometers. Microseisms, which are the continuous vibrations of the ground induced among others by ocean waves, have been extensively studied since the early days of seismology mostly because of their presence in all seismic records.

In 2019, we concluded a pilot demonstration of the usefulness of analogue seismograms to improve the database of ocean storms before the 1980s by providing additional data for the quantitative validation of ocean wave modelling, in particular for extreme events. We presented a method for automatic digitisation of paper seismograms to extract microseismic ground-motion periods and amplitudes. The digitised time series is processed and compared with modelled microseisms levels computed using a numerical ocean wave model.

As a case study, we focussed on one month of data recorded at the Royal Observatory of Belgium from January to February 1953, around the North Sea Flood event. This event was a tragic storm surge that flooded the lowlands of England, the Netherlands, and Belgium on 1 February 1953, causing 2551 deaths. Before the flood event, the reconstructed ground motions show clear storm signatures that we related to specific sources in the North Atlantic Ocean. However, the models of the North Sea Flood event predict much smaller microseismic amplitudes compared to the observational data when the storm reached its maximum in the southern North Sea (see the grey zone at the beginning of the E2 period on Figure 10). The study of primary microseism generation, specifically in the North Sea, remains an active field of investigations and should soon provide new modelling theories to compare with our results.

This study illustrates the need to preserve our archives. In seismology, as well as in climatology, new techniques allow interpreting old data to make important discoveries. Here, this study is a first successful proof of concept for the purpose of present-day analyses of constructing twentieth-century ocean-climate models.

Reference: Lecocq, T., Ardhuin, F., Collin, F., Camelbeeck, T., 2020. On the Extraction of Microseismic Ground Motion from Analog Seismograms for the Validation of Ocean-Climate Models. Seismological Research Letters, 91, 1518–1530. https://doi.org/10.1785/0220190276.

Gravimetry

The sensitivity of superconducting gravimeter is so large that it can also serve as a pluviometer

In Belgium, gravity (g) is close to 9.81 m/s². This value is essentially due to the gravitational attraction of the Earth. However, it is not constant. Tidal forces, induced by the relative movements of the Sun and the Moon, cause small variations. Climate-related variations are also observed, such as the amount of water in the soil varies over the seasons. During the winter, well-filled aquifers locally increase the Earth's mass and surface gravity.

Figure 11: Left: The superconducting gravimeter of Membach (Credit: E. Coveliers). Right: Detail drawing of the sensor with the levitating sphere. (Credit: B. Frederick)

These variations, of the order of one billionth of g, are extremely small and measured by the superconducting gravimeter of the Royal Observatory of Belgium. Geophysicists have long known that precipitation, by feeding water reservoirs in the ground, influences gravity. Hence, we wondered whether the gravimeter might be used to verify the measurements of the weather radar.

Figure 12: The weather radar of Wideumont.

For the first time, scientists from the Royal Observatory of Belgium and the Royal Meteorological Institute compared the data of a meteorological radar of Wideumont (Figure 12) with those of the superconducting gravimeter of Membach (Figure 11).

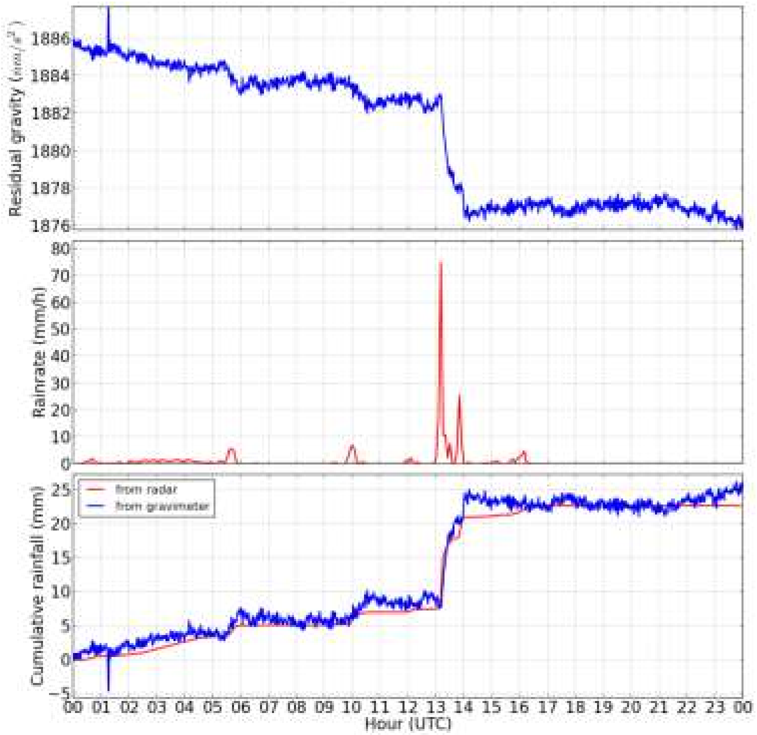

Figure 13: Evolution of the gravity measured at Membach (top), the intensity of precipitation estimated by the radar (middle) and the cumulative amount of precipitation (bottom) on 24 July 2017. The cumulative precipitation estimated from the gravimeter and radar appears in blue and red respectively. Although their measurement principles are very different, the estimates obtained from the two instruments are remarkably consistent.

Data from both instruments were analysed over the period 2003–2017 and more than 500 episodes of intense precipitation were identified. The results show that the gravimeter has proven invaluable for estimating the amount of precipitation accumulated over a large area. Like a gigantic rain gauge, it captures rain, hail or snowfall within a 400 m radius. This instrument is, therefore, an interesting new source for *in situ* observations to validate precipitation observations from remote sensing instruments such as radars and meteorological satellites. Precipitation measurement is essential for monitoring and refining weather forecasts and for studying the impact of climate change on the hydrological cycle.

This study got in 2018 the Jim Dooge Award of the European Geoscience Union (https://www.hydrology-and-earth-system-sciences.net/about/jim_dooge_award.html) and its results were published in 2019 in the journal Hydrology and Earth System Sciences of the European Geosciences Union.

Reference: Delobbe, L., Watlet, A., Wilfert, S., Van Camp, M., 2019, Exploring the use of underground gravity monitoring to evaluate radar estimates of heavy rainfall. Hydrology and Earth System Sciences, 23, 93–105. 10.5194/hess-23-93-2019. https://www.hydrol-earth-syst-sci.net/23/93/2019/hess-23-93-2019.html

Global Navigation Satellite Systems

Impact of GSM signals on GNSS high precision applications

Today, GNSS (Global Navigation Satellite System, e.g. American GPS, Russian GLONASS, European Galileo, Chinese Beidou) supports many applications going from positioning of public and private transportation (navigation), network synchronisation, surveying and mapping, to specific public and scientific applications. With classical mass-market receivers, the GNSS positioning accuracy is at the level of a few metres in real time (the accuracy can be of a few centimetres with Real-Time-Kinematic, a differential technique relying on the use of additional signals transmitted by a reference station). Positioning at a few millimetres is also possible by using a high-precision antenna and receivers linked to atomic clocks.

This kind of high-precision GNSS stations provides the possibility of further geophysical applications and research. For example, scientists of the GNSS research group of the Royal Observatory of Belgium use GNSS signals to realise the space and time reference systems, to determine atmospheric variables, to determine atmospheric parameters and to monitor solar radio bursts. All these applications rely on high-performing permanent GNSS stations located in a quiet electromagnetic environment.

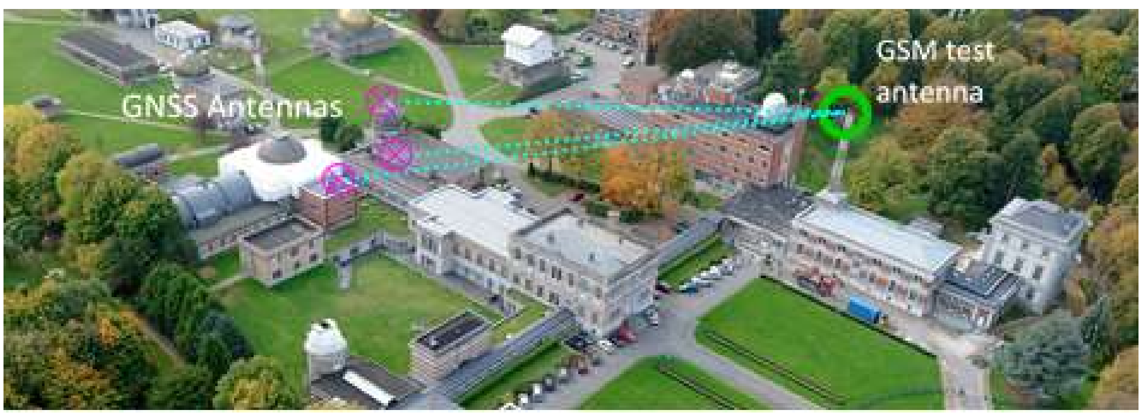

Figure 14: Antenna test setup.

With the increasing number of telecommunication antennas, there is a growing risk of interferences between the GSM frequency bands (around 0.9 GHz and around 1.8 GHz) and the GNSS frequency bands (1.2 GHz to 1.6 GHz). Those interferences are susceptible to affect the quality of our permanent GNSS stations. GNSS signals are indeed vulnerable as the signal is emitted from solar-powered satellites at roughly 22,000 km above the Earth. The power received on the ground is therefore very weak, and several orders of magnitudes lower than the power of the GSM signals.

In 2019, scientists of our GNSS research group realised a study of the possible interferences due to GSM signals on GNSS high precision measurements. With the collaboration of a telecommunication operator, a relay antenna was set up on a mast in the Space Pole site (Royal Meteorological Institute Building, see Figure 14) with the emission cone oriented towards our GNSS antennas. Two different campaigns were realised, with two different heights of the GSM antenna. In both cases, the emission intensity was set up to the maximal exposure value of 6 V/m, in a narrowband of GSM frequencies close to the GNSS bands: 947.2 MHz and

1825.6 MHz. The GSM signal intensity measured near the GNSS antennas ranged between 0.9 V/m and 1.7 V/m.

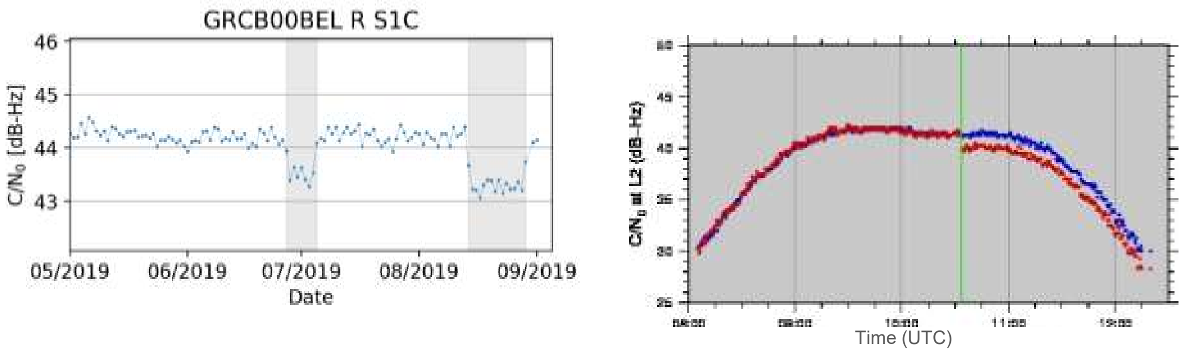

Figure 15: (left) Daily mean variations of the GNSS carrier-to-noise density ratio (from May to September 2019). The grey zones correspond to the two campaigns of emission of telecommunication signals from the relay antenna. (right) Brutal power decrease of the signal received (in red) compared to the normal values (in blue) for a given satellite. The vertical green line shows the epoch of the activation of the campaign on 14/08/2018.

During these two campaigns, the scientists observed a reduction of the carrier-to-noise density ratio (C/N0) of the GNSS signals due to a noise increase around the GNSS antennas. This C/N0 reduction was quantified for each of our GNSS stations, equipped with different receivers and antenna types. An example of C/N0 variations is shown in Figure 15 where the two GSM antenna emission campaigns are depicted in grey zones; a decrease of about 1 dB-Hz is clearly visible during both campaigns. Such interference would therefore directly affect our solar radio bursts monitoring based on GNSS C/N0 measurements, as it reaches their detection level. Besides this C/N0 fade, no impact was observed on our applications based on the pseudo-range and carrier phase measurements such as positioning, atmosphere sounding and remote clock comparisons. However, the 1 dB drop due to the change in the electromagnetic environment reaches the internationally established threshold for harmful interferences, known as the Interference Criterion Protection (IPC), and could jeopardise the receiver measurements.

This study therefore stressed the need to avoid any new telecommunication antenna in the neighbourhood of our GNSS permanent stations. Avoiding this allows to maintain the quality of the measurements, as needed for high-precision applications, and in particular, for the detection of solar radio bursts.

GNSS interferometric reflectometry to measure snow melting in Antarctica

The melting of Antarctic glaciers has a large impact on global sea level rise. In 2018, Shepherd et al.[1] estimated that, between 2012 and 2017, Antarctica lost on average 220 Gt of ice per year, five times more than what was observed between 1992 and 2002. To give an example, the ice lost between 2012 and 2017 corresponds to a roughly 30-meter thick ice layer of the size of Belgium.

These estimations heavily rely on the knowledge of a quantity called ice mass balance, considered as the ‘health status’ of the glacier system. The ice mass balance represents the balance between how much mass the system has received (the input flux) and how much it has lost (the output flux). The input flux, also known as ‘surface mass balance’, consists of all the processes affecting the addition or removal of snow on top of the ice sheet. Scientists monitor these processes with various techniques. However, due to the harsh environmental conditions in Antarctica and the elevated operational costs, *in situ* data remain scarce. Snowfall for example, is the primary ice sheet mass input and is mainly derived from satellite-borne altimetry, ice core studies or regional climate models.

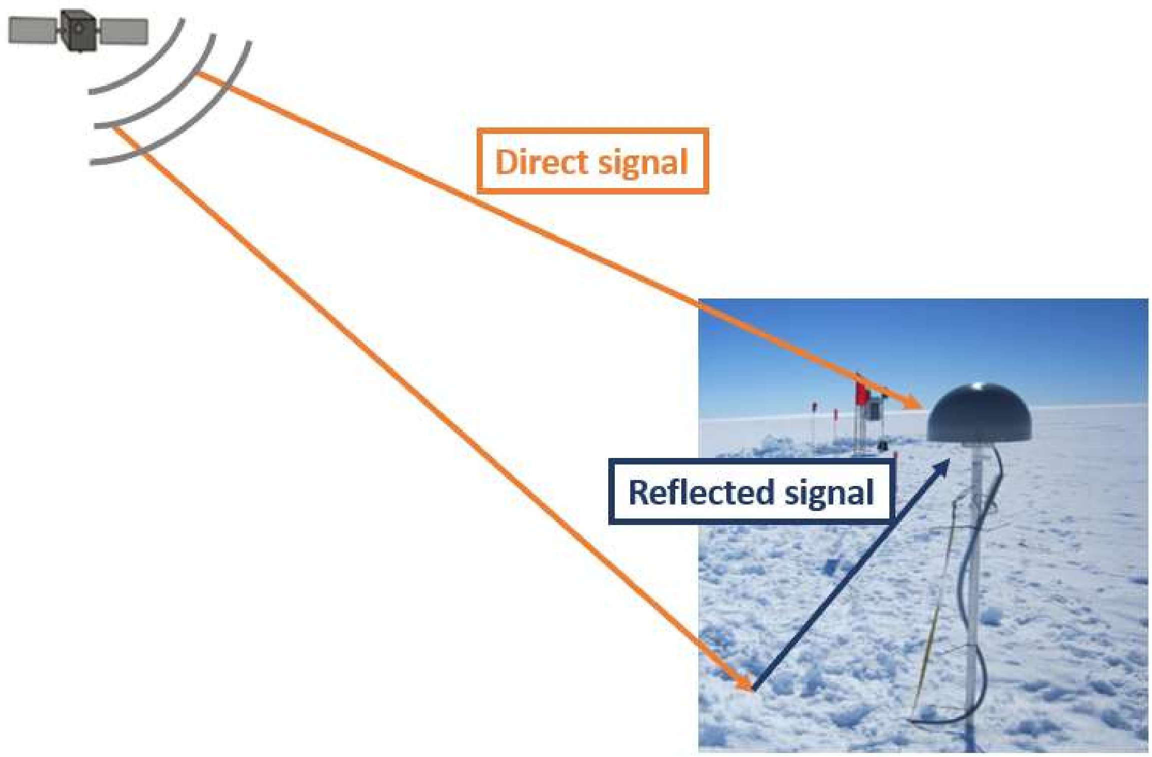

Figure 16: Scheme of the signals used for GNSS Interferometric Reflectometry (GNSS-IR). The picture shows the ROB1 station installed by ROB in East Antarctica in 2012.

Since 1995, GNSS antennas have been deployed in Antarctica to monitor ice flow, crustal deformation and seismic activities, resulting nowadays in a network of hundreds of stations. Some of these are located in the open field and not on the rocks, thus enabling GNSS Interferometric Reflectometry (GNSS-IR) studies to

---

1 Shepherd, A., Ivins, E., Rignot, E. et al. Mass balance of the Antarctic Ice Sheet from 1992 to 2017. Nature 558, 219–222 (2018). https://doi.org/10.1038/s41586-018-0179-y

retrieve local information on snow accumulation or ablation, contributing to more reliable surface mass balance assessments.

GNSS-IR uses signal-to-noise ratio measurements to sense the antenna near-field environment. The interferences between the direct signals and the signals reflected on the snow depend on the antenna height above the ground, and hence on the snow elevation (see Figure 16).

We applied our GNSS-IR analysis on the measurements from different regions of Antarctica. As an example, Figure 17 shows the results obtained for the ROB1 antenna, deployed in the snow by the Royal Observatory of Belgium on the Derwael Ice Rise, in the coastal Dronning Maud land, East Antarctica, and LPRD station, located on the Leppard Glacier in the Antarctic Peninsula. ROB1 provided continuous data from late 2012 to early 2016. Our results highlight an annual variation of snow accumulation in April-May (~30–50 cm) and ablation during spring/summer period. It is not possible, however, to establish a trend suggesting ice/snow meltdown.

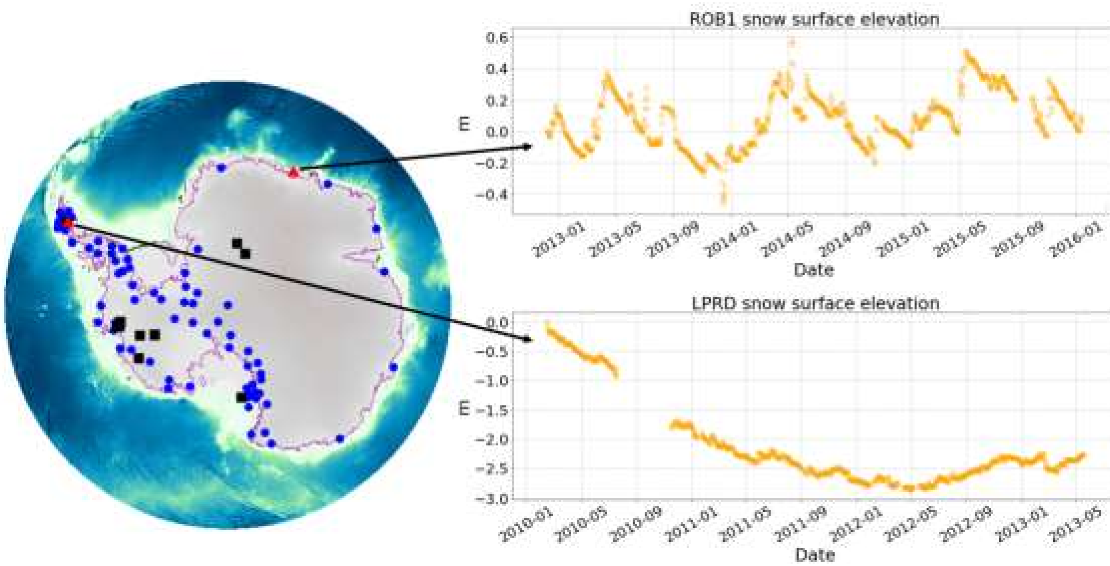

Figure 17: Comparison between snow height variations at ROB1 (East Antarctica) and LPRD (Antarctic Peninsula).

Due to its position on an Ice Rise, the ROB1 station is a very peculiar one: it does not undergo any horizontal motion throughout the years. This is not the case for most of the other antennas in the network, located on the flowing glacier slopes. For these stations (e.g. LPDR, our second case study), the glacier slope must therefore be subtracted from the results. In order to do this, we used the Reference Elevation Model of Antarctica REMA[2], a high-resolution topographical model of Antarctica. The final snow surface elevation at the LPRD location is also reported in Figure 17: from 2010 to 2012, we observe a global decrease of the snow level of about three metres, followed by a more stable period.

This study highlighted GNSS antennas potential in helping the Antarctic Surface Mass Balance assessment with local measurements over long periods.

[2] Howat, I. M., Porter, C., Smith, B. E., Noh, M.-J., and Morin, P.: The Reference Elevation Model of Antarctica, The Cryosphere, 13, 665–674, https://doi.org/10.5194/tc-13-665-2019, 2019.

Planetary Science

Mercury's crustal thickness controlled by mantle melt production

Mercury's crust has a complex structure resulting from a billion years of volcanism. Major magmatic activity terminated about 3.5 Ga ago. That means that the lava records the early stages of the thermal and compositional evolution of the planet and can be used to constrain melting conditions of the mantle. Contrary to Earth, plate tectonics do not recycle and deform surface materials. On Mercury, layer upon layer of effusive and intrusive volcanism have transformed the primary crust into a complex secondary crust showing large regional variations in its properties.

Between 2011 and 2015, the spacecraft MESSENGER identified surface variations in the abundance of chemical elements, from which was inferred the existence of at least six different geochemical terranes in the northern hemisphere. The two largest terranes are the magnesium-poor northern volcanic plains and a magnesium-rich region in the western hemisphere making up about 7% and 11% of the surface, respectively. While the former is a huge area of flood basalts, the later terrane is of unknown origin and was initially thought to be due to a giant impact. Elucidating the origin of the various terranes cannot be done without reconstructing at least in part the history of crustal formation processes. This requires an interdisciplinary approach merging geological analysis with geodesy.

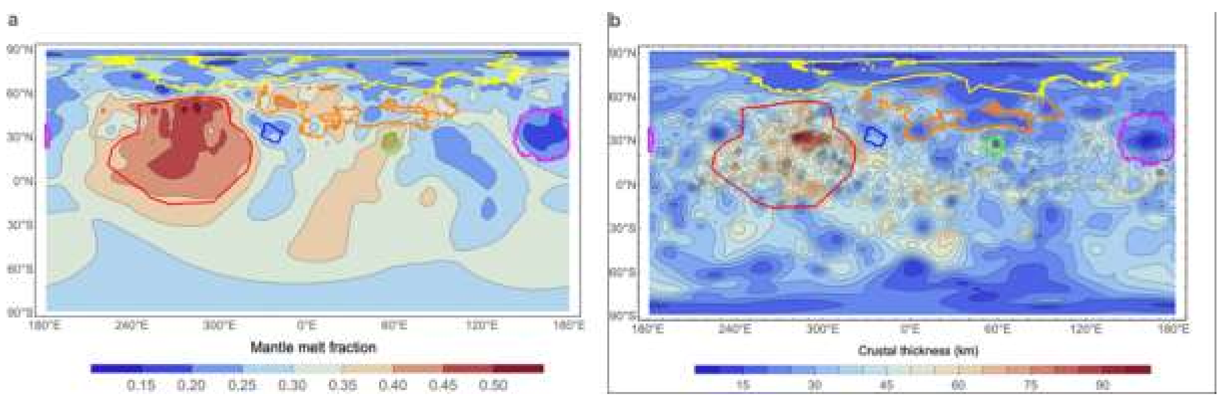

Figure 18: (a) Degree of partial melting of Mercury's mantle obtained from surface compositional data. Colour lines delimit geochemical terranes (magnesium-rich terrane in red, northern volcanic plains in yellow and orange, the Caloris impact basin in pink). (b) Crustal thickness of Mercury if laterally variable density.

Such a study was undertaken by researchers in geodesy of the Royal Observatory of Belgium, and researchers in geology of the University of Liège and the KU Leuven. In the geological part of the study, the surface chemical data was converted into a distribution of surface minerals. From this distribution, variations of the surface density and the degree of the partial melting of the mantle (or mantle productivity) could be deduced. Although Mercury's crust cannot be divided into continental lighter crust and oceanic denser crust, the minerals present in the magnesium-rich terrane result in a much denser crust whereas the northern flood basalt is of relatively lower density. In parallel, mantle productivity is much higher in the magnesium-rich terrane (Figure 18a).

In the geodesy part of the study, global models of crustal thickness were computed by inverting Mercury's latest gravity field and topography data and by using as input the variable density of surface minerals deduced from the geological analysis (Figure 18b). In the northern hemisphere, where the resolution of geochemical and geophysical data is the highest, mantle melt production and crustal thickness are well correlated: the higher the degree of melting, the thicker the crust (Figure 19). This correlation is robust for a wide class of crustal models, and holds as long as the lateral variations of crustal density at depth reflect those at the surface. Including crustal density variations completely changes the predictions for the crustal thickness of the magnesium-rich terrane, which becomes an area where the crust is thickest instead of being thinnest. Hence, this region cannot be an outcrop of the mantle but formed as a result of the highest degree of partial melting in Mercury's mantle. This melting led to the intrusion and eruption of magnesium-rich lava and the formation of a thick crust.

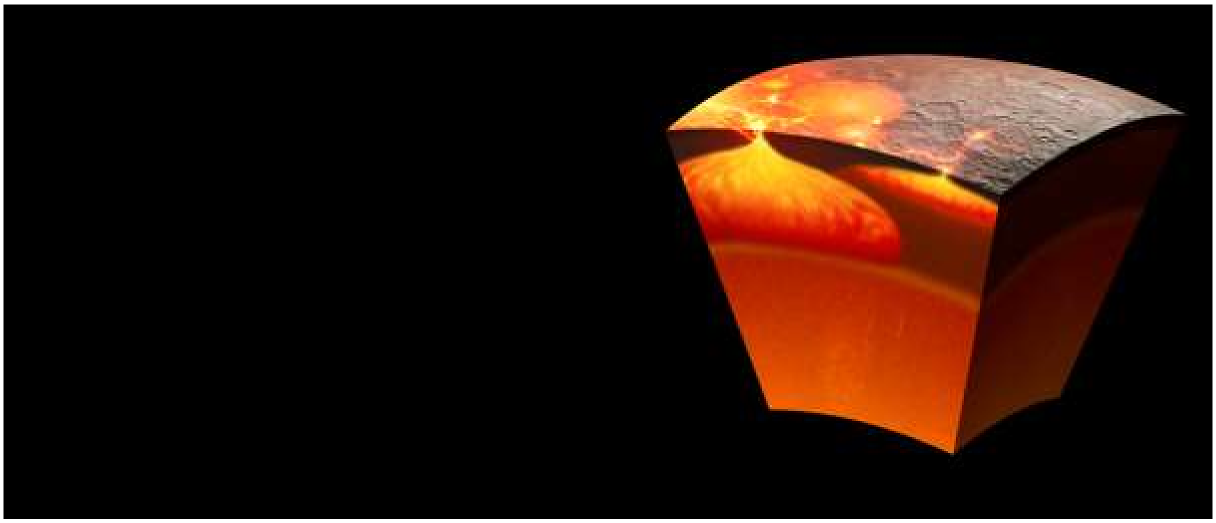

Figure 19: (Left) Crustal thickness as a function of mantle productivity for Mercury's north hemisphere. The middle curve shows the moving average of the scatter plot while the top and bottom curves delimit the 95% confidence level. The straight line represents the least-squares fit. (Right) Partial melting of the mantle and production of the secondary crust on Mercury. Deep and extensive melting of the mantle in some regions produced a thick crust while shallow and low-degree melting produced a thinner crust (copyright Mark Garlick).

Briefly, a simple scenario of heterogeneous mantle melting followed by melt extraction and secondary crust production explains at least 50% of the crustal thickness variability. High degrees of mantle melting produced a large volume of magnesium-rich lava that accumulated to produce a thick crust. Conversely, magnesium-poor lava was produced by a lower degree of partial mantle melting and formed a thinner crust (Figure 19). While this mechanism can be considered as dominant, other processes such as impacts, tectonics, and hidden heterogeneity of the crust and mantle also contribute to crustal formation and perturb the correlation between crustal thickness and mantle productivity.

A link between crustal thickness and mantle melt production had previously been identified on Earth. For example, one commonly explains the large difference between the lower average thickness of the oceanic crust and the thicker oceanic plateaus by mantle plumes being hotter than the surrounding mantle. Those hotter mantle plumes lead to a higher rate of mantle melting responsible for the chemical and physical characteristics of oceanic plateaus. On Mars, a link has been established between the density of erupted basalt forming the crust and the temperature conditions of partial melting in the mantle. In conclusion, the correlation we observe at the planetary scale on Mercury between mantle melt production and the thickness of the crust might be a general feature of secondary magmatic crusts of terrestrial planets.

Reference: This research was published in Geophysical Research Letters (M. Beuthe, B. Charlier, O. Namur, A. Rivoldini, and T. Van Hoolst, Geophys. Res. Lett. (2020), 47, e2020GL087261).

Mars surface-atmosphere interactions: Methane

Surface atmosphere interactions remain among the yet to be understood processes on Mars. Take for example methane (CH_4): different studies claimed its presence or non-presence in the atmosphere of the planet over the last two decades. Such studies raised numerous, still unanswered questions about methane generation and destruction mechanisms. The ESA Mars Express orbiter observed methane in 2003. In the same period, ground-based observations detected large methane plumes over the Martian region called Syrtis Major (see Gloesener, 2019 and Temel et al., 2019 for a review of observations).

Figure 20: NASA's MSL rover (left). Schematic of ESA's TGO and observations (middle). Upper limits for CH_4 obtained by TGO and compared to seasonally variable background methane as measured by MSL (Korablev et al., 2019) (right).

One of the key goals of the ESA Trace Gas Orbiter (TGO) Mission on the red planet, to which the Royal Observatory of Belgium contributes, is to gain a better understanding of methane and other atmospheric gases. Those gases are present in small concentrations (less than 1% of the atmosphere) but could be evidence for possible biological or geological activity. Preliminary observations of TGO (Korablev et al., 2019; Vandaele et al., 2019) showed no detection of methane in the atmosphere while the Mars Science Laboratory (MSL) in the Gale crater continued to detect methane emissions (see Figure 20). Reconciliation between the TGO findings and the background methane concentrations found in the Gale crater would require an unknown process that can rapidly remove or sequester methane from the lower atmosphere before it spreads globally.

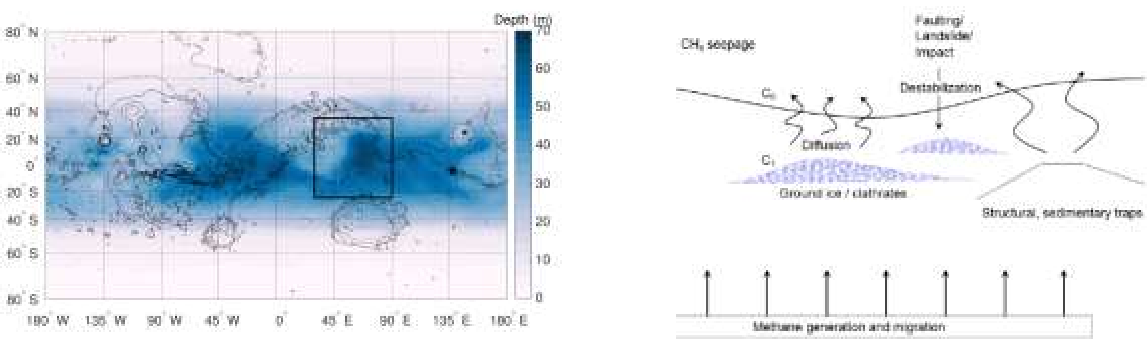

Figure 21: Depth (m) of the top of the clathrate stability zone in present-day Martian subsurface for CH_4-rich clathrates formed from a gas phase with 90% of methane. Local detections of methane are reported in black: a black star represents Gale Crater, while the Syrtis Major area is included in the black rectangle (left). Schematic of methane migration and storage in the Martian crust and subsequent release into the atmosphere (right) – (Gloesener, 2019).

In order to interpret the *in situ* and remote methane observations, a study including both subsurface methane transport and atmospheric transport was developed and applied to local and global observations (see Temel et al., 2019 and Pla-García et al., 2019). After its generation at depth, Martian methane can migrate upwards and be either directly released at the surface or trapped in subsurface reservoirs, such as clathrates. There, it could accumulate over a long time before being episodically liberated during destabilising events. The CH_4 source depths in our subsurface model are determined by the stability zone of clathrate hydrates (see Figure 21). On present-day Mars, the stability conditions of CH_4-rich clathrates are met at a depth of a few metres in high-latitude regions and at a few tens of metres deep at the equator (Gloesener et al., under review).

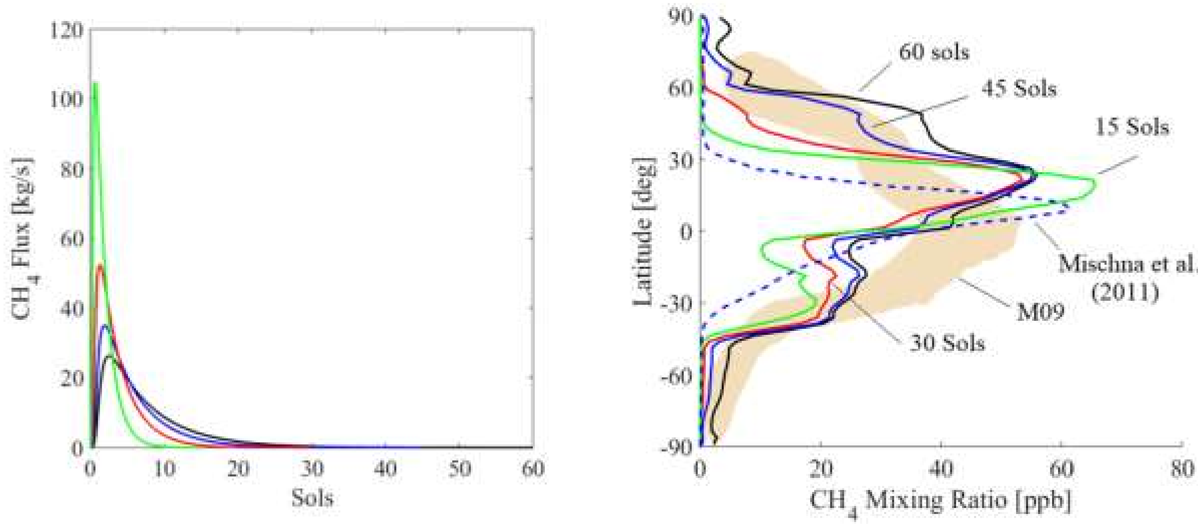

Figure 22: Time-variable CH_4 emission fluxes over the Syrtis Major area determined for various emission duration (green: 15 sols – red: 30 sols – blue: 45 sols – black: 60 sols; 1 sol = 1 Martian day) and considered as inputs in the general circulation model (left). Latitudinal methane concentrations simulated for the different emission scenario during ground-based observations of Mumma et al. (2009) (M09) and for a source location at (0 °N, 50 °E) (right). The instantaneous release scenario (Mischna et al., 2011) is shown for comparison (Temel et al., 2019).

The large methane plumes observed in Syrtis Major area in 2003 were simulated using a general circulation model, with time-variable CH_4 emission fluxes as inputs (Temel et al., 2019). The calculations of these fluxes are based on the destabilisation of shallow subsurface reservoirs and subsequent methane diffusion through the soil. The atmospheric transport and mixing of released methane have been tested for different emission duration and source locations. An emission scenario of 45 Martian days initiated from (50 °E, 10 °S) and during which a total amount of about 90,000 metric tons of methane is released provided the best agreement with the reported observations and with a better degree of accuracy than previously published studies (see Figure 22). Such a scenario corresponds to a subsurface source located at a depth of ~27 m.

The *in situ* detection of methane at Gale crater by the Mars Science Laboratory Curiosity rover has garnered significant attention because of the potential implications for habitability. Major unresolved questions regarding this detection include: (1) Where is the methane released? (2) How large is the release region? (3) For how long is methane released? To address the release location of methane, its spatial extent, and the magnitude and duration of the release, atmospheric circulation simulations were performed using tracers to study transport and mixing of methane at Gale crater (Pla-García et al., 2019). The aim of this work was to test whether methane releases inside or outside Gale crater are consistent with MSL observations. The results show that diffusive release of methane inside Gale crater is consistent with the low background levels observed by MSL – mean value of 0.41 parts per billion by volume (ppbv) – but cannot be responsible for CH_4 spikes (~7 ppbv) (see Figure 23). To explain these high and sporadic CH_4 levels, other gas transport processes such as advection should be investigated.

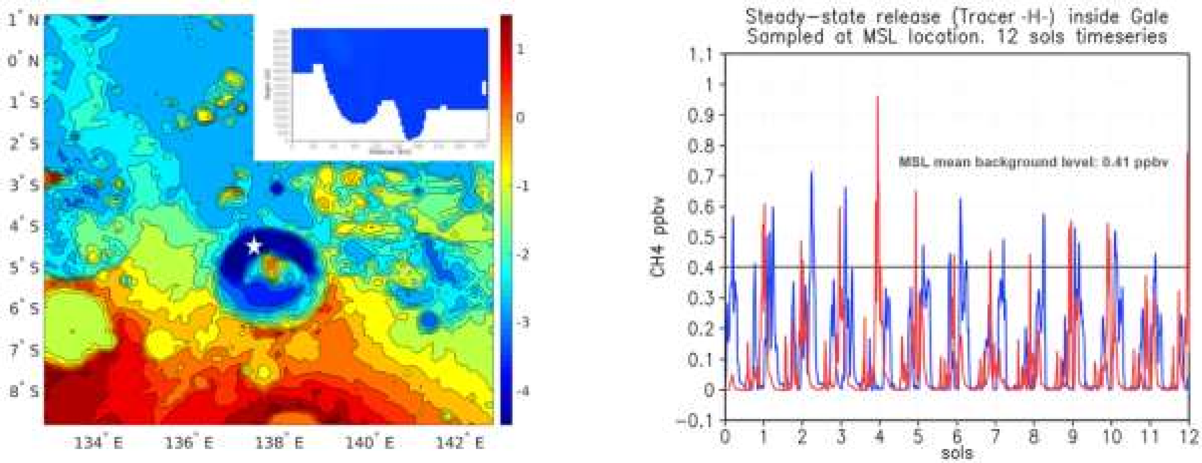

Figure 23: The topography of the Gale crater is shown as colour-coded elevation (km) from the Mars Orbiter Laser Altimeter (MOLA). White cross is the MSL Curiosity rover location. The upper figure shows the north-south cross-section view of the crater (altitude in m) (left). Simulated methane abundances over time (1 sol = 1 Martian day) at MSL location for a steady state release inside Gale crater (right). Blue and red correspond to a methane release during the northern summer and winter solstices respectively (Pla-García et al., 2019).

List of papers and reports mentioned above

Banfield, D. et al., including Karatekin, Ö. and Van Hove, B., 2020. The Atmosphere of Mars as Observed by InSight. Nature Geoscience, 13, 3, 190-98, DOI: 10.1038/s41561-020-0534-0.

Gloesener, E., 2019. Methane clathrate hydrate stability in the martian subsurface and outgassing scenarios, PhD thesis, Université catholique de Louvain, Louvain-la-Neuve.

Gloesener, E., Karatekin, Ö., Dehant, V., 2020, Stability and composition of CH_4-rich clathrate hydrate in the present martian subsurface, Icarus, 353, article id. 114099, DOI: 10.1016/j.icarus.2020.114099.

Korablev, O. et al., including Karatekin, Ö., 2019. No detection of methane on Mars from early ExoMars Trace Gas Orbiter observations, Nature, 568, 7753, 517-520.

Pla-García, J., Rafkin, S. C. R., Karatekin, Ö., Gloesener, E., 2019. Comparing MSL Curiosity rover TLS-SAM methane measurements with Mars Regional Atmospheric Modeling System (MRAMS) atmospheric transport experiments, J. Geophys. Res. Planets, DOI: 10.1029/2018JE005824.

Temel, O., Karatekin, Ö., Gloesener, E., Mischna, M. A., van Beeck, J., 2019. Atmospheric transport of subsurface, sporadic, time-varying methane releases on Mars, Icarus, 325, 39-54.

Temel, O. et al., including Karatekin, Ö. and Van Hoolst, T., Large eddy simulations of the Martian convective boundary layer: Towards developing a new planetary boundary layer scheme, Atmospheric Research (Under review).

Vandaele, A.-C. et al., including Karatekin, Ö., 2019. Martian dust storm impact on atmospheric H2O and D/H observed by ExoMars Trace Gas Orbiter, Nature, Volume 568, Issue 7753, 521-525.

Solar Physics

PROBA2: 10 Years of Observations

On November 2, 2019, the PROBA2 ESA micro-satellite celebrated 10 years of operations. PROBA2 is the second of the European Space Agency's (ESA) fleet of PROBA satellites. It hosts 17 new technological developments including two main solar instruments (SWAP and LYRA) designed for studying all events on the Sun that might have implications on the solar-terrestrial connection.

SWAP provides images of the solar corona filtered at a wavelength around 17.4 nm, a bandpass that corresponds to a temperature of roughly 1 million degrees. This allows us to see the hot solar atmosphere while filtering out the relatively cooler solar surface. SWAP observes an exceptionally wide field-of-view (FOV), allowing it to see more structures around the edge of the Sun. A good example is reported in a paper published by O'Hara et al. 'Exceptional Extended Field-of-view Observations by PROBA2/SWAP on 2017 April 1 and 3.' Observing the structured nature of the extended solar atmosphere is one of SWAP's most important tasks.

Figure 24 shows SWAP images from each year of the mission. The Sun undergoes an 11-year activity cycle, where solar activity, such as the magnitude and number of flares and coronal mass ejections, fluctuates. The images in Figure 24 reflect this variability through the changing number of coronal holes (the dark regions) and of active regions (the bright structures), which are often the source of the more dramatic solar activity.

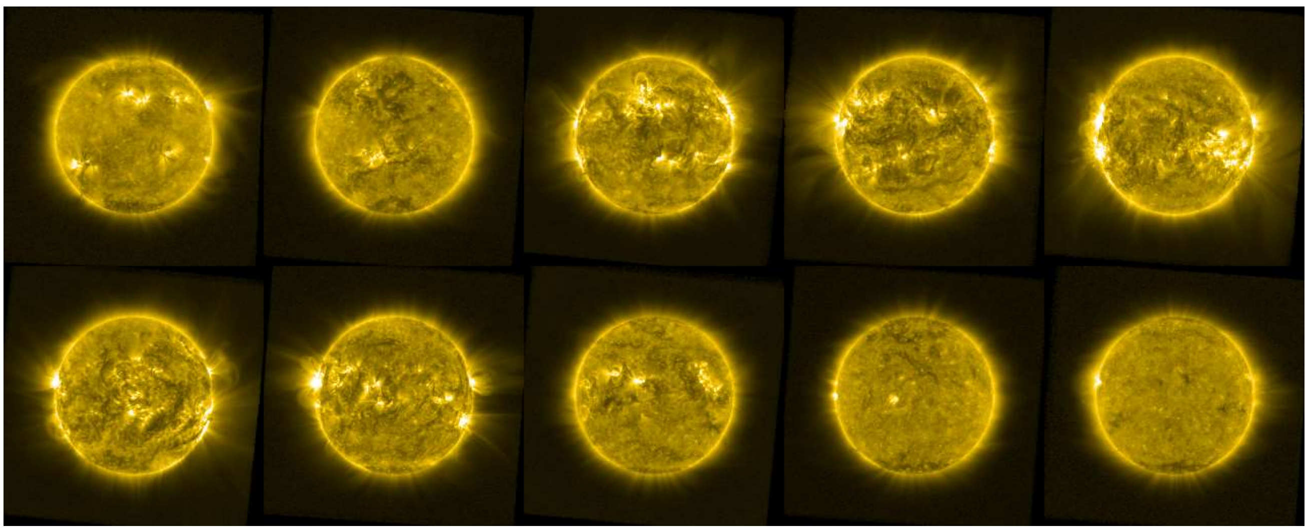

Figure 24: Ten years of SWAP observations, from 2010 to 2014 on the top row and from 2015 to 2019 on the bottom row, showing the changing face of the solar atmosphere.

LYRA is a solar UV-EUV radiometer, monitoring the Sun through four channels relevant to Solar Physics, Space Weather and Aeronomy, and hosts one of the first Lyman-Alpha irradiance monitors. Unlike the SWAP imager, LYRA observes the Sun as a star, that is, as a single data point. The extremely high-cadence (up to 100 measurements per second) of LYRA is required for the detailed study of transient solar events such as solar flares. In particular, LYRA was able to characterise the strongest flare of the current solar cycle, on the 6th of September 2017, and make rare observations in its Lyman-Alpha and Herzberg channels (Figure 25). LYRA detected small-amplitude oscillations called quasi-periodic pulsations in its rising phase. Such oscillations can only be made with high cadence observations, like those of LYRA. These observations are shedding new light on the flaring mechanism itself.

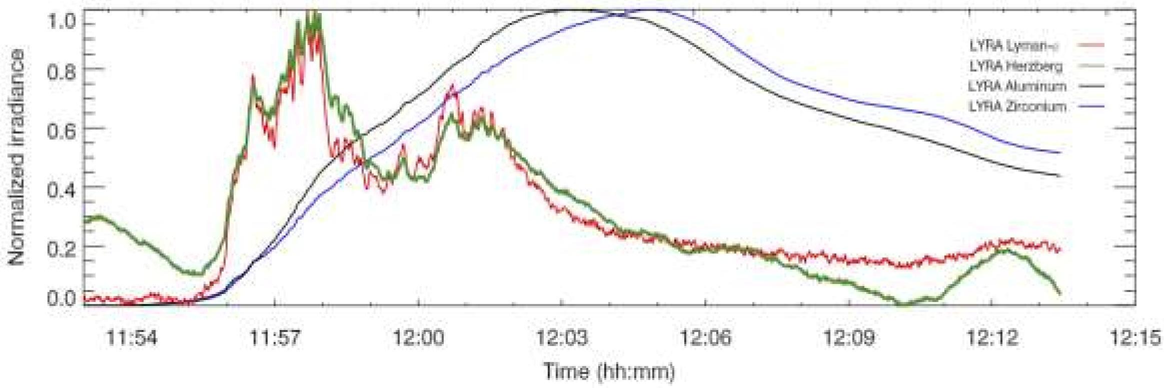

Figure 25: LYRA light curves of the 6 September 2017 X9.3 flare.

Space Weather. SWAP and LYRA were originally designed for studying the Sun and energetic events, such as solar flares, coronal holes and CMEs, that might have implications on the solar-terrestrial connection. Naturally, the observations have become an integral part of several solar-monitoring space weather forecasting centres, including the Regional Warning Center at the Royal Observatory of Belgium.

Figure 24 above highlighted long-term changes in the Sun. Active regions (the bright structures) and coronal holes (the dark regions) can be seen varying over time, both of which can have implications for space weather on Earth. SWAP and LYRA are also monitoring more transient, energetic and eruptive phenomena such as flares and CMEs, Figure 26 below shows SWAPs ability to track eruptions into the extended solar atmosphere. Two papers, published last year, highlight PROBA2's ability to track space weather events: 'Multipoint Study of Successive Coronal Mass Ejections Driving Moderate Disturbances at 1 AU' by Palmerio et al. and 'Large non-radial propagation of a coronal mass ejection on January 2011 24.' by Cécere et al.

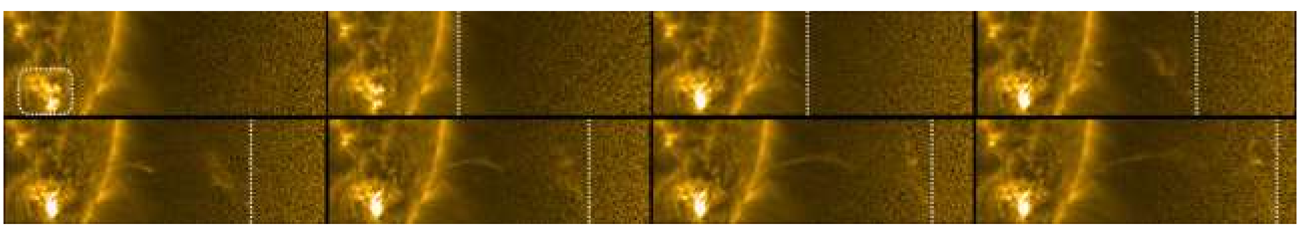

Figure 26: A flare (top left panel) and eruption observed by SWAP on April 1, 2017. The eruption was traced to over 1-Solar Radii, highlighted by the dashed line.

Vital Statistics from launch to the 10-year anniversary. PROBA2 was launched under the ESA Technology, Engineering and Quality Directorate (D/TEC). After launch, the ESA Science Directorate (D/SCI) supported the scientific exploitation of the PROBA2 science instruments and the Belgian PI-teams were supported by PRODEX. At the time of the 10-year anniversary, PROBA2 had:

- Been in orbit for 3653 days.
- Orbited the Earth ~53,000 times.
- Produced ~30,000 LYRA data files.
- Produced ~2,090,000 SWAP images.
- Passed our ground stations in Redu, Belgium and Svalbard, Norway (Arctic) 32,453 times.
- Helped produce over 100 peer-reviewed papers, the full list can be seen here.

- Run 8 guest investigator programs from 2010 to 2018, and welcomed 64 teams, 81 team members from 16 countries.

What next for the PROBA2 mission? As discussed above, the Sun undergoes an 11-year activity cycle, and next year will mark the 11th anniversary of the PROBA2 mission and therefore the monitoring of the Sun for a full solar cycle. This landmark period will allow PROBA2 to probe the Sun's evolution over the long term, comparing two solar minimum periods. The instruments themselves are proving robust in the harsh radiation environment. The detectors, which had never been used in space before, still produce a clean signal, with very low levels of noise. SWAP has seen less than 10% degradation in the number of active pixels, a remarkable number after 10 years of operations.

To celebrate 10 years of observations, the PROBA2 team are putting together a 10-year anniversary topical collection of articles. Those articles are a follow-up of the successful 2013 Topical Issue that highlighted the scientific and operational achievements after the first two years of the mission. The 10-year anniversary edition will report on the health and status of the mission and various studies ranging from the middle corona to solar flares.

With a 2-day PROBA2 Symposium, organised at the ground station in Redu, we celebrated the achievements after nine years of smooth operations by summarising the findings, reflecting on the experiences, brainstorming on the lessons-learned, and looking into the challenges for the future. PROBA2 is ready for the next 10 years!

Long-term evolution of the solar corona in PROBA2 data

We studied the evolution of the solar corona observed throughout solar cycle 24 (from 2010 to 2019), by using PROBA2/SWAP images, PROBA2/LYRA irradiance time series, and the latest version of the International Sunspot Number dataset.

The SWAP EUV imager is monitoring both the changes on the solar disk and the changes in the large-scale off-limb features, which can be seen to vary throughout the solar cycle. These large-scale structures trace out magnetic field lines, which are seen due to hot plasma trapped on them. In a standard SWAP image, the signal-to-noise in these regions is too small to distinguish individual structures. However, D. B. Seaton developed an image processing method, which employs image stacking and median filtering techniques to improve the signal-to-noise and enhance the signatures of structures in these regions. One can easily see the evolution of large-scale structures in solar corona throughout SC24 by examining different Carrington rotation (CR) stacked images throughout the PROBA2 mission.

A CR is a period of time chosen to represent one rotation of the Sun, allowing the comparison of features such as sunspot groups or active regions. A period of 27.275 days was chosen to represent a single rotation that greatly resembles the recurrence time of features near the equator.

Figure 27 compares three stacked images of the Sun taken at different times during the solar cycle. The left image of Figure 27 shows the Sun on 30-Jan-2010 at the beginning of PROBA2 observations, which corresponds to the period when solar activity was increasing. The central image shows the Sun on 15-Oct-2014, at one of the peaks in the solar cycle when the Sun exhibited most of its activity. Finally, the right panel of Figure 27 shows the Sun on 2-Jun-2019, taken during the minimum phase of the solar cycle.

The changes in the large-scale off-limb structure can clearly be seen between the different phases of the solar cycle, when the overlying structures become more complicated at solar maximum. They were visible from around March 2011 to around March 2016, meaning they were absent at the minimum phase of the solar cycle. A fan-like structure in the northern hemisphere was seen to persist for more than 11 CRs (February 2014 to March 2015) and was observed out to 1.6 solar radii. These complicated field structures are generated by the evolving magnetic field and can drive solar activity and space weather.

Figure 27: SWAP stacked images showing the solar corona at three moments of time between January 2010 and June 2019.

From the synoptic maps (see Figure 28), one can see the evolution of the active regions over a full CR as well as the evolution of coronal holes.

A SWAP synoptic map (or a latitude-time map) is constructed by extracting 3 degree-wide vertical stripes from individual stacked images. Each stripe is averaged into a single vertical line to remove artefacts. Those artefacts might be created by events such as cosmic rays and Solar Energetic Particles striking the detector, or from radiation from the Earth's radiation belts and the South Atlantic Anomaly. A Carrington Rotation's worth of images are then put together side by side to create an image such as that seen in Figure 28.

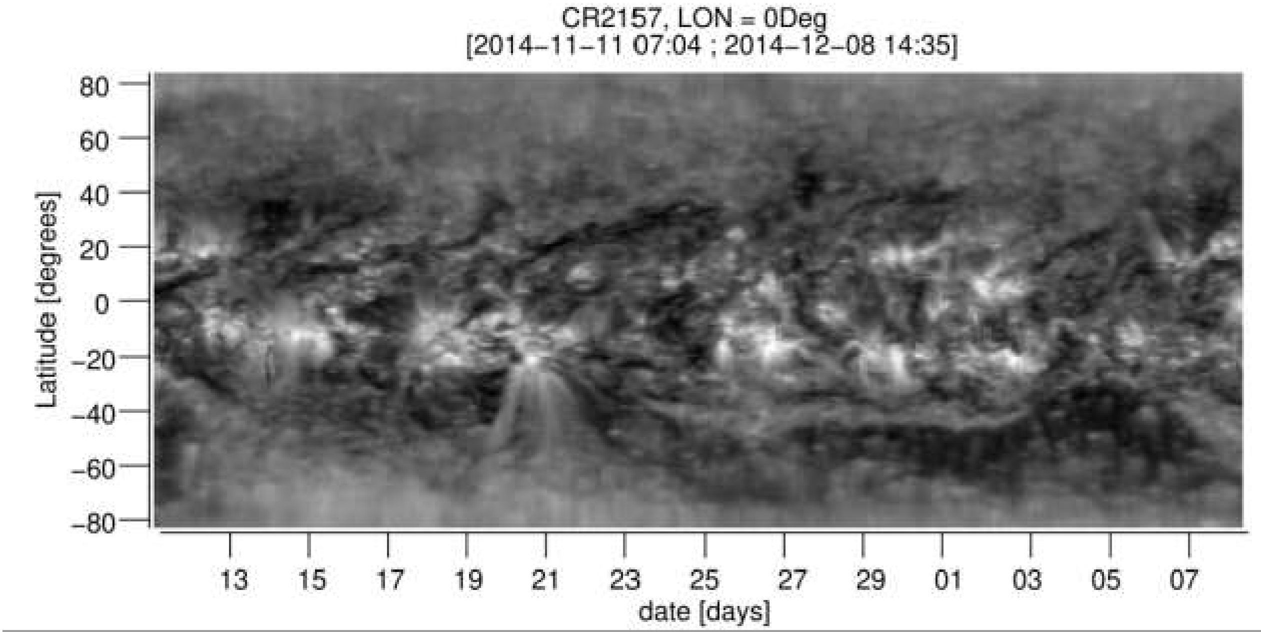

Figure 28: SWAP Synoptic Map of the Sun from 11-Nov-2014 to 8-Dec-2014. The image is constructed from the central meridian of the CR 2157 stacked images.

By inspecting all the synoptic maps, one can see that more active regions started to appear (starting in the northern hemisphere) in February 2011. They became less frequent from December 2016, reaching a very low number from September 2017, indicating the transition from solar minimum to maximum and back.

The coronal holes at the north pole were present from February 2010 to October 2011, with some short intermittent periods. No Coronal Holes were observed between November 2011 and June 2015, with some short intermittent periods also. They started to develop again in July 2015 and remained visible until June 2019 (end of our dataset). At the south pole, the Coronal Holes were present from February 2010 to May 2012, with some intermittent periods. No Coronal Holes were observed between June 2012 and May 2014. They started to develop again in June 2014 and remained visible until June 2019. The start of the development of the (polar) coronal holes were associated with peaks that we observed at both poles in SWAP data.

When observing the Sun for a long period of time, one can see that features on its surface, and in its outer atmosphere do not rotate at the same rate. This is because the Sun is not a solid body, but a big ball of magnetised plasma, whose rotation is variable with position and height in the solar atmosphere. We found that the average rotation speed, for bright regions between latitudes of -40 and +40 degrees was approximately 14 degrees/day. The average rotation rate of bright features at latitudes of +15, 0, and −15 degrees was around 15 degrees/day throughout the period studied.

We also observed that the three datasets used in this study (SWAP on-disk average brightness; LYRA signals and International Sunspot Number) had a high degree of correlation (around 0.9), all following the evolution.

This work was published in Solar Physics in the frame of PROBA2 special issue '10 Years of solar Observations'.

Astronomy and Astrophysics

First Results with the NASA Space Mission TESS

NASA's Transiting Exoplanet Survey Satellite or TESS is an all-sky survey mission whose aim is to discover exoplanets around nearby bright stars. TESS was launched on April 18, 2018, aboard a SpaceX Falcon-9 rocket.

The satellite searches for exoplanets by looking for small periodic dips in the star light curves. This requires that the exoplanets cross in front of stars as viewed by the spacecraft, thus blocking a fraction of the light from their host stars. This method is called the 'transit method' (Figure 29). The transit method allows a very precise measure of a planet's orbital period. The depth of the folded transit light curve can reveal the planet's size compared to the star's size, and the width can reveal the duration of the transit.

TESS surveys over 200,000 of the brightest dwarf stars near the Sun with four wide-field optical CCD cameras to search for transiting exoplanets. The stars observed are typically 30 to 100 times brighter than those observed by the Kepler mission, which enables follow-up observations with both ground-based and space-based telescopes. Photometry of these pre-selected targets is recorded every 2 minutes. TESS also obtains full-frame images of the entire field-of-view (24° × 96°) at a cadence of 30 minutes to allow for additional science. Based on the first four sectors of TESS data (released in 2019), about 370 TESS objects of interest have been identified. In its first year, TESS discovered 21 planets outside the solar system.

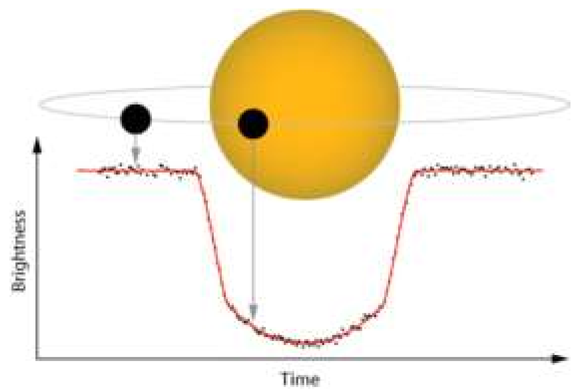

Figure 29: The transit method of detecting exoplanets involves monitoring the brightness of stars to identify periodic drops caused by planets crossing in front and blocking a fraction of their light as viewed by the spacecraft. Image credit: NASA.

Additional science goals with TESS also consist of in-depth studies of the stars which were monitored in exquisite detail during a period of 27 successive days. In particular, the astronomers can collect novel information about the internal structure and the properties of variable and/or pulsating stars. A pulsating star is a star whose internal layers undergo periodic oscillations due to an intrinsic (pulsation) mechanism. Two members of the Astronomy & Astrophysics Department are members of the TASC (TESS Asteroseismic Science Operations Center) Workgroup 4. The TASC groups all astronomers that study asteroseismolgy (study of the internal vibration of the stars) of A/F-type stars on and near the main sequence observed by TESS.

The pulsating stars of main-sequence A/F-type (hereafter named δ Scuti or γ Doradus stars) are in a state of transition of their envelopes where the outgoing energy experiences the change from radiative (for hotter envelopes) to convective transport (for cooler envelopes). Such stars may pulsate in two distinct regimes of frequencies caused by two mechanisms: that of the acoustic modes and that of the gravity modes. Some stars, called hybrid stars, pulsate in both regimes simultaneously. Knowledge of their fundamental stellar parameters along with that of their pulsation characteristics – which allow probing the stellar interiors – helps refine the physics of the stellar models.

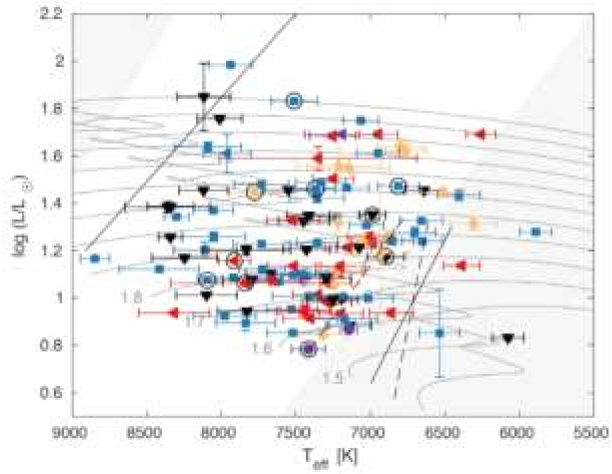

Figure 30: Location of the intermediate-mass A- and F-type stars observed by TESS in Sectors 1 and 2 in the HR diagram. Constant stars are shown as black triangles, δ Sct stars as blue squares, γ Dor stars as violet circles, hybrids or suspected hybrids as yellow diamonds, and high-amplitude δ Sct stars as red triangles. Stars marked with a black circle are known binary stars. The blue and red edges of the δ Sct instability domain are shown as black lines (following Pamyatnykh, 2000, and Dupret et al., 2005, respectively).

The first results on the A- and F-type δ Scuti and γ Doradus stars (concerning 141 objects) observed by TESS in the Sectors 1 and 2 were presented by Antoci et al. (2009). We used the 2-minute cadence TESS data of 117 stars to classify their behaviour in variability and place them in the Hertzsprung-Russell diagram using the Gaia Data Release 2 parallaxes (Figure 30). Included are also the first members of two classes of classical pulsators, namely γ Doradus and SX Phoenicis, the latter being a candidate blue straggler.

The TESS data for our sample of 117 intermediate-mass pulsating stars allow the first large-scale confrontation ever between theoretical models of pulsation driving in the classical instability strip and systematic high-quality observations. We showed that mixing processes in the outer envelope play an important role, and derived an empirical estimate of 74% for the amplitude suppression factor as a consequence of the TESS passband relative to the Kepler one. Our sample also contains many high-frequency pulsators, which were lacking in the Kepler data set. The additional data allows us to probe the variability of hot young δ Scuti stars as well as to identify promising targets for future in-depth asteroseismic modelling studies.

Reference: "The first view of δ Scuti and γ Doradus stars with the TESS mission", Antoci, Cunha, Bowman and 63 co-authors 2019, MNRAS 490, 4040 (https://publi2-as.oma.be/record/4536)

STARLAB

STARLAB – Evolved stars and their shells: Laboratories for stellar physics is a Belspo supported network in the context of BRAIN-be (Belgian Research Action through Interdisciplinary Networks) that operated between 15 December 2014 and 30 September 2019. The network consisted of three partners: the Institut d'Astronomie et d'Astrophysique of the ULB (PI: Prof. Dr. Alain Jorissen), the Instituut voor Sterrenkunde of the KU Leuven (Co-PI: Prof. Dr. Christoffel Waelkens) and the Operational Direction of Astronomy and Astrophysics of the Royal Observatory of Belgium (Co-PI: Dr. Martin Groenewegen). In each institute, several other senior and junior staff were involved; at the Royal Observatory of Belgium these were Dr. Griet Van de Steene, M.Sc. Dries Nicolaes and Dr. Joachim Wiegert.

The research in STARLAB focused on stars with mass between 0.8 to 8 times the solar mass (denoted low- and intermediate-mass stars) that dominate the stellar population in our Galaxy. During their ascent of the asymptotic giant branch (AGB) phase, low- and intermediate-mass stars are the source of a rich nucleosynthesis, forging mainly carbon and elements heavier than iron through the so-called s-process. Because mixing processes bring these elements to their surface, the envelope composition of AGB stars is altered, and some of these stars will turn into carbon stars. As stellar winds disperse the AGB envelope, molecules and dust grains form in a circumstellar envelope surrounding the star. As it expands, the shell eventually merges with the interstellar medium where it releases the products of the stellar nucleosynthesis, thus contributing to the chemical evolution of the galaxy.

Although the star global evolution is well known, major uncertainties still affect our understanding of key physical and chemical processes. For instance, major shortcomings remain in the description of convection and internal mixing, mass loss, dust formation and gas-phase reactions in thick circumstellar shells, and for binary systems, in the description of mass and angular momentum transfer between the stellar components.

The goal of this project was to boost our understanding of (some of) the physical and chemical processes at work in low- and intermediate-mass stars. The work was divided into three work packages:

- WP1: 'Diagnostics of nucleosynthesis and mixing in stars'. The results on this topic culminated in the PhD thesis by Shreeya Shetye, a join thesis between ULB and KU Leuven.
- WP2: 'Uncovering the link between the various classes of binaries involving evolved low- and intermediate-mass stars.' The results on this topic culminated in the PhD thesis 'Barium stars as tracers of binary evolution in the Gaia era' by Ana Escorza, a joint thesis between KU Leuven and ULB.
- WP 3: 'Circumstellar matter on different spatial scales: signatures of mass-loss processes and of binary interaction'. This research involved KU Leuven (Prof. Dr. Leen Decin) and the Royal Observatory of Belgium.

A major paper was published by Nicolaes et al. They analysed PACS (55 µm – 190 µm) and SPIRE (200 µm– 680 µm) high-resolution spectra for 27 M stars (23 oxygen-rich AGB stars including a few OH/IR stars, and 3 red supergiant stars), 3 S-type stars, and 10 carbon-rich stars. In fact, they analysed all AGB stars observed with ESA's Herschel satellite mission in broadband spectral mode. They presented a library containing the reduced spectra (see the example in Figure 31 on the left), the lines that are measured in the spectra with wavelengths, intensity, potential identification, and the continuum spectra, i.e. the full spectra with all identified lines removed (the right panel in Figure 31). Some simple analysis was presented, but the main aim was to release this rich dataset to the public.

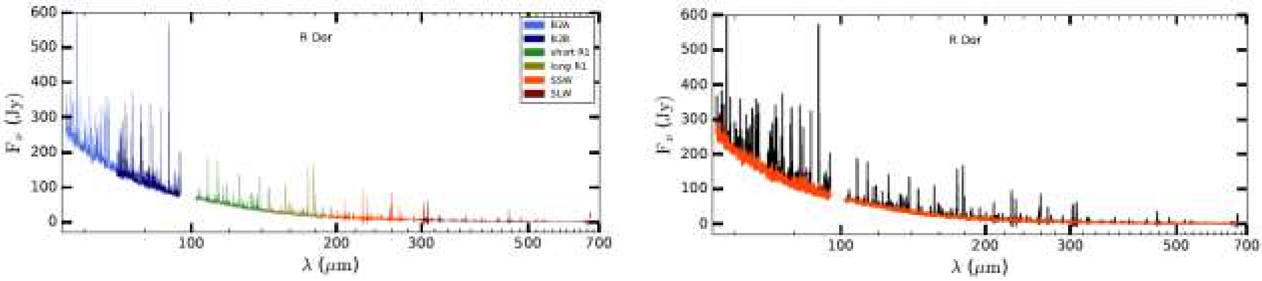

Figure 31: Left: Different parts of the PACS (55 µm – 190 µm) and SPIRE (200 µm– 680 µm) high-resolution spectra for for 27 M stars (23 oxygen-rich AGB stars including a few OH/IR stars, and 3 red supergiant stars), 3 S-type stars, and 10 carbon-rich stars merged together. Right: continuous spectra with all identified lines removed.

A second paper was published by Wiegert et al. It is a theoretical investigation, addressing the following questions:

1. Is it possible to identify features in spectral energy distributions that are caused by specific dust-cloud morphologies?
2. Are these signatures unique to specific morphologies?

We also investigated the possibility of the opposite case where different morphologies with different dust masses possibly give rise to the same spectral energy distribution. With this, we evaluated by how much dust shell masses may be misestimated when adopting an incorrect dust morphology. It was decided to use EP Aquarii as a benchmark star for this study, because this star likely belongs to a binary system, as revealed by the spiral structure characterising its circumstellar dust shell. The impact of the circumstellar geometry on the spectral energy distribution was evaluated. In particular, scientists evaluated whether dusty spirals (associated with binary systems) leave a specific signature in the spectral energy distribution that would permit to distinguish them from spherical circumstellar. The parameter space has been explored using the RADMC-3D code, by evaluating the impact on the mass loss rate on the geometry (spiral vs spherical with the same dust mass) and on the inclination of the spiral plane with respect to the plane of the sky.

The most important results are presented in Figure 32 revealing that the spectral energy distribution alone cannot be used to discriminate between different circumstellar geometries. It was concluded that the knowledge of the circumstellar geometry is necessary to obtain accurate circumstellar dust masses and consequently, accurate mass-loss rates.

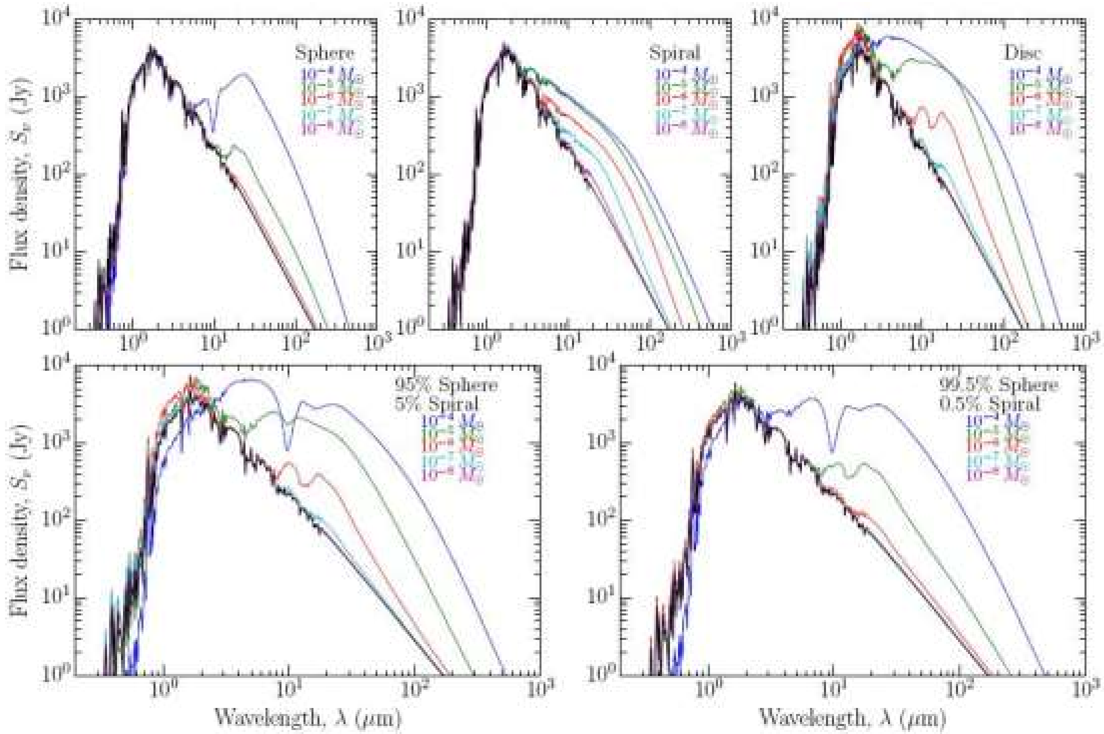

Figure 32: All face-on, 5 to 5000 au simulated SEDs, and the stellar SEC MARCS model (in black). The dust masses are 10-4 (blue), 10-5 (green), 10-6 (red), 10-7 (cyan), and 10-8 of the magnitude of the Sun (magenta). Top row shows SEDs from CSE with 100% sphere, spiral and disc respectively while the second row shows combined sphere-spiral model SEDs.

POEMS: Physics Of Extreme Massive Stars

EC Horizon 2020 Project

POEMS is a project top-ranked by the European Commission for receiving funding from the European Union (2019–2022; MC-RISE Horizon 2020). It aims at studying massive stars in extreme phases of their evolution. The knowledge achieved within this project will help understanding the fate of massive stars such as energetic supernova explosions and black hole formation.

In the frame of POEMS, scientists of five European countries, including Alex Lobel of the Royal Observatory of Belgium, established a multidisciplinary international network between researchers from Europe and from four countries in South America and Asia. This network will foster research collaboration on different aspects of the project, by supporting exchange visits of scientific staff and by educating young researchers and students in the field.

Science Goals

Massive stars are extreme engines, enriching their environments with chemically processed material throughout their entire lifetime, and triggering star and planet formation. Despite their importance for the cosmic evolution, their evolutionary path up to their deaths such as spectacular supernova explosions is not well known. Scientists lack precise knowledge of the physical mechanisms behind stellar winds and mass eruptions. The goal of POEMS is to elucidate these processes generating mass loss in massive stars during extreme phases of their evolution. It is developing cutting-edge numerical codes suitable to describe large-scale environments and the star and stellar wind chemical and dynamic evolution. Confronting predictions from the numerical models with observations will allow the collaboration project to derive the first extensive and comprehensive set of physical parameters.

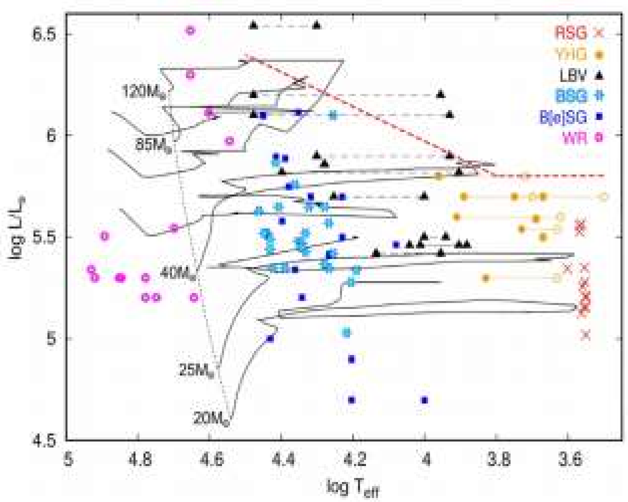

Figure 33: Location of various types of evolved massive stars in the H-R diagram (black drawn solid lines show evolutionary tracks). Yellow symbols mark Yellow Hypergiants (YHG). Credit: EC Horizon 2020 POEMS project.

The evolutionary path of massive stars consists in various extreme transition phases in which these stars shed huge amounts of material into their environments, typically via episodic, sometimes even eruptive events. These objects are luminous super- or hypergiants populating the upper part of the Hertzsprung-Russell (H-R) diagram, and ranging from spectral type O to F or later (see Figure 33). Sophisticated stellar (evolutionary) models critically depend on the input physics. Any uncertainty of the input parameters consequently results in large inaccuracies on the output of numerical simulations. The mass loss rate is one of the most crucial parameters for massive star evolution. Hence, understanding the mechanisms behind these ejection phases and exploring the mass lost during the eruptive events is essential for establishing reliable laws for the mass loss throughout the entire stellar evolution.

POEMS at the Royal Observatory of Belgium

Winds

Massive stars drive energetic winds. These can at first be smooth. At larger distances from the stellar surface, the wind material can form clumps of different sizes and density. The clumps cause variability in observed stellar spectra. The properties of the winds and the clumping can be determined by investigating spectroscopic observations from various epochs. In the POEMS work package shared between the Royal Observatory of Belgium (Alex Lobel), Univ. Valparaíso (M. Curé, Chile) and Univ. Pontifica Católica Valparaíso (A. Christen, Chile), high-resolution spectra of four massive O-type stars have been analysed and modelled in detail.

We developed numerical codes that can reproduce the wide variety of line shapes in these spectra observed with the Mercator Telescope at La Palma. Selected line profiles have been theoretically calculated using a new multi-Castor Abbott & Klein-like prescription, providing new and improved stellar and wind parameters for these hot massive stars. The study yielded mass-loss rates that are larger than the values published in previous studies. They represent considerable improvement in spectroscopic mass-loss rate calculations in present-day massive stars research. A publication is in preparation. This research collaboration is also part of a PhD dissertation at the Univ. Valparaíso. The PhD degree was awarded to A. Gormaz in November 2019.

Pulsations

Stellar pulsations are caused by expansions and contractions in the outer layers of the atmosphere. If a star pulsates radially, it swells and shrinks. However, most stars pulsate in non-radial modes, which leads to a deformation of the stellar surface. Neighbouring regions on the stellar surface move in opposite directions, while other regions do not move at all. Pulsations also cause variability in spectroscopic lines. To disentangle between variations due to pulsations and clumps in the winds, high-quality spectral monitoring over many pulsation cycles is crucial.

Many evolved massive stars are surrounded by dense material accumulating in rings or shells. This material has been ejected from the star during eruptive events. The ejected material is often dense and cool enough for efficient molecule and dust condensation. However, the physical mechanism causing mass ejections is currently unknown. An innovative way to approach this subject is to analyse whether mass eruptions can be triggered by stellar pulsations. This hypothesis is being tested in POEMS with extensive numerical simulations of the dynamics within the diluted atmospheres of evolved massive stars.

How yellow hypergiant stars repeatedly cool and heat up

Yellow Hypergiants (YHGs) are huge, luminous stars. They are fifteen to twenty times heavier than the Sun and shine 500,000 times brighter. The atmospheres of these stars can be so huge that, if they replaced our Sun, they would stretch beyond the orbit of Jupiter. A notorious YHG is Rho Cassiopeiae that showed a massive outburst event in 2000 clearly linked to strong atmospheric pulsations. The Egg Nebulae hosts a YHG surrounded by dust shells caused by strong eruption events in the past (see Figure 34).

Figure 34: The Egg Nebula: a Yellow Hypergiant surrounded by two ejected dust shells. Credit: ESO Very Large Telescope.

In 2019, Alex Lobel of the Royal Observatory of Belgium published research results of the analysis of long-term photometric monitoring of four YHGs in collaboration with Drs A. Van Genderen (Univ. Leiden, Netherlands), C. de Jager, and H. Nieuwenhuijzen (SRON, Netherlands), and amateur astronomers. An Astronomy and Astrophysics paper was published in Nov 2019 describing the results. Because their study uses a very long series of measurements, they could demonstrate in detail how these extreme stars get warmer over decades and cool down in a few years.

Figure 35: The Yellow Hypergiant HR 5171A observed towards the Gum 48d Nebula. Credit: NASA Spitzer Space Telescope.

The large mass-loss rates of YHGs can increase the circumstellar absorption causing redder and variable B−V colour indexes. This property of YHGs is unpredictable and explains why spectroscopic temperatures (reddening independent) are always higher than photometric ones, although the difference decreases with effective temperature. The study revealed that besides HR 8752, the other three YHGs show blue loop evolution in similar cycles over the last 70 years. The cycle begins with a cool star. In a few decades, the average atmospheric temperature increases to about 8000 degrees. At 8000 degrees, however, the atmosphere becomes unstable due to strongly amplified pulsations. At a certain moment, the entire atmosphere erupts. As a result, it cools down quickly and a self-accelerating process occurs in which electrons attach themselves to hydrogen ions and a lot of ionisation energy is released. This cools the atmosphere even further. The cooling from 8000 degrees to 4000 degrees takes only two years. Then the cycle starts again from the beginning, only with a slightly less massive star. Eventually the YHG is thought to transform into a hotter star ending its life in a supernova explosion.

The research results also show that YHG HR 5171A (see Figure 35) is only subject to one source of light variation, not by two as recent literature suggested.

Links:
http://stelweb.asu.cas.cz/~kraus/POEMS/
https://www.astro.oma.be/en/astronomers-show-how-giant-stars-repeatedly-cool-and-heat-up/
http://www.sci-news.com/astronomy/yellow-hypergiants-07692.html
https://www.knack.be/nieuws/wetenschap/supernova-vele-hete-sterren-eindigen-als-een-ontploffing/article-normal-1530827.htmlh
http://alobel.freeshell.org/rcas.html

The project RUSTICCA: revalorising the Ukkel Schmidt Telescope

The prehistory of RUSTICCA

The Royal Observatory has a long tradition of astrometry of Solar System objects, in particular asteroids (minor planets). It started in 1924 at the Triplet, which is a large-field refractor, but with rather poor optics. In 1933, the Double Astrograph was purchased, an astrograph with two tubes and much better optics (Figure 36). At that time, there was virtually no light pollution and with an exposure time of 1 hour, the limit was around magnitude 17. Even after one hour of exposure, between the stars the photographic plates were perfectly transparent. While stars appeared as little circles on the images, minor planets appeared as short dashes due to their motion.

With the Double Astrograph, numerous minor planets were discovered and observed. The most famous ones are the minor planet (2101) Adonis, one of the first discovered Earth-grazing asteroids, by Eugène Delporte in 1936, and comet Arend-Roland in 1956 by Sylvain Arend and Georges Roland, which became visible to the naked eye in 1957.


Figure 36: The Double Astrograph was active in the period 1933–1995, but mostly in 1933–1960. With this instrument Comet Arend-Roland was discovered in 1956.

After WWII, the Ukkel night sky started to deteriorate, and the limit magnitude of observation at the Double Astrograph went down to 14–15. Moreover, the accuracy of the astrometry also declined. Whereas it could be better than 1 arcsecond in the early days, errors of more than 2 arcseconds were common in the 1980s. The increased sky background on the plates caused an increased noise, and measuring accurate positions – at that time still by eye – became more difficult.

The last discovery at the Double Astrograph occurred in 1965. It was no longer possible to discover new asteroids from Ukkel, due to the increased light pollution and the fact that more and more of the brighter minor planets were discovered elsewhere. The Ukkel observers continued the tradition by moving to other telescopes in dark areas, such as the ESO telescopes in La Silla in Chile, or the Observatoire de Haute Provence in France. Although astronomers were no longer motivated to observe from Ukkel, there were still a few sporadic observations at the Double Astrograph in the 1980s and early 1990s. However, it was clear that continuing the old photographic astrometric observations had no more sense.

RUSTICCA started in 1993

In 1993, the Royal Observatory of Belgium obtained a LOTTO-grant to purchase a CCD camera. A CCD camera offers a lot of advantages compared to the photographic technique. While a grain on a photographic plate is either black or white, a CCD pixel can have up to 65,535 grey values. Moreover, removing the sky background from a digital image is a simple operation on a computer. Hence, an object in the sky no longer had to stand out from the sky background, but only from the noise caused by this background. Furthermore, the signal-to-noise ratio can easily be increased by summing individual exposures. Thus, much fainter objects can be

Figure 37: The UkkelUccle Schmidt Telescope was the instrument most fit to hold the CCD camera purchased in 1995. It was active in the RUSTICCA project 1995–2016.

observed with the CCD technology. Photometry is also possible, since a CCD camera has a linear response to the amount of light.

The CCD camera was not installed on the Double Astrograph. Instead, it was mounted on the Ukkel Schmidt Telescope (Figures 37 and 38), which was at that time no longer in use. This telescope has a rather short focal length of 2.05 m when using the prime focus, and a main mirror of 1.2 m diaphragmed to 0.85 cm.

Figure 38: The CCD camera is mounted at the prime focus of the UkkelUccle Schmidt Telescope, i.e. inside the tube. To fix the camera the old plate holder was used, but had to be moved up by about 30 centimetres.

The Schmidt design allows a large distortion-free field of view. This has several advantages. Firstly, this design produces sharper images than an astrograph, concentrating the light on a smaller surface and hence increasing the signal-to-noise ratio. Secondly, a Schmidt telescope has a mirror as main optical device, and has virtually no chromatic aberration. The Double Astrograph, on the other hand, was designed to produce "sharp" images only in blue light, while a CCD camera is sensitive in the red part of the spectrum. Thirdly, the larger aperture of the Ukkel Schmidt Telescope compared to the Double Astrograph increases the speed by a factor of ~4.5 in exposure time. Finally, the Ukkel Schmidt Telescope would be easier to automate than the Double Astrograph for remote control.

After purchase, installation and initial tests of the camera, a field observed at the Double Astrograph some time earlier was observed for comparison. It showed that the limit magnitude was pushed back from 14 to about 21, a gain of a factor of more than 200. In operational mode, a more realistic magnitude limit under good weather conditions is between 20 and 20.5 (Figure 39). The accuracy improved a lot, and, for bright enough objects, the measurements could give the precision of 0.1 arcseconds, competitive with the best differential astrometry in the 1990s.

The telescope became operational by the end of 1996. At this time, the completeness of the known minor planet population was up to magnitude 16, leaving a myriad of minor planets still to be discovered and in the range of the new equipment.

The project was called "RUSTICCA", standing for "Revalorising the Ukkel Schmidt Telescope by Installing a Ccd CAmera". Its logo, shown on the top of the first page, is formed by all the letters of the word RUSTICCA and shows a schematic representation of the Ukkel Schmidt Telescope. At the start, the core of the RUSTICCA team of observers consisted of two people, Eric Elst and Thierry Pauwels. In 2004, a new staff member, Peter De Cat, joined the team.

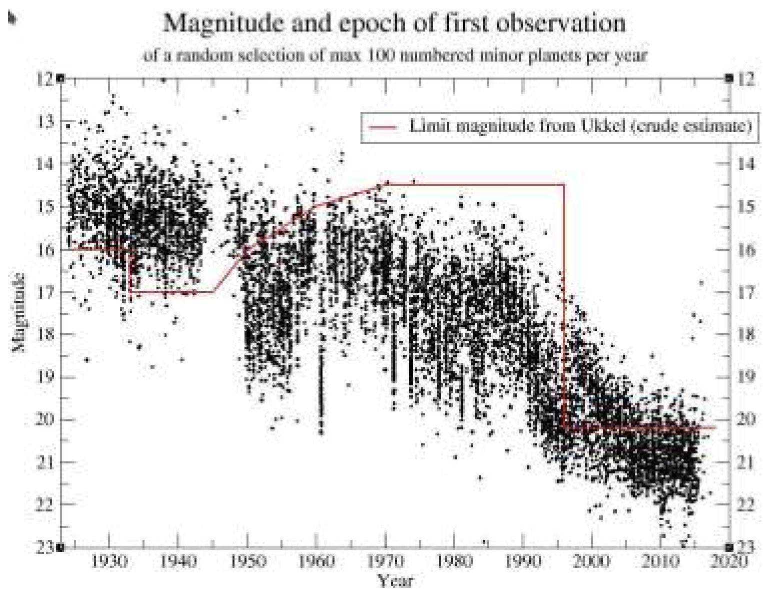

Figure 39: This plot shows for a selection of numbered asteroids the magnitude at the moment of their earliest observation. For each year, the sample was restricted to 100 randomly selected asteroids. This means that each dot in 1930-1940 represents only 1 or 2 asteroids, while in the period 2000-2010 each dot stands for 100 or more objects. The red line is a very crude estimate of the limit magnitude with the Ukkel equipment, first with the Triplet, then the Double Astrograph and finally the RUSTICCA project. One can see that in the 1970, and even in the 1960 detecting new objects became very unlikely. With the RUSTICCA equipment, a myriad of undiscovered objects became observable.

RUSTICCA at cruise speed

Routine observations started in late 1996, and unidentified asteroids were immediately detected. Officially, discovering an asteroid is a long process. Actually, automatically assigning the discovery to the first observation would encourage observers to scrutinise as many different fields as possible in the sky to maximise their discovery number. They should better concentrate on the follow-up of their discoveries. Otherwise, it would not be possible to compute orbits, and one would be left with a lot of 'discovered' asteroids, which would be lost again. Therefore, follow-up observations are required to secure a first crude orbit and to allow recovery after the asteroid has passed conjunction with the Sun and has been unobservable for many months. The asteroid is officially labelled only when a very accurate orbit is determined (usually after at least 4 years of observations, but sometimes it may take 20 years or more). It gets a permanent number, and the discovery is officially announced. Only then is it decided which observer gets the credit for the discovery. He/she may not have been the one who observed it first, as the latter could have given insufficient follow-up observations to secure a first orbit.

In the first years of the project, there were so many unknown objects that it was common to have 10 unidentified asteroids on a single CCD frame, although the field of view is only 45′ × 30′ (compared to the 8° × 8° of the photographic plates at the Double Astrograph). Since each asteroid has its own motion in the sky, all these asteroids fitting in a single frame on the first night, one needed several frames in the next nights for the follow-up observations. In these follow-up frames new asteroids coming from other directions would appear, which also had to be followed up, requiring an ever-increasing number of frames to follow them all. It was a real challenge to get all the necessary follow-up observations before they would fade due to their orbit

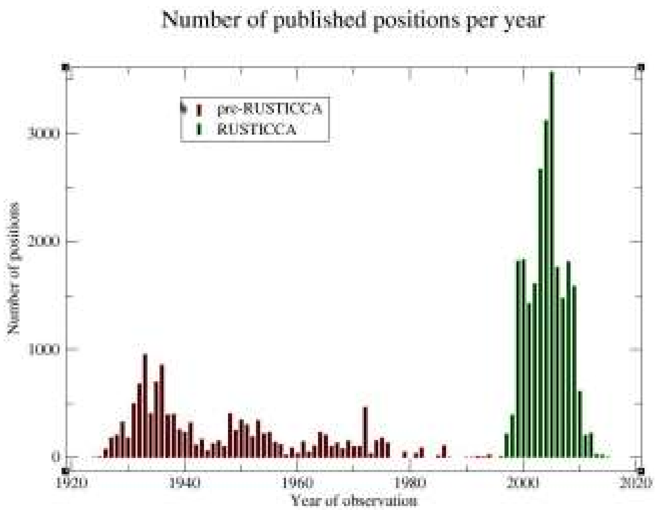

Figure 40: The number of published positions per year from the UkkelUccle site. The CCD technique is clearly a lot more efficient than the photographic technique.

bringing them further away from the Earth. The Belgian weather and the fact that observations of the faintest object about one week around full moon are unusable even add to the challenge.

The most prolific period was 1999–2005 (Figure 40). Before 1999, we still had to learn how to observe efficiently and how to process the observations. We had to write the reduction pipeline software to derive the accurate positions from the raw CCD images (Figure 41). Besides, the computer speed and the hard disk capacity were still problematic in the starting phase. Using 3 to 5 computers in parallel in the late 1990s, it took almost 18 hours to process one night of observations, while, later, a single desktop PC would process the observations about twice as fast as the images arrived during the night.

Figure 41: Stars and asteroids both look as dots on the images. To discriminate between stars and asteroids, the motion of the object has to come out. By taking a series of pictures, superimpose them, and then colour code them, moving objects immediately stand out and are easily detected.

Observations are not evenly spread over the year, as can be seen in Figure 42. One expects very few observations during the holiday period of July and August, but the decline starts already in mid-April. The reasons are the nights being short in May and June, and the minor planets being very low in the sky and difficult to observe. Even more surprising may be the fact that September, October and December are in general more productive than January to March. The reason is that new asteroids are preferably discovered in the second half of the night, before their opposition, when they are still getting brighter, so that they can be followed for a longer time.

Objects discovered in the first half of the night rapidly get too faint to be still observable, and are in general more difficult to follow. In September, asteroids are high in the sky in the second half of the night, and low in the sky in the first half of the night. Combined with nights that are getting longer and longer, this creates the ideal conditions to search for new asteroids. In February and March, the reverse happens. Asteroids are high in the sky in the first half of the night and low in the sky in the second half of the night. This means that they are either difficult to detect, or difficult to follow up. Even more striking is the very pronounced dip in November. We do not have a real explanation for that, other than that the weather conditions might be systematically worse in November.

One of the major achievements of the project was probably the discovery in 2005 of (314,082) Dryope (the discovery was announced only in 2012). This asteroid turned out to be a PHA, a so-called potentially hazardous asteroid, which could pose a threat to the Earth, since any impact hazard cannot be ruled out. This discovery was a real thriller and could only be achieved thanks to the cooperation of all the RUSTICCA team observers.

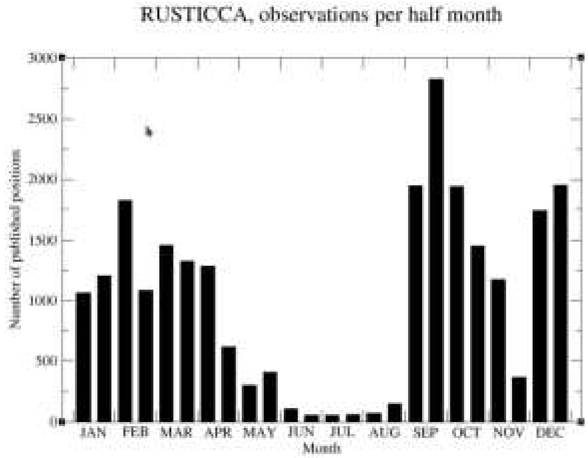

Figure 42: Published positions are not evenly distributed during the year. See the main text for a discussion.

Although the initial intention of RUSTICCA was to do astrometry of minor planets, other observations have also been performed. In the late 1990s, under the impulse of Henri Boffin, some cataclysmic variables were observed photometrically. In 1997, under the impulse and with the participation of Piërre Vingerhoets, we started to observe the so-called PHEMUs, mutual phenomena of the Galilean satellites of Jupiter (one satellite occulting or eclipsing another satellite). Detailed photometry of such events gives more accurate information on the positions of the satellites than traditional astrometry can provide. Such events occur in seasons every ~5.5 years, and we observed events in the seasons of 1997, 2003, 2009 and 2015. However, these observations were not easy, since neither the equipment nor the reduction pipeline were optimised for such photometry.

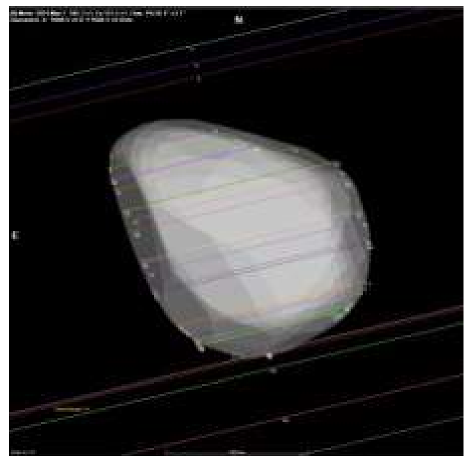

Figure 43: An example of the result of a multi-site campaign observing the occultation of a star by an asteroid. By plotting the precise instants of disappearance and reappearance of the star together with the radial position of the observer compared to the motion of the asteroid, the complete profile of the asteroid can be reconstructed. Also negative observations, i.e. without occultations, are important, since they put an upper limit on the size of the asteroid.

PLANOCCULT-observations, occultations of stars by minor planets, were a bit more successful. These were also in cooperation with Piërre Vingerhoets. These observations give very accurate position information for both the star and the minor planet. Moreover, if enough observers can give precise timings of the star disappearance and reappearance, an accurate profile of the minor planet can be deduced, giving its size and shape (Figure 43). Due to the rather large uncertainty of a minor planet position compared to its size, there is only a small probability for an observer to be in the occultation path. Yet, out of 82 attempted events in 2003–2016, we could derive accurate disappearance and reappearance timings for 8 events, the last one being in 2016. These observations could still be useful, but their number does not justify keeping the telescope operational, considering the cost of staff to keep everything in good shape.

The decline of RUSTICCA

RUSTICCA was a low-cost upgrade of a telescope, giving a new life to an otherwise no longer used instrument. Thanks to this upgrade, productivity increased compared to the 1930–1960 period. However, due to the weather and light pollution in Brussels, the RUSTICCA project could never achieve an output comparable to the new sites in very dark locations and equipped with cutting-edge technology telescopes. In the beginning, the Ukkel site was still ranked 17th worldwide for the number of discovered asteroids. But rapidly, other sites became orders of magnitude more efficient, and Ukkel dropped below the threshold to be listed as one of the

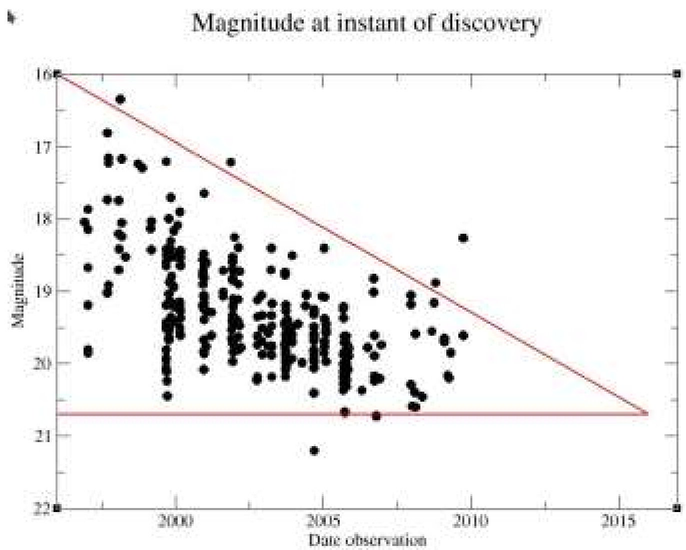

Figure 44: The magnitude of the new RUSTICCA detections at the epoch of their first observation. The lower horizontal red line corresponds to the limit of the capabilities of the RUSTICCA equipment, the upper diagonal red line represents the limit above which detection of new objects is rather unlikely. Both lines meet around 2016.

50 most prolific sites. Yet, Ukkel still was holding a world record for some time. With discoveries of asteroids starting in 1924, and continuing into the 2000s, Ukkel had almost 80 years of discoveries from the same site, being the longest in the world. However, when Heidelberg-Königstuhl, which had been discovering asteroids from 1891 to 1962, resumed the observations of minor planets in 2003, Ukkel lost that record, too.

After 2005, the productivity started to decrease. We estimate that the number of observable minor planets with the RUSTICCA equipment amount roughly to 300,000. At the start of the project, only some 5,000 were already numbered, and maybe another 15,000 were already observed, leaving 280,000 asteroids still to be discovered. As the present number of numbered asteroids already exceeds 500,000, it means there is hardly any left to be discovered. Also, the accuracy of the observations is increasing worldwide. In particular, the satellite Gaia will set new norms, with its positional accuracy being better than 0.001 arcseconds.

An extrapolation performed around 2008 predicted the last discovery of RUSTICCA to be expected around 2014 (Figure 44). However, with less valuable results, observers became less motivated, which causes an earlier decline of the observation frequency. In 2012, an unidentified asteroid was found on our images for the last time. Still, this was an important observation. Almost 2 years before the launch of Gaia, we found a new asteroid in conditions similar to the conditions in which Gaia would find new asteroids. This was an ideal opportunity to test the follow-up procedure for Gaia alerts, and to do a general rehearsal for the team of ground-based observers that was being set in place to follow up Gaia discoveries.

The coup de grâce for RUSTICCA came in 2017, when there was a complete refurbishing of the dome, putting the telescope out of use for a full year. Observers lost the routine, the equipment did not get the maintenance, and after the works were finished, only one last attempt to observe was made in June 2019, but it failed because of technical problems.

Still, the whole RUSTICCA project got a very important spin-off. While observers were getting expertise on astrometry of asteroids, they could use this expertise in the framework of the Gaia DPAC (Data Processing and Analysis Consortium), in particular on the work on ‘Astrometric reduction of Solar System Objects’.

Outreach and communication

Astronomy Day on September 21, 2019

On the occasion of the 100th anniversary of the International Astronomical Union (IAU), the Royal Observatory of Belgium has opened its doors on September 21 for an Astronomy Day, an event organised by the Planetarium of Brussels, in collaboration with the FFAAB (Fédération Francophone des Astronomes Amateurs de Belgique) and the VVS (Vereniging Voor Sterrenkunde).

The event lasted from 13:00 to midnight. Statistics from the Public Observatory's machines show that more than 2400 visitors attended the event.

Activities of the Royal Observatory of Belgium included visits to the telescopes and the museum and scientific experiments. The amateur astronomers presented their clubs and activities to the public and organised observation sessions during the day (for the Sun) and at night (for the stars). Lectures given by scientists as well as amateur astronomers were given throughout the day. The Planetarium also organised activities such as the animation tent for children, the mobile planetarium and a VR (Virtual Reality) application for observing the sky at night.

Exhibition at the Royal Palace in 2019

As each year, the Royal Palace in Brussels opened its doors to the public in summer 2019 (from July 23 to August 25). The theme of this exhibition was "The Moon: between dream and reality". In collaboration with the SPF Chancellery of the Prime Minister, the Royal Observatory of Belgium and the nine other federal scientific institutes, the National Geographic Institute and the Federal Science Policy Office offered an original vision of art and science revolving closely or remotely around the Moon, the Earth's only natural satellite that captivated and still captivates humanity's imagination.

A photograph of the Moon taken by Paul Van Cauteren and Dr. Patricia Lampens, collaborators at the Observatory, had the honour to be used as a visual for the exhibition. The public could also view three of their photographs of the Moon on-site, one of which was taken during the total lunar eclipse on January 21, 2019.

The Observatory also exhibited a superconducting gravimeter, an instrument designed to measure gravity variations. These latter are influenced by, among other things, tidal forces, which are themselves generated by the Sun and the Moon. The Observatory has world-renowned expertise on Earth tides and gravimetry. The displayed gravimeter, manufactured by GWR, is one of the first two superconducting gravimeters in Europe and operated from 1982 to 2000.

Asgard IX – Meet and Greet

In April, the Planetarium team organised the ninth edition of the Asgard Contest geared toward primary and high school classes. Like every year, the finalists of the contest spent a day at the Space Pole site, during which the balloon launch of their experiments is the climax. This year, the Planetarium organised two additional activities for Asgard: sessions in which scientists explain science topics in their fields to teenagers and a "Meet and Greet" afternoon in which scientists from different fields present themselves and their research.

Information to the public

In 2019, the Communication and Information service replied to questions from authorities, public and media sent by email (766), by telephone (184), by letter or fax (22), and in the social networks of the Observatory (Facebook and Twitter, 14), in totality 1195 replies. Other questions come from authorities (courts, police, army, Belgocontrol, Meteowing, Royal Meteorological Institute…). As usual, most questions were about sunset and sunrise, astronomical phenomena, calendar and time, satellite and space station flybys and the history of the Observatory. This is also the first year that the service received questions concerning the Starlink satellite constellations, of which the first launch dated from end 2019.

The Communication and Information service was regularly in contact with the media (TV, radio and written press) and press agencies (Belga, Thomsons Reuters…). The service gave information to them on some occasions (Day of the Astronomy). Other members of the Royal Observatory of Belgium appeared in news items on other topics (Solar Orbiter, 10th anniversary of PROBA2, LaRa and ExoMars 2020…).

Public tours of the Observatory are no more organized. Group visits are still organised on special occasions. The individual visitors were mainly journalists, other media-related people, photographs, historians and students. The Communication and Information service presented the ‘History and activities of the Royal Observatory of Belgium’ as an introductory talk to some of the visiting groups and guided these in the institute.

Website, news, press releases and social media

In 2019, the main website of the Observatory (https://www.astro.oma.be) got 328,369 visits. The content of the information web pages was regularly updated. In 2018, 15 topics were published in the “News” section of the ROB website (always in 3 languages: NL/FR/EN), including 8 press releases.

On 31 December 2019, the Facebook page of the Observatory had 817 likes (with 231 new likes since end 2018), its Twitter account 606 followers (165 new followers) and its YouTube account 23 videos. The themes of the published posts and videos are related to all services of the institutes, comprising shared posts from the Planetarium Facebook page, from the Seismologie.be Facebook page and Twitter account, from the EUI Twitter account and also from the Royal Belgian Institute of Spatial Aeronomy and the Royal Meteorological Institute. The most popular Facebook post of this year is a post about the recalibration of the sunspot number and about the solar influence on climate. On Twitter, the video of Mercury’s transit was the most popular of the year.

The Planetarium

Daily Activities

In 2019, the Planetarium welcomed 46,226 paying visitors. A total of 1657 sessions were given, divided between 222 courses for school groups (including 40 workshops) and 1395 film screenings (individual visits, families, tourists). The Planetarium is open nearly every day of the year, including weekends and public holidays, 361 opening days in 2019. In addition to lectures and films, 'live' sessions (Rendez-vous@Planetarium) using the historical Zeiss projector are regularly offered throughout the year: they allow the public to discover the starry sky in an interactive and lively way and are a great success.

In 2019, the Facebook page of the Planetarium saw a clear increase in visibility with 2018 followers (of which 1947 likes) recorded at the end of the year, which is an increase of +683 (respectively +646) compared to the previous year.

Special Events

In addition to its daily activities, the Planetarium fully plays its role as an educational, cultural and science-promoting actor, organising or promoting a whole series of special activities. It is estimated that 4400 people participated in 2019 in one or another of the activities organised by the Planetarium, including 3150 that took place extra muros.

Highlight: International Astronomical Union Centenary Celebrations

The year 2019 was highlighted by the celebration of the 100th anniversary of the International Astronomical Union (IAU). On this occasion, an exceptional meeting (a bridging event) between visually impaired people and astronomers from the IAU (Wanda Diaz-Merced) and Belgium was organised at the Planetarium on February 18.

It is also to pursue this desire to open the Planetarium to new audiences that a new planetarium show, The Sky in Your Hands, adapted for visually impaired people, was added to the Planetarium's offer for groups. This film created by 'Astronomers Without Borders' required the 3D printing of dozens of tactile spheres representing the constellations evoked in the film. This production could be carried out in-house thanks to the support of different teams in the Observatory.

The preview of 'De Hemel binnen handbereik / Le Ciel dans vos mains' took place on April 10 in the presence of the President of the IAU at the opening of the 100th anniversary flagship event co-organised by the IAU and the Royal Observatory of Belgium and its Planetarium at the Palais des Académies from April 11 to April 13.

This international conference welcomed both professional scientists (including Nobel Prize winners) and amateur astronomers.


On April 12, Japanese astronauts Chiaki Mukai and American astronaut John Grunsfeld on the fringe of the flagship event gave a conference opened to the public. This lecture launched the day dedicated to amateur astronomers on April 13 (Amateur Day, Palais des Académies).




A big Astronomy Day organized on September 21 by the Observatory, the Planetarium, the Fédération Francophone des Astronomes Amateurs de Belgique and the VVS took place on the Observatory site, with many activities and presentations during the day, and observations in the evening. It was greatly appreciated by the many people who came for the occasion.

The closing of the IAU100 celebrations in Belgium took place on December 5 with the presentation of the documentary Tintin Moonwalker in collaboration with the Moulinsart Foundation. This film parallels Hergé's visions and the first exploits of the conquest of space.

Yet more activities that took place in 2019

- Performances of the theatre creation 'Het puntje van de tong' on January 11, February 11, March 11, April 11, May 11 and June 11.
- The Smurf exhibition developed together with several scientists from the Observatory and the Peyo Foundation was inaugurated on January 26 in the exhibition hall of the Planetarium.
- The Museum Night Fever was hosted at the Planetarium on February 23, including a demonstration (in the dark) of a lightsaber fight.
- The final selection for the CANSAT competition (school projects to launch scientific experiments with rockets) took place on March 20.
- The Planetarium participated in the 'Printemps des Sciences' on March 29 with special sessions for school groups.
- The Planetarium hosts the groups participating in the ASGARD project on April 25.
- A lecture (Alex Karl, BIRA-IASB) was given on the occasion of Asteroid Day on June 30.
- Two lectures (Sarah Baatout, SCK-CEN) for the general public on the occasion of the 50th anniversary of the Apollo flight were given on July 8 and 12.
- Electronic music concerts were held on May 24 and 25.
- The Planetarium organized and hosted the FNRS/ROB Astronomy Day on June 14.
- A new edition of the 'Poetry under the Stars' event was held on September 14.
- The Planetarium took part in the 'Nocturnes des Musées bruxellois' on October 3.
- It organised the 'Night of Darkness' on October 12 at the Rouge-Cloître
- The Planetarium's new inflatable planetarium was installed on the forecourt of the Atomium on October 30 for a special day of entertainment.
- The Planetarium took part in the 'Dag van de Wetenschap' on November 24.
- The event planned for the launch of the CHEOPS mission on December 13 was hosted in the dome of the Planetarium.

Annex 1: Publications

Publications with peer review

[1] Antoci, V. ; Cunha, M. S. ; Bowman, D. M. ; and 63, more ; (incl. De Cat, P. ; and Lampens, P.)
The first view of Delta Scuti and Gamma Doradus stars with the TESS mission
Monthly Notices of the Royal Astronomical Society, 490, pp. 4040-4059, 2019.
https://doi.org/10.1093/mnras/stz2787

[2] Asvestari, E.; ; Heinemann, S. G.; ; Temmer, M.; ; Pomoell, J.; ; Kilpua, E.; ; Magdalenic, J.; ; Poedts, S.
Reconstructing Coronal Hole Areas With EUHFORIA and Adapted WSA Model: Optimizing the Model Parameters
Journal of Geophysical Research: Space Physics, 124 issue 11, pp 8280-8297, 2019.
http://dx.doi.org/%2010.1029/2019JA027173

[3] Baland, R.-M. ; Coyette, A. ; Van Hoolst, T.
Coupling between the spin precession and polar motion of a synchronously rotating satellite. Application to Titan
Celestial Mechanics and Dynamical Astronomy, Vol 131, pp. eid 11, 2019.
http://dx.doi.org/10.1007/s10569-019-9888-2

[4] Barnes, D. ; Davies, J. ; Harrison, R. ; Byrne, J. ; Perry, C. ; Bothmer, V. ; Eastwood, J. ; Gallagher, P. ; Kilpua, E. ; Moestl, C. ; Rodriguez, L. ; Rouillard, A. ; Odstrcil, D.
CMEs in the Heliosphere: II. A Statistical Analysis of the Kinematic Properties Derived from Single-Spacecraft Geometrical Modelling Techniques Applied to CMEs Detected in the Heliosphere from 2007 to 2017 by STEREO/HI-1
Solar Physics, 294, Article number: 57, 2019. http://dx.doi.org/10.1007/s11207-019-1444-4

[5] Bergeot, Nicolas ; Witasse, Olivier ; Le Maistre, Sebastien ; Blelly, Pierre-Louis ; Kofman, Wlodek ; Peter, Kerstin ; Dehant, Veronique ; Chevalier, Jean-Marie
MoMo: a new empirical model of the Mars ionospheric total electron content based on Mars Express MARSIS data
Journal of Space Weather and Space Climate, 9, 2019. http://dx.doi.org/10.1051/swsc/2019035

[6] Bertrand, Bruno ; Govaerts, Jan
Mass generation in Abelian U(1) gauge theories: A rich network of dualities
Journal of Mathematical Physics, 60 issue 102904, 2019. http://dx.doi.org/10.1063/1.5109628

[7] Besliu-Ionescu, Diana ; Talpeanu, Dana-Camelia ; Mierla, Marilena ; Maris Muntean, Georgeta
On the prediction of geoeffectiveness of CMEs during the ascending phase of SC24 using a logistic regression method
Journal of Atmospheric and Solar-Terrestrial Physics, 192, number 105036, 2019.
https://doi.org/10.1016/j.jastp.2019.04.017

[8] Beuthe, Mikael
Enceladus's crust as a non-uniform thin shell: II tidal dissipation
Icarus, 332, pp. 66-91, 2019. http://dx.doi.org/10.1016/j.icarus.2019.05.035

[9] Bowman, D.M. ; Burssens, S. ; Pedersen, M.G. ; Johnston, C. ; Aerts, C. ; Buysschaert, B. ; Tkachenko, A. ; Rogers, T.M. ; Edelmann, P.V.F. ; Ratnasingam, R.P. ; Simón-Díaz, S. ; Moravveji, E. ; Pope, B.J.S. ; White, T.R. ; De Cat, P.
Blue supergiants reveal low-frequency internal gravity waves in high-precision space photometry
Nature Astronomy, 3, pp. 760-765, 2019. https://doi.org/10.1038/s41550-019-0768-1

[10] Brenguier, F. ; Boué, P. ; Ben-Zion, Y. ; Vernon, F. ; Johnson, C.W. ; Mordret, A. ; Coutant, O. ; Share, P.-E. ; Beaucé, E. ; Hollis, D. ; Lecocq, T.

Train traffic as a powerful noise source for monitoring active faults with seismic interferometry
Geophysical Research Letters, 46 issue 16, 2019. http://dx.doi.org/10.1029/2019GL083438

[11] Brenguier, F. ; Mordret, A. ; Lynch, R. ; Courbis, R. ; Campbell, X. ; Boué, P. ; Chmiel, M. ; Mao, S. ; Takano, T. ; Lecocq, T. ; van der Veen, W. ; Postif, S. ; Hollis, D.
Monitoring of fields using body and surface waves reconstructed from passive seismic ambient noise
SEG Technical Program Expanded Abstracts, pp. 3036-3040, 2019.

[12] Bruyninx, C. ; Legrand, J. ; Fabian, A. ; Pottiaux, E.
GNSS Metadata and Data Validation in the EUREF Permanent Network
GPS Solutions, 23 issue 4, 2019. https://doi.org/10.1007/s10291-019-0880-9

[13] Camelbeeck, T. ; Lombardi, D. ; Collin, F. ; Rapagnani, G. ; Martin, H. ; Lecocq, T.
Contribution of the seismic monitoring at the Belgian Princess Elisabeth base to East Antarctica ice sheet dynamics and global seismicity studies
Bulletin of the Royal Academy for Overseas Sciences, 63 issue 2017-1, pp. 163–179, 2019.
https://doi.org/10.5281/zenodo.3693877

[14] Camelbeeck, T. ; Vanneste, K. ; Lecocq, T.
Natural and man-induced destructive earthquakes in stable continental regions
in press to Bulletin of the Royal Academy for Overseas Sciences, 2019.

[15] Cébron, David ; Laguerre, Raphael ; Noir, Jerome ; Schaeffer, Nathanael
Precessing spherical shells: flows, dissipation, dynamo and the lunar core
Geophysical Journal International, 217 issue 2, pp. 926-949, 2019.
http://dx.doi.org/10.1093/gji/ggz037

[16] Cecere, Mariana ; Sieyra, M.V. ; Cremades, H. ; Mierla, M. ; Sahade, A. ; Stenborg, G. ; Costa, A. ; West, M.J. ; D'Huys, E.
Large non-radial propagation of a coronal mass ejection on 2011 January 24
Advances in Space Research, Volume 65, Issue 6, 15 March 2020, Pages 1654-1662, 2019.
https://doi.org/10.1016/j.asr.2019.08.043

[17] Çelik, Onur ; Sánchez, Joan Pau ; Karatekin, Özgür ; Ritter, Birgit
A comparative reliability analysis of ballistic deployments on binary asteroids
Acta Astronautica, 156, pp. 308-316, 2019. http://dx.doi.org/%2010.1016/j.actaastro.2018.03.020

[18] Chmiel, M. ; Mordret, A. ; Boué, P. ; Brenguier, F. ; Lecocq, T. ; Courbis, R. ; Hollis, D. ; Campman, X. ; Romijn, R. ; Van der Veen, W
Ambient noise multimode Rayleigh and Love wave tomography to determine the shear velocity structure above the Groningen gas field
Geophysical Journal International, Volume 218, Issue 3, September 2019, Pages 1781–1795, 2019.
https://doi.org/10.1093/gji/ggz237

[19] Chmiel, M. ; Mordret, A. ; Boué, A. ; Boué, P. ; Brenguier, F. ; Lecocq, T. ; Courbis, R. ; Hollis, D. ; Campman, X. ; Romijn, R. ; VanderVeen, W. ; Arndt, N. ; Beauprêtre, S. ; Lynch, R. ; Gradon, C.
Ambient noise multimode Rayleigh and Love wave tomography to determine the shear velocity structure above the Groningen gas field
SEG Technical Program Expanded Abstracts, pp. 3031-3035, 2019.
http://dx.doi.org/10.1190/segam2019-3216087.1

[20] Cunha, M. S. ; Antoci, V. ; Holdsworth, D. L. ; Kurtz, D. W. ; Balona, L. A. ; Bognár, Zs ; Bowman, D. M. ; Guo, Z. ; Kołaczek-Szymański, P. A. ; Lares-Martiz, M. ; Paunzen, E. ; Skarka, M. ; Smalley, B. ; Sódor, Á. ; Kochukhov, O. ; Pepper, J. ; Richey-Yowell, T. ; Ricker, G. R. ; Seager, S. ; Buzasi, D. L. ; Fox-Machado, L. ; Hasanzadeh, A. ; Niemczura, E. ; Quitral-Manosalva, P. ; Monteiro, M. J. P. F. G. ;

Stateva, I. ; De Cat, P. ; García Hernández, A. ; Ghasemi, H. ; Handler, G. ; Hey, D. ; Matthews, J. M. ; Nemec, J. M. ; Pascual-Granado, J. ; Safari, H. ; Suárez, J. C. ; Szabó, R. ; Tkachenko, A. ; Weiss, W. W.
Rotation and pulsation in Ap stars: first light results from TESS sectors 1 and 2
Monthly Notices of the Royal Astronomical Society, 487 issue 3, pp. 3523-3549, 2019.
https://doi.org/10.1093/mnras/stz1332

[21] De Cat, P. ; Lampens, P. ; Joshi, S. ; De Becker, M. ; Jorissen, A.
Proceedings of the 2nd BINA workshop: BINA as an expanding international collaboration
Bulletin de la Société Royale des Sciences de Liège, 88 issue October 2019, pp. 1-18, 2019.
https://doi.org/10.25518/0037-9565.8620

[22] Decraemer, Bieke ; Zhukov, Andrei ; Van Doorsselaere, Tom
Three-dimensional Density Structure of a Solar Coronal Streamer Observed by SOHO/LASCO and STEREO/COR2 in Quadrature
The Astrophysical Journal, 883 issue 2, 2019. http://dx.doi.org/10.3847/1538-4357/ab3b58

[23] Dehant, V. ; Debaille, V. ; Dobos, V. ; Gaillard, F. ; Gillmann, C. ; Goderis, S. ; Grenfell, J.L. ; Höning, D. ; Javaux, E.J. ; Karatekin, Ö. ; Morbidelli, A. ; Noack, L. ; Rauer, H. ; Scherf, M. ; Spohn, T. ; Tackley, P. ; Van Hoolst, T. ; Wünnemann, K.
Geoscience for understanding habitability in the solar system and beyond
Space Science Reviews, 215 issue 42, pp. 48p, 2019. http://dx.doi.org/10.1007/s11214-019-0608-8

[24] Dehghanian, M. ; Ferland, G. J. ; Peterson, B. M. ; Kriss, G. A. ; Korista, K. T. ; Chatzikos, M. ; Guzmán, F. ; Arav, N. ; De Rosa, G. ; Goad, M. R. ; Mehdipour, M. ; van Hoof, P. A. M.
A Wind-based Unification Model for NGC 5548: Spectral Holidays, Nondisk Emission, and Implications for Changing-look Quasars
The Astrophysical Journal, 882 issue 2, pp. L30, 2019. http://dx.doi.org/10.3847/2041-8213/ab3d41

[25] Dehghanian, M. ; Ferland, G. J. ; Kriss, G. A. ; Peterson, B. M. ; Mathur, S. ; Mehdipour, M. ; Guzmán, F. ; Chatzikos, M. ; van Hoof, P. A. M. ; Williams, R. J. R. ; Arav, N. ; Barth, A. J. ; Bentz, M. C. ; Bisogni, S. ; Brandt, W. N. ; Crenshaw, D. M. ; Dalla Bontà, E. ; De Rosa, G. ; Fausnaugh, M. M. ; Gelbord, J. M. ; Goad, M. R. ; Gupta, A. ; Horne, Keith ; Kaastra, J. ; Knigge, C. ; Korista, K. T. ; McHardy, I. M. ; Pogge, R. W. ; Starkey, D. A. ; Vestergaard, M.
Space Telescope and Optical Reverberation Mapping Project. X. Understanding the Absorption-line Holiday in NGC 5548
The Astrophysical Journal, 877 issue 2, pp. 119 (10 pages), 2019. http://dx.doi.org/10.3847/1538-4357/ab1b48

[26] Delobbe, L. ; Watlet, A. ; Wilfert, S. ; Van Camp, M.
Exploring the use of underground gravity monitoring to evaluate radar estimates of heavy rainfal
Hydrology and Earth System Sciences, 23, pp. 93-105, 2019. http://dx.doi.org/10.5194/hess-23-93-2019

[27] Emel'yanov, N. V. ; Arlot, J.-E. ; Zhang, X. L. ; Bradshaw, J. ; De Cat, P. ; Han, X. L. ; Ivantsov, A. ; Jindra, J. ; Maigurova, N. ; Manek, J. ; Pauwels, T. ; Pomazan, A. ; Vingerhoets, P.
Astrometric Results for Observations of Jupiter's Galilean Satellites During Mutual Occultations and Eclipses in 2009 and 2014–2015
Solar System Research, 53, pp. 436–442, 2019. https://doi.org/10.1134/S0038094619060017

[28] Ferri, F. ; Karatekin, Ozgur ; Lewis, S.R. ; Forget, F. ; Aboudan, A. ; Bettanini, C. ; Colombatti, G. ; Debei, S. ; Van Hove, Bart ; Dehant, Veronique ; Harri, A.-M. ; Leese, M. ; Mäkinen, T. ; Millour, E. ; Muller-Wodarg, I. ; Ori, G.G. ; Paris, S. ; Patel, M. ; Schoenenberger, M. ; Herath, J. ; Silii, T. ; Spiga, A. ; Tokano, T. ; Towner, M. ; Withers, P. ; Asmar, S. ; Plettemeier, D.
ExoMars Atmospheric Mars Entry and Landing Investigations and Analysis (AMELIA)

Space Science Review, 215 issue 8, pp. 1-21, 2019. http://dx.doi.org/10.1007/s11214-019-0578-x

[29] Gaia Collaboration: Eyer, L., and 454 coauthors, including Blomme R., Cuypers J., Frémat Y., Lobel A., Pauwels T.
Gaia Data Release 2. Variable stars in the colour-absolute magnitude diagram
Astronomy & Astrophysics, 623, pp. A110, 2019. https://doi.org/10.1051/0004-6361/201833304

[30] Garbin, Esteban ; Defraigne, Pascale ; Krystek, Piotr ; Piriz, Ricardo ; Bertrand, Bruno ; Waller, Pierre
Absolute calibration of GNSS timing stations and its applicability to real signals
Metrologia, 56 issue 1, 2018. https://doi.org/10.1088/1681-7575/aaf2bc

[31] Garcia, Raphael F. ; Khan, Amir ; Drilleau, Mélanie ; Margerin, Ludovic ; Kawamura, Taichi ; Sun, Daoyuan ; Wieczorek, Mark A. ; Rivoldini, Attilio ; Nunn, Ceri ; Weber, Renee C. ; Marusiak, Angela G. ; Lognonné, Philippe ; Nakamura, Yosio ; Zhu, Peimin
Lunar Seismology: An Update on Interior Structure Models
Space Science Reviews, 215 issue 8, Article number 50, 2019. http://dx.doi.org/10.1007/s11214-019-0613-y

[32] Garcia-Moreno, David ; Gupta, Sanjeev ; Collier, Jenny S. ; Oggioni, Francesca ; Vanneste, Kris ; Trentesaux, Alain ; Verbeeck, Koen ; Versteeg, Wim ; Jomard, Hervé ; Camelbeeck, Thierry ; De Batist, Marc
Middle-Late Pleistocene landscape evolution of the Dover Strait inferred from buried and submerged erosional landforms
Quaternary Science Reviews, 203, pp. 209-232, 2019.
https://doi.org/10.1016/j.quascirev.2018.11.011

[33] Gérard, Jean-Claude ; Gkouvelis, Leo ; Ritter, Birgit ; Hubert, Benoit ; Jain, Sonal K. ; Schneider, Nick M.
MAVEN-IUVS Observations of the CO2+ UV Doublet and CO Cameron Bands in the Martian Thermosphere: Aeronomy, Seasonal, and Latitudinal Distribution
Journal of Geophysical Research: Space Physics, Volume 124, Issue 7, 2019.
http://dx.doi.org/10.1029/2019JA026596

[34] Ghazoui, Z. ; Bertrand, S. ; Vanneste, Kris ; Yokoyama, Y. ; Nomade, J. ; Gajurel, A.P. ; van der Beek, P.A.
Potentially large post-1505 AD earthquakes in western Nepal revealed by a lake sediment record
Nature Communications, 10, pp. 2258, 2019. http://dx.doi.org/10.1038/s41467-019-10093-4

[35] Gillmann, Cedric ; Forget, Francois ; Baudin, Baptiste ; Palumbo, Ashley ; Head, James ; Karatekin, Ozgur
The environmental effects of very large bolide impacts on early Mars explored with a hierarchy of numerical models
Icarus, 335, 113419, 2019. https://doi.org/10.1016/j.icarus.2019.113419

[36] Gobron, K. ; de Viron, O. ; Wöppelmann, G. ; Poirier, E. ; Ballu, V. ; Van Camp, M.
Assessment of tide gauges biases and precisions by the combination of multiple co-located time series
Journal of Atmospheric and Oceanic Technology, 36 (10): pp 1983–1996, 2019.
http://dx.doi.org/10.1175/JTECH-D-18-0235.1

[37] Goldman, S.R. ; Boyer, M.L. ; McQuinn, K.B.W. ; Whitelock, P.A. ; McDonald, I. ; van Loon, J.Th. ; Skillman, E.D. ; Gehrz, R.D. ; Javadi, A. ; Sloan, G.C. ; Jones, O.C. ; Groenewegen, M.A.T. ; Menzies, J.W.
An infrared census of dust in nearby galaxies with Spitzer (DUSTiNGS), V. The period-luminosity relation for dusty metal-poor AGB stars

ApJ, 877, pp. 502, 2019. https://doi.org/10.3847/1538-4357/ab0965

[38] González, J.F. ; Briquet, M. ; Przybilla, N. ; Nieva, M.-F. ; De Cat, P. ; Saesen, S. ; Hubrig, S. ; Thoul, A. ; Pápics, P.I. ; Palaversa, L. ; Naef, D. ; Neveu-Van Malle, M. ; Järvinen, S. ; Pollard, K.R. ; Kilmartin, P. ; Mowlavi, N. ; Butler, K.
HD96446: a long-period binary with a strongly magnetic He-rich primary with beta Cep pulsations
Astronomy & Astrophysics, 626 issue A94, pp. 1-15, 2019. https://doi.org/10.1051/0004-6361/201935177

[39] Groenewegen, M.A.T. ; Cioni, M.-R.L. ; Girardi, L. ; de Grijs, R. ; Ivanov, V.D. ; Marconi, M. ; Muraveva, T. ; Ripepi, V. ; van Loon, J.Th.
The VMC Survey XXXIII. The tip of the red giant branch in the Magellanic Clouds
A&A, 622, pp. A63, 2019. https://doi.org/10.1051/0004-6361/201833904

[40] Guzmán, F. ; Chatzikos, M. ; van Hoof, P. A. M. ; Balser, Dana S. ; Dehghanian, M. ; Badnell, N. R. ; Ferland, G. J.
H-, He-like recombination spectra - III. n-changing collisions in highly excited Rydberg states and their impact on the radio, IR, and optical recombination lines
Monthly Notices of the Royal Astronomical Society, 486 issue 1, pp. 1003-1018, 2019. http://dx.doi.org/10.1093/mnras/stz857

[41] Handler, G. ; Pigulski, A. ; Daszyńska-Daszkiewicz, J. ; Irrgang, A. ; Kilkenny, D. ; Guo, Z. ; Przybilla, N. ; Kahraman Aliçavus, F. ; Kallinger, T. ; Pascual-Granado, J. ; Niemczura, E. ; Różański, T. ; Chowdhury, S. ; Buzasi, D.L. ; Mirouh, G.M. ; Bowman, D.M. ; Johnston, C. ; Pedersen, M. ; Simón-Díaz, S. ; Moravveji, E. ; Gazeas, K. ; De Cat, P. ; Vanderspek, R.K. ; Ricker, G.R.
Asteroseismology of massive stars with the TESS mission: the runaway β Cep pulsator PHL 346 = HN Aqr
Astrophysical Journal Letters, 873 issue L4, pp. 1-7, 2019. https://doi.org/10.3847/2041-8213/ab095f

[42] Hinterreiter, J. ; Magdalenic, J. ; Temmer, M. ; Verbeke, C. ; Jebaraj, I.J. ; Samara, E. ; Asvestari, E. ; Poedts, S. ; Pomoell, J. ; Kilpua, E. ; Rodriguez, L. ; Scolini, C. ; Isavnin, A.
Assesing the background solar wind modelled by EUHFORIA
Solar Physics, 294, Article number: 17, 2019. http://dx.doi.org/10.1007/s11207-019-1558-8

[43] Huang, Wei ; Defraigne, Pascale ; Signorile, Giovanna ; Sesia, Ilaria
Improved Multi-GNSS PPP Software for Upgrading the DEMETRA Project Time Monitoring Service
Sensors, 19 issue 20, pp. 4389-4410, 2019. http://dx.doi.org/10.3390/s19204389

[44] Joshi, S. ; De Cat, P.
Overview of the BINA Activities
Bulletin de la Société Royale des Sciences de Liège (en ligne), Volume 88 - Année 2019, Actes de colloques, 2nd Belgo-Indian Network for Astronomy & Astrophysics (BINA) workshop - October 2018 - Brussels, Belgium, 2019. https://doi.org/10.25518/0037-9565.8625

[45] Joshi, Y. C. ; De Cat, P. ; Panchal, A. ; Goswami, A. ; Lampens, P. ; Vermeylen, L. ; Maurya, J.
Optical characterization and Radial velocity monitoring of Exoplanet and Eclipsing Binary candidates
Bulletin de la Société Royale des Sciences de Liège, 88 issue October 2019, pp. 82-88, 2019. https://doi.org/10.25518/0037-9565.8685

[46] Katsavrias, Ch ; Sandberg, I ; Li, W ; Podladchikova, 0 ; Daglis, I ; Papadimitriou, C ; Aminalragia-Giamini, S
Highly relativistic electron flux enhancement during the weak geomagnetic storm of April–May 2017

Journal of Geophysical Research, Space Physics, Volume 124, Issue 6, p 4402-4413, 2019. https://doi.org/10.1029/2019JA026743

[47] Katz, D. ; Sartoretti, P. ; Cropper, M. ; Panuzzo, P. ; Seabroke, G. M. ; Viala, Y. ; Benson, K. ; Blomme, R. ; Jasniewicz, G. ; Jean-Antoine, A. ; Huckle, H. ; Smith, M. ; Baker, S. ; Crifo, F. ; Damerdji, Y. ; David, M. ; Dolding, C. ; Frémat, Y. ; Gosset, E. ; Guerrier, A. ; Guy, L. P. ; Haigron, R. ; Janßen, K. ; Marchal, O. ; Plum, G. ; Soubiran, C. ; Thévenin, F. ; Ajaj, M. ; Allende Prieto, C. ; Babusiaux, C. ; Boudreault, S. ; Chemin, L. ; Delle Luche, C. ; Fabre, C. ; Gueguen, A. ; Hambly, N. C. ; Lasne, Y. ; Meynadier, F. ; Pailler, F. ; Panem, C. ; Royer, F. ; Tauran, G. ; Zurbach, C. ; Zwitter, T. ; Arenou, F. ; Bossini, D. ; Gerssen, J. ; Gómez, A. ; Lemaitre, V. ; Leclerc, N. ; Morel, T. ; Munari, U. ; Turon, C. ; Vallenari, A. ; Žerjal, M.
Gaia Data Release 2. Properties and validation of the radial velocities
Astronomy & Astrophysics, 622, pp. A205, 19 pp., 2019. https://doi.org/10.1051/0004-6361/201833273

[48] Kenyeres, A. ; Baron, A. ; Bruyninx, C. ; Caporali, A. ; De Doncker, F. ; Droscak, B. ; Duret, A. ; Franke, P. ; Georgiev, I. ; Bingley, R. ; Huisman, L. ; Jivall, L. ; Khoda, O. ; Kollo, K. ; Kurt, A.I. ; Lathinen, S. ; Legrand, J. ; Magyar, B. ; Mesmaker, D. ; Morozova, K. ; Nagl, J. ; Ozdemir, S. ; Papanikolaou, X. ; Parseulinas, E. ; Stangl, G. ; Ryczywolsk, M. ; Tangen, O.B. ; Valdes, M. ; Zurutuza, J. ; Weber, M.
Regional integration of long-term national dense GNSS network solutions
GPS Solutions, 23 issue 4, 2019. https://doi.org/10.1007/s10291-019-0902-7

[49] Kilpua, Emilia K. J.; ; Good, Simon W.; ; Palmerio, Erika; ; Asvestari, Eleanna; ; Lumme, Erkka; ; Ala-Lahti, Matti; ; Kalliokoski, Milla M. H.; ; Morosan, Diana E.; ; Pomoell, Jens; ; Price, Daniel J.; ; Magdalenic, Jasmina; ; Poedts, Stefaan; ; Futaana, Yoshifumi
Multipoint Observations of the June 2012 Interacting Interplanetary Flux Ropes
Frontiers in Astronomy and Space Sciences, 6, 2019. http://dx.doi.org/10.3389/fspas.2019.00050

[50] Korablev, Oleg ; Avandaele, Ann Carine ; Montmessin, Franck ; Fedorova, Anna A. ; Trokhimovskiy, Alexander ; Forget, Francois ; Lefevre, Franck ; Daerden, Frank ; Thomas, Ian R. ; Trompet, Lov<c ; Erwin, Justin T. ; Aoki, Shohei ; Robert, S√©verine ; Neary, Lori ; Viscardy, S√©bastien ; Grigoriev, Alexey V. ; Ignatiev, Nikolay I. ; Shakun, Alexey ; Patrakeev, Andrey ; Belyaev, Denis A. ; Bertaux, Jean-Loup ; Olsen, Kevin S. ; Baggio, Lucio ; Alday, Juan ; Ivanov, Yuriy S. ; Ristic, Bojan ; Mason, Jon ; Willame, Yannick ; Depiesse, Cedric ; Hetey, Laszlo ; Berkenbosch, Sophie ; Clairquin, Roland ; Queirolo, Claudio ; Beeckman, Bram ; Neefs, Eddy ; Patel, Manish R. ; Bellucci, Giancarlo ; Lopez-Moreno, Jose-Juan ; Wilson, Colin F. ; Etiope, Giuseppe ; Zelenyi, Lev ; Svedhem, H√•kan ; Vago, Jorge L. ; Alonso-Rodrigo, Gustavo ; Altieri, Francesca ; Anufreychik, Konstantin ; Arnold, Gabriele ; Bauduin, Sophie ; Bolsee, David ; Carrozzo, Giacomo ; Clancy, R. Todd ; Cloutis, Edward ; Crismani, Matteo ; da Pieve, Fabiana ; D'Aversa, Emiliano ; Duxbury, Natalia ; Encrenaz, Therese ; Fouchet, Thierry ; Funke, Bernd ; Fussen, Didier ; Garcia-Comas, Maia ; Gerard, Jean-Claude ; Giuranna, Marco ; Gkouvelis, Leo ; Gonzalez-Galindo, Francisco ; Grassi, Davide ; Guerlet, Sandrine ; Hartogh, Paul ; Holmes, James ; Hubert, Benov√Æt ; Kaminski, Jacek ; Karatekin, Ozgur ; Kasaba, Yasumasa ; Kass, David ; Khatuntsev, Igor ; Kleinbehl, Armin ; Kokonkov, Nikita ; Krasnopolsky, Vladimir ; Kuzmin, Ruslan ; Lacombe, Gav©tan ; Lanciano, Orietta ; Lellouch, Emmanuel ; Lewis, Stephen ; Luginin, Mikhail ; Liuzzi, Giuliano ; Lopez-Puertas, Manuel ; Lopez-Valverde, Miguel ; Maattinen, Anni ; Mahieux, Arnaud ; Marcq, Emmanuel ; Martin-Torres, Javier ; Maslov, Igor ; Medvedev, Alexander ; Millour, Ehouarn ; Moshkin, Boris ; Mumma, Michael J. ; Nakagawa, Hiromu ; Novak, Robert E. ; Oliva, Fabrizio ; Patsaev, Dmitry ; Piccialli, Arianna ; Quantin-Nataf, Cathy ; Renotte, Etienne ; Ritter, Birgit ; Rodin, Alexander ; Schmidt, Fr√©d√©ric ; Schneider, Nick ; Shematovich, Valery ; Smith, Michael D. ; Teanby, Nicholas A. ; Thiemann, Ed ; Thomas, Nicolas ; Vander Auwera, Jean ; Vazquez, Luis ; Villanueva, Geronimo ; Vincendon, Matthieu ; Whiteway, James ; Wilquet,

Valerie ; Wolff, Michael J. ; Wolkenberg, Paulina ; Yelle, Roger ; Young, Roland ; Zasova, Ludmila ; Zorzano, Maria Paz
No detection of methane on Mars from early ExoMars Trace Gas Orbiter observations
Nature Geoscience, 568 issue 7753, pp. 517-520, 2019. http://dx.doi.org/%2010.1038/s41586-019-1096-4

[51] Koubský, P. ; Harmanec, P. ; Brož, M. ; Kotková, L. ; Yang, S. ; Božić, H. ; Sudar, D. ; Frémat, Y. ; Korčáková, D. ; Votruba, V. ; Škoda, P. ; Šlechta, M. ; Ruždjak, D.
Properties and nature of Be stars. 31. The binary nature, light variability, physical elements, and emission-line changes of HD 81357
Astronomy & Astrophysics, 629, pp. A105 (14pp), 2019. http://dx.doi.org/10.1051/0004-6361/201834597

[52] Kraemer, K.E. ; Sloan, G.C. ; Keller, L.D. ; McDonald, I. ; Zijlstra, A.A. ; Groenewegen, M.A.T.
Stellar Pulsation and the Production of Dust and Molecules in Galactic Carbon Stars
ApJ, 877, pp. 82, 2019. https://doi.org/10.3847/1538-4357/ab4f6b

[53] Kraus, M. ; Kolka, I. ; Aret, A. ; Nickeler, D.H. ; Maravelias, G. ; Eenmäe, T. ; Lobel, A. ; Klochkova, V. G
A new outburst of the yellow hypergiant star Rho Cas
Monthly Notices of the Royal Astronomical Society, Vol. 483, Issue 3, 3792, 2019. https://doi.org/10.1093/mnras/sty3375

[54] Krupar, V.; ; Magdalenic, J.; ; Eastwood, J. P.; ; Gopalswamy, N.; ; Kruparova, O.; ; Szabo, A.; ; Němec, F.
Statistical Survey of Coronal Mass Ejections and Interplanetary Type II Bursts
The Astrophysical Journal, 882 issue 2, 92, 2019. http://dx.doi.org/10.3847/1538-4357/ab3345

[55] Lampens, P. ; Vermeylen, L. ; De Cat, P. ; Van Cauteren, P.
Eclipse mapping of Algol-type systems with oscillating delta Scuti type components
Bulletin de la Société Royale des Sciences de Liège, 88 issue October 2019, pp. 89-94, 2019. https://doi.org/10.25518/0037-9565.8694

[56] Laverick, M. ; Lobel, A. ; Royer, P. ; Merle, T. ; Martayan, C. ; van Hoof, P. A. M. ; Van der Swaelmen, M. ; David, M. ; Hensberge, H. ; Thienpont, E.
The Belgian repository of fundamental atomic data and stellar spectra (BRASS). II. Quality assessment of atomic data for unblended lines in FGK stars
Astronomy and Astrophysics, 624, pp. A60 (51 pages), 2019. http://dx.doi.org/10.1051/0004-6361/201833553

[57] Leka, K. D. ; Park, Sung-Hong ; Kusano, Kanya ; Andries, Jesse ; Barnes, Graham ; Bingham, Suzy ; Bloomfield, D. Shaun ; McCloskey, Aoife E. ; Delouille, Veronique ; Falconer, David ; Gallagher, Peter T. ; Georgoulis, Manolis K. ; Kubo, Yuki ; Lee, Kangjin ; Lee, Sangwoo ; Lobzin, Vasily ; Mun, JunChul ; Murray, Sophie A. ; Hamad Nageem, Tarek A. M. ; Qahwaji, Rami ; Sharpe, Michael ; Steenburgh, Robert A. ; Steward, Graham ; Terkildsen, Michael
A Comparison of Flare Forecasting Methods. II. Benchmarks, Metrics, and Performance Results for Operational Solar Flare Forecasting Systems
The Astrophysical Journal Supplement Series, 243 issue 2, p 36, 2019. https://doi.org/10.3847/1538-4365/ab2e12

[58] Leka, K. D. ; Park, Sung-Hong ; Kusano, Kanya ; Andries, Jesse ; Barnes, Graham ; Bingham, Suzy ; Bloomfield, D. Shaun ; McCloskey, Aoife E. ; Delouille, Veronique ; Falconer, David ; Gallagher, Peter T. ; Georgoulis, Manolis K. ; Kubo, Yuki ; Lee, Kangjin ; Lee, Sangwoo ; Lobzin, Vasily ; Mun, JunChul ; Murray, Sophie A. ; Hamad Nageem, Tarek A. M. ; Qahwaji, Rami ; Sharpe, Michael ; Steenburgh, Robert A. ; Steward, Graham ; Terkildsen, Michael

A Comparison of Flare Forecasting Methods. III. Systematic Behaviors of Operational Solar Flare Forecasting Systems
The Astrophysical Journal, 881 issue 2, article id. 101, 13 pp, 2019. https://doi.org/10.3847/1538-4357/ab2e11

[59] Le Maistre, Sébastien ; Rivoldini, Attilio ; Rosenblatt, Pascal
Signature of Phobos'interior structure in its gravity field and libration
Icarus, 321, pp 272-290, 2019 https://doi.org/10.1016/j.icarus.2018.11.022

[60] Lilensten, Jean ; Belehaki, Anna ; Watermann, Jürgen ; Janssens, Jan ; Henri, Agnès
JSWSC: recent developments and further advances
Journal of Space Weather and Space Climate, 9, E2, 5 pp, 2019.
http://dx.doi.org/10.1051/swsc/2019011

[61] Lobel, Alex ; Royer, Pierre ; Martayan, Christophe ; Laverick, Michael ; Merle, Thibault ; Van der Swaelmen, Mathieu ; van Hoof, Peter A. M. ; David, Marc ; Hensberge, Herman ; Thienpont, Emmanuel
The Belgian Repository of Fundamental Atomic Data and Stellar Spectra (BRASS)
Atoms, 7 issue 4, pp. 105 (11 pages), 2019. http://dx.doi.org/10.3390/atoms7040105

[62] Lognonne, Philippe ; Banerdt, W.B. ; Giardini, D. ; Pike, W.T. ; Christensen, U. ; SEIS team, including ; Dehant, Veronique
SEIS: The Seismic Experiment for Internal Structure of InSight
Space Science Reviews - InSight pre-launch special issue, 215, pp. 12, 2019.
http://dx.doi.org/10.1007/s11214-018-0574-6

[63] Lombardi, D. ; Gorodetskaya, I. ; Barruol, G. ; Camelbeeck, T.
Thermally induced icequakes detected on blue ice areas of the East Antarctic ice sheet
Annals of Glaciology, Volume 60, Issue 79, p 45-66, 2019. https://doi.org/10.1017/aog.2019.26

[64] Lopes, R. M. C. ; Wall, S. D. ; Elachi, C. ; Birch, S. P. D. ; Corlies, P. ; Coustenis, A. ; Hayes, A. G. ; Hofgartner, J. D. ; Janssen, M. A. ; Kirk, R. L. ; LeGall, A. ; Lorenz, R. D. ; Lunine, J. I. ; Malaska, M. J. ; Mastroguiseppe, M. ; Mitri, G. ; Neish, C. D. ; Notarnicola, C. ; Paganelli, F. ; Paillou, P. ; Poggiali, V. ; Radebaugh, J. ; Rodriguez, S. ; Schoenfeld, A. ; Soderblom, J. M. ; Solomonidou, A. ; Stofan, E. R. ; Stiles, B. W. ; Tosi, F. ; Turtle, E. P. ; West, R. D. ; Wood, C. A. ; Zebker, H. A. ; Barnes, J. W. ; Casarano, D. ; Encrenaz, P. ; Farr, T. ; Grima, C. ; Hemingway, D. ; Karatekin, Ozgur. ; Lucas, A. ; Mitchell, K. L. ; Ori, G. ; Orosei, R. ; Ries, P. ; Riccio, D. ; Soderblom, L. A. ; Zhang, Z.
Titan as Revealed by the Cassini Radar
Space Science Reviews, 215 issue 4, Article number: 33, 2019.
http://dx.doi.org/%2010.1007/s11214-019-0598-6

[65] Lopez, R. A. ; Shaaban, S. M. ; Lazar, M. ; Poedts, S. ; Yoon, P. H. ; Micera, A. ; Lapenta, G.
Particle-in-cell simulations of the whistler heat-flux instability in the solar wind conditions
ApJL, 882 issue 1, pp. L8, 2019. http://dx.doi.org/10.3847/2041-8213/ab398b

[66] Marini, E. ; Dell'Agli, F. ; García-Hernandez, D.A. ; Groenewegen, M.A.T. ; Puccetti, S. ; Ventura, P. ; Villaver, E.
Do evolved stars in the LMC show dual dust chemistry?
MNRAS, 488, pp. L85, 2019. https://doi.org/10.1093/mnrasl/slz105

[67] Mathieu, Sophie ; von Sachs, Rainer ; Ritter, Christian ; Delouille, Véronique ; Lefèvre, Laure
Uncertainty Quantification in Sunspot Counts
The Astrophysical Journal, 886 issue 1, 2019. http://dx.doi.org/10.3847/1538-4357/ab4990

[68] McDonald, I. ; Boyer, M.L. ; Groenewegen, M.A.T. ; Lagadec, E. ; Richards, A.M.S. ; Sloan, G.C. ; Zijlstra, A.A.

Circumstellar CO in metal-poor stellar winds: the highly irradiated globular cluster star 47 Tucanae V3
MNRAS, 484, pp. L85, 2019. https://doi.org/10.1093/mnrasl/slZ009

[69] Mkrtichian, D. ; Engelbrecht, C. ; Lampens, P. ; Lehmann, H. ; A-thano, N. ; Gunsriwiwa, K.
A spectroscopic survey of oEA stars
Bulletin de la Société Royale des Sciences de Liège, 88 issue October 2019, pp. 256-261, 2019.

[70] Nanni, A. ; Groenewegen, M.A.T. ; Aringer, B. ; Rubele, S. ; Bressan, A. ; van Loon, J.Th. ; Goldman, S.R.
The mass-loss, expansion velocities and dust production rates of carbon stars in the Magellanic Clouds
MNRAS, 487, pp. 502, 2019. https://doi.org/10.1093/mnras/stz1255

[71] O'Hara, J. ; Mierla, M. ; Podladchikova, O. ; D'Huys, E. ; West, M. J.
Exceptional Extended Field-of-view Observations by PROBA2/SWAP on 2017 April 1 and 3
The Astrophysical Journal, Volume 883, Number 1, 2019. https://doi.org/10.3847/1538-4357/ab3b08

[72] Opgenoorth, H. ; Wimmer-Schweingruber, R. ; Belehaki, A. ; Berghmans, D. ; Hapgood, M. ; Hesse, M. ; Kauristie, K. ; Lester, M. ; Lilensten, J. ; Messerotti, M. ; Temmer, M.
European Space Weather Activities: Assessment and Recommendations for a Consolidated European Approach to Space Weather – as Part of a Global Space Weather Effort
Journal of Space Weather and Space Climate, 9, pp. A37, 2019.
https://doi.org/10.1051/swsc/2019033

[73] Palmerio, E. ; Scolini, C. ; Barnes, D. ; Magdalenic, J. ; West, M. ; Zhukov, A. ; Rodriguez, L. ; Mierla, M. ; Good, S. ; Morosan, D. ; Kilpua, E. ; Pomoell, J. ; Poedts, S.
Multipoint Study of Successive Coronal Mass Ejections Driving Moderate Disturbances at 1 au
The Astrophysical Journal, 878 issue 1, 2019. https://doi.org/10.3847/1538-4357/ab1850

[74] Pastorelli, G. ; Marigo, P. ; Girardi, L. ; Chen, Y. ; Rubele, S. ; Trabucchi, M. ; Aringer, B. ; Bladh, S. ; Bressan, A. ; Montalban, J. ; Boyer, M.L. ; Dalcanton, J. ; Eriksson, K. ; Groenewegen, M.A.T. ; Höfner, S. ; Lebzelter, T. ; Nanni, A. ; Rosenfield, P. ; Wood, P.R. ; Cioni, M.-R.L.
Constraining the thermally pulsing asymptotic giant branch phase with resolved stellar populations in the Small Magellanic Cloud
MNRAS, 485 issue 5666, 2019. https://doi.org/10.1093/mnras/stz725

[75] Pedersen, M.G. ; Chowdhury, S. ; Johnston, C. ; Bowman, D.M. ; Aerts, C. ; Handler, G. ; De Cat, P. ; Neiner, C. ; David-Uraz, A. ; Buzasi, D. ; Tkachenko, A. ; Símon-Díaz, S. ; Moravveji, E. ; Sikora, J. ; Mirouh, J.M. ; Lovekin, C.C. ; Cantiello, M. ; Daszyńska-Daszkiewicz, J. ; Pigulski, A. ; Vanderspek, R.K. ; Ricker, G.R.
Diverse Variability of O and B Stars Revealed from 2-minute Cadence Light Curves in Sectors 1 and 2 of the TESS Mission: Selection of an Asteroseismic Sample
Astrophysical Journal Letters, 872, pp. L9, 2019. https://doi.org/10.3847/2041-8213/ab01e1

[76] Pla-Garcia, J. ; Rafkin, S. C. R. ; Karatekin, Ö. ; Gloesener, E.
Comparing MSL Curiosity rover TLS-SAM methane measurements with Mars Atmospheric Modeling System atmospheric transport experiments
JGR Planets, 124:8, pp 2141-2167, 2019.

[77] Podladchikova, T ; Veronig, A ; Dissauer, K ; Temmer, M ; Podladchikova, O
3D Reconstructions of EUV Wave Front Heights And Their Influence On Wave Kinematics
The Astrophysical Journal, Volume 877, Issue 2, article id. 68, 14 pp., 2019.
https://doi.org/10.3847/1538-4357/ab1b3a

[78] Pou, L. ; Mimoun, D. ; Lognonne, P. ; Garcia, R. F. ; Karatekin, Ozgur ; Nonon-Latapie, M. ; Llorca-Cejudo, R.
High Precision SEIS Calibration for the InSight Mission and Its Applications
Space Science Reviews, 215 issue 1, article number 6, 2019. http://dx.doi.org/10.1007/s11214-018-0561-y

[79] Ragosta, F. ; Marconi, M. ; Molinaro, R. ; Ripepi, V. ; Cioni, M.-R.L. ; Moretti, M.-I. ; Groenewegen, M.A.T. ; Choudhury, S. ; de Grijs, R. ; van Loon, J.Th. ; Oliveira, J.M. ; Ivanov, V.D. ; Gonzalez-Fernandez, C.
The VMC survey – XXXV. model fitting of LMC Cepheid light curves
MNRAS, 490, pp. 4975, 2019. https://doi.org/10.1093/mnras/stz2881

[80] Rekier, J. ; Trinh, A. ; Triana, Santiago Andres ; Dehant, V.
Inertial modes in near-spherical geometries
Geophysical Journal International, 216 issue 2, pp. 777-793, 2019. http://dx.doi.org/10.1093/gji/ggy465

[81] Rekier, J. ; Trinh, A. ; Triana, S.A. ; Dehant, V.
Internal energy dissipation in Enceladus's ocean from tides and libration and the role of inertial waves
J. Geophys. Res. Planets, 124, pp. 2198-2212, 2019. http://dx.doi.org/10.1029/2019JE005988

[82] Ritter, Birgit ; Gérard, Jean-Claude ; Gkouvelis, Leo ; Hubert, Benoit ; Jain, Sonal K. ; Schneider, Nicholas M.
Characteristics of Mars UV Dayglow Emissions From Atomic Oxygen at 130.4 and 135.6 nm: MAVEN/IUVS Limb Observations and Modeling
Journal of Geophysical Research: Space Physics, Volume 124, Issue 6. https://doi.org/10.1029/2019JA026669

[83] Rochus, P. ; Auchere, F. ; Berghmans, D. ; Harra, L. ; Schmutz, W. ; Schühle, U. ; Addison, P. ; Appourchaux, T. ; Aznar Cuadrado, R. ; Baker, D. ; Barbay, J. ; Bates, D. ; BenMoussa, A. ; Bergmann, M. ; Beurthe, C. ; Borgo, B. ; Bonte, K. ; Bouzit, M. ; Bradley, L. ; Büchel, V. ; Buchlin, E. ; Büchner, J. ; Cabé, F. ; Cadiergues, L. ; Chaigneau, M. ; Chares, B. ; Choque Cortez, C. ; Coker, P. ; Condamin, M. ; Coumar, S. ; Curdt, W. ; Cutler, J. ; Davies, D. ; Davison, G. ; Defise, J.-M. ; Del Zanna, G. ; Delmotte, F. ; Delouille, V. ; Dolla, L. ; Dumesnil, C. ; Dürig, F. ; Enge, R. ; François, S. ; Fourmond, J.-J. ; Gillis, J.-M. ; Giordanengo, B. ; Gissot, S. ; Green, L. ; Guerreiro, N. ; Guilbaud, A. ; Gyo, M. ; Haberreiter, M. ; Hafiz, A. ; Hailey, M. ; Halain, J.-P. ; Hansotte, J. ; Hecquet, C. ; Heerlein, K. ; Hellin, M.-L. ; Hemsley, S. ; Hermans, A. ; Hervier, V. ; Hochedez, J.-F. ; Houbrechts, Y. ; Ihsan, K. ; Jacques, L. ; Jérôme, A. ; Jones, J. ; Kahle, M. ; Kennedy, T. ; Klaproth, M. ; Kolleck, M. ; Koller, S. ; Kotsialos, E. ; Kraaikamp, E. ; Langer, P. ; Lawrenson, A. ; Le Clech', J.-C. ; Lenaerts, C. ; Liebecq, S. ; Linder, D. ; Long, D. M. ; Mampaey, B. ; Markiewicz-Innes, D. ; Marquet, B. ; Marsch, E. ; Matthews, S. ; Mazy, E. ; Mazzoli, A. ; Meining, S. ; Meltchakov, E. ; Mercier, R. ; Meyer, S. ; Monecke, M. ; Monfort, F. ; Morinaud, G. ; Moron, F. ; Mountney, L. ; Müller, R. ; Nicula, B. ; Parenti, S. ; Peter, H. ; Pfiffner, D. ; Philippon, A. ; Phillips, I. ; Plesseria, J.-Y. ; Pylyser, E. ; Rabecki, F. ; Ravet-Krill, M.-F. ; Rebellato, J. ; Renotte, E. ; **Rodriguez, L.** ; Roose, S. ; Rosin, J. ; Rossi, L. ; Roth, P. ; Rouesnel, F. ; Roulliay, M. ; Rousseau, A. ; Ruane, K. ; Scanlan, J. ; Schlatter , P. ; Seaton, D. B. ; Silliman, K. ; Smit, S. ; Smith, P.J. ; Solanki, S.K. ; Spescha, M. ; Spencer, A. ; **Stegen, K.** ; Stockman, Y. ; Szwec, N. ; Tamiatto, C. ; Tandy, J. ; Teriaca, L. ; Theobald, C. ; Tychon, I. ; van Driel-Gesztelyi, L. ; Verbeeck, C. ; Vial, J.-C. ; Werner, S. ; West, M. J. ; Westwood, D. ; Wiegelmann, T. ; Willis, G. ; Winter, B. ; Zerr, A. ; Zhang, X. ; Zhukov, A. N.
The Solar Orbiter EUI instrument: The Extreme Ultraviolet Imager
in press to Astronomy and Astrophysics issue Special Issue on Solar Orbiter , 2019. https://doi.org/10.1051/0004-6361/201936663

[84] Rouillard, A.P. ; Pinto, R.F. ; Vourlidas, A. ; De Groof, A. ; ManyOtherAuthors, X. ; Berghmans, D. ; Nicula, B. ; Kraaikamp, E. ; Parenti, S. ; Rodriguez, L. ; Verbeeck, C. ; Zhukov, A.N.
Models and data analysis tools for the Solar Orbiter mission
in press to Astronomy and Astrophysics, 2019. https://doi.org/10.1051/0004-6361/201935305

[85] Sarkar, Ranadeep; Srivastava, Nandita; Mierla, Marilena; West, Matthew J.; D'Huys, Elke
Evolution of the Coronal Cavity From the Quiescent to Eruptive Phase Associated with Coronal Mass Ejection
The Astrophysical Journal, Volume 875, Issue 2, article id. 101, 16 pp, 2019.
https://doi.org/10.3847/1538-4357/ab11c5

[86] Schleutker, Thorn ; Gulhan, Ali ; Van Hove, Bart ; Karatekin, Ozgur
ExoMars Flush Air Data System: Experimental and Numerical Investigation
Journal of Spacecraft and Rockets, vol. 56, issue 4, pp. 971-982, 2019.
https://doi.org/10.2514/1.A34185

[87] Schmidtke, G ; Finsterle, W ; Van Ruymbeke, M ; Haberreiter, M ; Schafer, R ; Zhu, P ; Brunner, R
Solar autocalibrating XUV-IR spectrometer system (SOLACER) for the measurement of solar spectral irradiance
Applied Optics, vol 58, issue 22, pp 6182-6192, 2019. https://doi.org/10.1364/AO.58.006182

[88] Scolini, C. ; Rodriguez, L. ; Mierla, M. ; Pomoell, J. ; Poedts, S.
Observation-based modelling of magnetised Coronal Mass Ejections with EUHFORIA
Astronomy and Astrophysics, 626, A122, 2019. https://doi.org/10.1051/0004-6361/201935053

[89] Shestov, S V ; Zhukov, A N ; Seaton, D B
Modeling and removal of optical ghosts in the PROBA-3/ASPIICS externally occulted solar coronagraph
Astronomy and Astrophysics, 622 issue A101, pp. 1-14, 2019. http://dx.doi.org/10.1051/0004-6361/201834584

[90] Stopa, J. ; Ardhuin, F. ; Stutzmann, E. ; Lecocq, T.
Sea state trends and variability: consistency between models, altimeters, buoys, and seismic data (1979-2016)
Journal of Geophysical Research: Oceans, 124 issue 6, pp. 3923-3940, 2019.
http://dx.doi.org/10.1029/2018JC014607

[91] Temel, O. ; Karatekin, Ö. ; Gloesener, E. ; Mischna, M. A. ; van Beeck, J.
Atmospheric transport of subsurface, sporadic, time-varying methane releases on Mars
Icarus, 325, pp. 39-54, 2019. http://dx.doi.org/10.1016/j.icarus.2019.02.014

[92] Terasaki, Hidenori ; Rivoldini, Attilio ; Shimoyama, Yuta ; Nishida, Keisuke ; Urakawa, Satoru ; Maki, Mayumi ; Kurokawa, Fuyuka ; Takubo, Yusaku ; Shibazaki, Yuki ; Sakamaki, Tatsuya ; Machida, Akihiko ; Higo, Yuji ; Uesugi, Kentaro ; Takeuchi, Akihisa ; Watanuki, Tetsu ; Kondo, Tadashi
Pressure and composition effects on sound velocity and density of core-forming liquids: Implication to core compositions of terrestrial planets
Journal of Geophysical Research: Planets, 124 issue 8, 2019.
http://dx.doi.org/10.1029/2019JE005936

[93] Triana, Santiago Andres ; Rekier, Jeremy ; Trinh, Antony ; Dehant, Veronique
The coupling between inertial and rotational eigenmodes in 2 planets with liquid cores
Geophys. J. Int., 2019 issue 2, pp. 1071-1086, 2019. http://dx.doi.org/10.1093/gji/ggz212

[94] Triantafyllou, A. ; Watlet, A. ; Le Mouélica, S. ; Camelbeeck, T. ; Civeta, F. ; Kaufmann, O. ; Quinif, Y. ; Vandycke, S.
3-D digital outcrop model for analysis of brittle deformation and lithological mapping (Lorette cave, Belgium)

Journal of Structural Geology, 120, pp. 55-66, 2019.https://doi.org/10.1016/j.jsg.2019.01.001

[95] Van Daele, Maarten ; Araya-Cornejo, Cristian ; Pille, Thomas ; Vanneste, Kris ; Moernaut, Jasper ; Schmidt, Sabine ; Kempf, Philipp ; Meyer, Inka ; Cisternas, Marco
Distinguishing intraplate from megathrust earthquakes using lacustrine turbidites
Geology, 47 issue 2, 2019. http://dx.doi.org/10.1130/G45662.1

[96] Vandaele, Ann Carine ; Korablev, Oleg ; Daerden, Frank ; Aoki, Shohei ; Thomas, Ian R. ; Altieri, Francesca ; Lopez-Valverde, Miguel ; Villanueva, Geronimo ; Liuzzi, Giuliano ; Smith, Michael D. ; Erwin, Justin T. ; Trompet, Loic ; Fedorova, Anna A. ; Montmessin, Franck ; Trokhimovskiy, Alexander ; Belyaev, Denis A. ; Ignatiev, Nikolay I. ; Luginin, Mikhail ; Olsen, Kevin S. ; Baggio, Lucio ; Alday, Juan ; Bertaux, Jean-Loup ; Betsis, Daria ; Bolse, David ; Clancy, R. Todd ; Cloutis, Edward ; Depiesse, Cedric ; Funke, Bernd ; Garcia-Comas, Maia ; Gerard, Jean-Claude ; Giuranna, Marco ; Gonzalez-Galindo, Francisco ; Grigoriev, Alexey V. ; Ivanov, Yuriy S. ; Kaminski, Jacek ; Karatekin, Ozgur ; Lefevre, Franck ; Lewis, Stephen ; Lopez-Puertas, Manuel ; Mahieux, Arnaud ; Maslov, Igor ; Mason, Jon ; Mumma, Michael J. ; Neary, Lori ; Neefs, Eddy ; Patrakeev, Andrey ; Patsaev, Dmitry ; Ristic, Bojan ; Robert, Severine ; Schmidt, Frederic ; Shakun, Alexey ; Teanby, Nicholas A. ; Viscardy, Sebastien ; Willame, Yannick ; Whiteway, James ; Wilquet, Valerie ; Wolff, Michael J. ; Bellucci, Giancarlo ; Patel, Manish R. ; Lopez-Moreno, Jose-Juan ; Forget, Francois ; Wilson, Colin F. ; Young, Roland ; Svedhem, H√¢kan ; Vago, Jorge L. ; Rodionov, Daniel
Martian dust storm impact on atmospheric H2O and D/H observed by ExoMars Trace Gas Orbiter
Nature, 568 issue 7753, pp. 521-525, 2019. http://dx.doi.org/%2010.1038/s41586-019-1097-3

[97] van Genderen, A. M. ; Lobel, A. ; Nieuwenhuijzen, H. ; Henry, G. W. ; de Jager, C. ; Blown, E. ; Di Scala, G. ; van Ballegoij, E. J.
Pulsations, eruptions, and evolution of four yellow hypergiants
Astronomy and Astrophysics, 631 issue November 2019, pp. A48, 1-26, 2019. https://doi.org/10.1051/0004-6361/201834358

[98] Van Hoolst, Tim ; Noack, Lena, ; Rivoldini, Attilio
Exoplanet interiors and habitability
Advances in Physics: X, 4 issue 1, 2019. http://dx.doi.org/10.1080/23746149.2019.1630316

[99] Van Hove, Bart ; Karatekin, Ozgur ; Schleutker, Thorn ; Gulhan, Ali
ExoMars Flush Air Data System: Entry Simulation and Atmospheric Reconstruction Method
Journal of Spacecraft & Rockets, 56:4, 1205-1220, 2019. https://doi.org/10.2514/1.A34187

[100] Van Noten, Koen ; Topal, S. ; Baykara, M.O. ; Özkul, M. ; Claes, Hannes ; Aratman, A. ; Swennen, Rudy
Pleistocene-Holocene tectonic reconstruction of the Ballık travertine (Denizli Graben, SW Turkey): (De)formation of large travertine geobodies at intersecting grabens
Journal of Structural Geology, 118, pp. 114-134, 2019. http://dx.doi.org/10.1016/j.jsg.2018.10.009

[101] Verbeeck, C ; Kraaikamp, E ; Ryan, D.F. ; Podladchikova, O
Solar flare distributions: lognormal instead of power law?
Astrophysical Journal, 884, Number 1, 2019. http://dx.doi.org/10.3847/1538-4357/ab3425

[102] Verbeurgt, J. ; Van Camp, M. ; Cornelis, S. ; Camelbeeck, T. ; De Sloover, L. ; Poppe, H. ; Declercq, P.-Y. ; Voet, P. ; Constales, D. ; Troch, P. ; De Maeyer, P. ; De Wulf, A.
The gravity database for Belgium
Geoscience Data Journal, Volume 6, Issue 2, pp. 116-125, 2019. https://doi.org/10.1002/gdj3.74

[103] Verhasselt, Katrijn ; Defraigne, Pascale
Multi-GNSS time transfer based on the CGGTTS
Metrologia, 56 issue 6, pp. 065003-065014, 2019. http://dx.doi.org/10.1088/1681-7575/ab3ed7

[104] Vincent, D. ; Lambrechts, J. ; Karatekin, Ö. ; Van Hoolst, T. ; Tyler, R.H. ; Dehant, V. ; Deleersnijder, E.
Normal modes and resonance in Ontario Lacus: a hydrocarbon lake of Titan
Ocean Dynamics, 69, pp. 1121-1132, 2019. http://dx.doi.org/10.1007/s10236-019-01290-2

[105] Wieczorek, Mark ; Beuthe, Mikael ; Rivoldini, Attilio ; Van Hoolst, Tim
Hydrostatic Interfaces in Bodies With Nonhydrostatic Lithospheres
Journal of Geophysical Research (Planets), 124, pp. 1410-1432, 2019.
http://dx.doi.org/%2010.1029/2018JE005909

Non-refereed publications

[106] Bacci, P. ; Maestripieri, M. ; Tesi, L. ; Fagioli, G. ; Mikuz, H. ; Facchini, M. ; Corradini, G. ; Coffano, A. ; Marinello, W. ; Micheli, M. ; Pizzetti, G. ; Soffiantini, A. ; Cernis, K. ; Selevicius, H. ; Haver, R. ; Gorelli, R. ; Jaeger, M. ; Prosperi, E. ; Prosperi, S. ; Aletti, A. ; Buzzi, L. ; Naves, R. ; Campas, M. ; Hasubick, W. ; Trondal, O. ; Tanga, P. ; Berthier, J. ; Carry, B. ; DellOro, A. ; Fedorets, G. ; Muinonen, K. ; Pauwels, T. ; Petit, J. M. ; Thuillot, W. ; Mignard, F. ; Pedro, D. ; Kadota, K. ; Abe, H. ; Seki, T. ; Sarneczky, K. ; Szakats, R. ; Gilmore, A. C. ; Kilmartin, P. M. ; Desmars, J. ; Baillie, K. ; Bouquillon, S. ; Delbo, M. ; Dennefeld, M. ; Robert, V. ; Souami, D. ; Spoto, F. ; Taris, F. ; Carlucci, T. ; Barache, C. ; Meech, K. J. ; Kleyna, J. ; Carcano, A. ; Colzani, E. ; Ventre, G. ; Bressan, F. ; Montanar, U. ; Pettarin, E. ; Rankin, D. ; Leonard, G. J. ; Pruyne, T. A. ; Groeller, H. ; Fuls, D. C. ; Christensen, E. J. ; Farneth, G. A. ; Gibbs, A. R. ; Grauer, A. D. ; Kowalski, R. A. ; Larson, S. M. ; Seaman, R. L. ; Shelly, F. C. ; Wierzchos, K. W. ; Moritz, N. ; Childs, W. ; Durig, D. T. ; Walker, G. C. ; Wilson, L. E. ; Keller, C. B. ; Seegars, J. C. ; Cline, D. M. ; Irwin, J. M. ; Kerrigan, D. M. ; Lang, C. O. ; Lewis, M. C. ; Schenk, A. M. ; King, V. R. ; Serra-Ricart, M. ; Lemes-Perera, S. ; Buri, J. ; James, N. ; Kocher, P. ; Bachini, M. ; Martinelli, F. ; Rinner, C. ; Kugel, F. ; Klotz, A. ; Nicolas, J. ; Shurpakov, S. ; Overhaus, C. ; Bryssinck, E. ; Soulier, J. -F. ; Diepvens, A. ; Lindner, P. ; Dangl, G. ; Mainzer, A. K. ; Bauer, J. M. ; Grav, T. ; Masiero, J. R. ; Cutri, R. M. ; Dailey, J. W. ; Kramer, E. ; Pittichova, J. ; Sonnett, S. ; Wright, E. L. ; Thorsteinson, S. ; Balam, D. D. ; Tremosa, L. ; Jahn, J. ; Al-Bussaidi, M. ; Takahashi, T. ; Armstrong, J. D. ; Carstens, R. ; Drummond, J. ; Bulger, J. ; Lowe, T. ; Schultz, A. ; Willman, M. ; Chambers, K. ; Magnier, E. ; Chastel, S. ; de Boer, T. ; Denneau, L. ; Fairlamb, J. ; Flewelling, H. ; Huber, M. ; Lin, C. -C. ; Ramanjooloo, Y. ; Wainscoat, R. ; Weryk, R. ; Dukes, T. ; Ban, L. ; Lee, L. K. ; Felber, T. ; Lutkenhoner, B. ; Maes, J. ; Paul, N. ; Gray, B. ; Sato, H. ; Prystavski, T. ; Suzuki, M. ; Romanov, F. D. ; Bell, C. ; Peterson, H. ; Z. T. F. Collaboration ; Bolin, B. T. ; Masci, F. J. ; Masek, M. ; Cole, M. ; Buczynski, D. ; Gonzalez, J. ; Hills, K. ; Garcia, F. ; Ory, M. ; Carson, P. ; Rubio, L. ; Morales, M. ; Demeautis, C. ; Adamovsky, M. ; Taccogna, F. ; Gerhard, C. ; Lombardo, M. ; Tombelli, M. ; Interrante, G. ; Mazzanti, Y. ; Grazzini, L. ; Mazzanti, A. ; Haeusler, B. ; Brosio, A. ; De Pieri, A. ; Korlevic, K. ; Hudin, L. ; Bertini, M. ; Franchini, L. ; Bellucci, P. ; Carballada, J. ; Hess, R. ; Alterdorfer, R. ; Riegler, A. ; Kurtze, L. ; Chen, T. ; Ikemura, T. ; Nohara, H. ; Denisenko, D. ; Camilleri, P. ; Williams, H. ; Lister, T. ; Bodewits, D. ; Kelley, M. ; Ye, Q. -Z. ; Tonry, J. ; Heinze, A. ; Weiland, H. ; Stalder, B. ; Fitzsimmons, A. ; Robinson, J. ; Young, D. ; Erasmus, N. ; Crowson, D. ; Cuppens, W. ; Flynn, R. L. ; Gasparovic, G. ; Chen, Y. ; Gasparovic, G. Y. ; Fornari, C. ; Reisenauer, E. ; Alonso, J. ; Lescano, A. ; Storey, D. ; Calvo, J. F. ; Limon, F. ; Farfan, R. ; Malagon, C. ; Munoz, M. ; Wells, G. ; Bamberger, D. ; Pratt, A. R. ; Williams, Gareth V. (216 authors)
Observations and Orbits of Comets
Minor Planet Electronic Circ. issue 2019-V116, 2019.
https://ui.adsabs.harvard.edu/abs/2019MPEC....V..116B/abstract

[107] Baland, R.-M. ; Yseboodt, M. ; Le Maistre, S. ; Rivoldini, A. ; Péters, M.-J. ; Van Hoolst, T. ; Dehant, V.
Rigid nutations of Mars
Proc. EPSC 2019, Geneva, Switzerland, 15-20 September 2019, pp. EPSC2019-488, 2019.

[108] Banerdt, W.B. ; Smrekar, S. ; Antonangeli, D. ; Asmar, S. ; Banfield, D. ; Beghein, C. ; Bowles, N. ; Bozdag, E. ; Chi, P. ; Christensen, U. ; Clinton, J. ; Collins, G. ; Daubar, I. ; Dehant, V. ; the SEIS, team
Insight - The First Three Months on Mars
Proc. 50th Lunar and Planetary Science Conference, held 18-22 March, 2019 at The Woodlands, Texas, LPI Contribution, 2132 issue 3109, 2019.

[109] Bergeot, N. ; Witasse, O. ; Le Maistre, S. ; Blelly, P.L. ; Kofman, W. ; Peter, K. ; Dehant, V. ; Chevalier, J.M.

A new empirical model for Mars Ionosphere to correct radio signal experiments
Proc. EPSC 2019, Geneva, Switzerland, 15-20 September 2019, pp. EPSC2019-642, 2019.

[110] Bertrand, Bruno ; Defraigne, Pascale
Fundamental physics tests using the propagation of GNSS signals
Proceedings of the 7th International Colloquium on Scientific and Fundamental Aspects of GNSS, 2019.

[111] Blanc, M. ; Prieto-Ballesteros, O. ; André, N ; Gómez-Elvira, J ; Jones, G ; Martins, Z ; Bunce, E ; Bills, B ; Choblet, G ; Cooper, J ; Hussmann, H ; Lara, L ; Jäggi, T ; Kempf, S ; Khurana, K ; Krupp, N ; Lainey, V ; Longobardo, A ; Masters, A ; Mimoun, D ; Montesi, L ; Saur, J ; Szegő, K ; Tosi, F ; Vance, S ; Van Hoolst , T ; Wagner, R ; Westal, F ; Volwerck, M ; Wurz, P
Joint Europa Mission (JEM). A multiscale, multi-platform mission to characterize Europa's habitability and search for extant life
White paper submitted to ESA's Voyage 2050 call, 2019.

[112] Bruyninx, C.
IAG Travaux 2015-2019, Sub-commission 1.3: Regional References Frames
IAG reports , 41, pp. 21-94, 2019. https://iag.dgfi.tum.de/en/iag-publications-position-papers/iag-reports-2019-online/

[113] Bruyninx, C. ; Brockmann, E. ; Kenyeres, A. ; Legrand, J. ; Liwosz, T. ; Pacione, R. ; Söhne, W. ; Völksen, C.
EPN Regional Network Associate Analysis Center Technical Report 2018
International GNSS Service Technical Report 2018, pp. 95-108, 2019.
https://doi.org/10.7892/boris.130408

[114] Bruyninx, C. ; Bergeot, N. ; Chevalier, J.-M. ; Fabian, A. ; Legrand, J. ; Pottiaux, E. ; Voet, P. ; De Doncker, F.
EUREF 2019 National report of Belgium
Proc. Symposium of the IAG Subcommission for Europe (EUREF) held in Tallin, Estonia, 22 -24 May, 2019, 2019. http://www.euref.eu/symposia/2019Tallinn/Belgium_national_report_2019.pdf

[115] Calders, S. ; Lamy, H. ; Anciaux, M. ; Ranvier, S. ; Martínez Picar, A. ; Verbeeck, C.
Towards an autonomous BRAMS network
Proceedings of the International Meteor Conference 2018, Pezinok, Slovakia, August 30 - September 2, 2019.

[116] Caldiero, A. ; Le Maistre, S. ; Marty, J.C. ; Dehant, V.
Accuracy of Phobos gravity field determination from radio-tracking of spacecraft flybys
Proc. EPSC 2019, Geneva, Switzerland, 15-20 September 2019, pp. EPSC2019-1734, 2019.

[117] Caldiero A. ; Karatekin Ö. ; Temel O. ; Romagnolo A.
Evolution of Mars polar caps extent from CRISM data
EPSC-DPS2019, Geneva, Switzerland, 15-20 September 2019, EPSC2019-1804, 2 pages.

[118] Carry, Benoit ; Spoto, Federica ; Thuillot, William ; David, Pedro ; Muinonen, Karri ; Fedorets, Grigori ; Berthier, Jerome ; Pauwels, Thierry ; Dell`Oro, Aldo ; Petit, Jean-Marc ; Tanga, Paolo
Gaia-FUN-SSO: Tracking Gaia asteroid discoveries
EPSC Abstracts, 13 issue EPSC-DPS2019-1409-1, 2019.
https://ui.adsabs.harvard.edu/abs/2019EPSC...13.1409C/abstract

[119] Choblet, G. ; Buch, A. ; Cadek, O. ; Camprubi-Casas, E. ; Freissenet, C. ; Hadman, M. ; Jones, G. ; Lainey, V. ; Le Gall, A. ; Lucchetti, A. ; MacKenzie, S. ; Mitri, G ; Neveu, M. ; Nimmo, F. ; Olsson-Francis, K. ; Panning, M. ; Saur, J. ; Postberg, F. ; Schmidt, J. ; Shibuya, T. ; Sekine, Y. ; Sotin, C. ;

Tobie, G. ; Soucek, O. ; Vance, S. ; Szopa, C. ; Brage, L. ; Tomohiro, U. ; Behounkova, M. ; Van Hoolst, T.
Enceladus as a potential oasis for life: Science goals and investigations for future explorations
White paper submitted to ESA's Voyage 2050 call, 2019.

[120] Cisneros González M.E., Bolsée D., Pereira N., Jacobs L., Van Laeken L., Gérard P., Cessateur G., Robert S., Vandaele A.C., Karatekin Ö., Giordanengo B., Gissot S., Romagnolo A., Ritter B., Langevin Y., Poulet F., Dumesnil C., Ruiz de Galarreta Fanjul C., Lecomte B., Arondel A., the MAJIS VIS-NIR detectors characterization team
Validation tests of the calibration bench for the characterization of MAJIS/JUICE VIS-NIR detectors
EPSC-DPS2019, Geneva, Switzerland, 15-20 September 2019, extended abstract, EPSC-DPS2019-551, 2 pages, 2019.

[121] Coyette A. ; Baland R.M. ; Van Hoolst T.
Influence of non-hydrostatic equilibrium and subsurface ocean flow on the polar motion of Titan
EPSC-DPS2019, Geneva, Switzerland, poster, 15-20 September 2019, extended abstract, EPSC-DPS2019-615, 2 pages, 2019.

[122] De Beck, E. ; Boyer, M.L. ; Bujarrabal, V. ; Decin, L. ; Fonfría, J.P. ; Groenewegen, M.A.T. ; Höfner, S. ; Jones, O. ; Kamiński, T. ; Maercker, M. ; Marigo, P. ; Matsuura, M. ; Meixner, M. ; Quintana Lacaci Martínez, G. ; Scicluna, P. ; Szczerba, R. ; Velilla Prieto, L. ; Vlemmings, W. ; Wiedner, M.
The fundamentals of outflows from evolved stars, An Astro2020 Science White Paper
arXiv, 1903.12025, 2019. https://arxiv.org/abs/1903.12025

[123] Debehogne, H. ; Elst, E. ; De Cat, P. ; Pauwels, T.
Minor Planet Observations [012 Uccle]
Minor Planet Circulars, pp. 115989, 2019.

[124] including Debehogne, H. ; De Cat, P. ; Pauwels, T. ; Elst, E.
Positions of minor planets observed with the Uccle Schmidt telescope
Minor Planet Circulars Supplement, pp. 1037339-1056900, 2019.

[125] including De Cat, P.
Positions of minor planets observed with the Uccle Schmidt telescope
Minor Planet Circulars Supplement, pp. 1031967-1037338, 2019.

[126] Dehant, V. ; Keppens, R. ; Decin, L.
Episode 5: There comes the Solar System / Etape 5 : L'origine de notre système solaire", Contribution to the Big-bang Route
UCLouvain-KULeuven, Episode 5, 2019.

[127] Dehant, V. ; Mackwell, S. ; Blanc, M.
Report from Horizon 2061 Synthesis Workshop Pillar 1: From Science questions to representative space missions
Proc. EPSC 2019, Geneva, Switzerland, 15-20 September 2019, pp. EPSC2018-217, 2019.

[128] Dehant, V. ; Le Maistre, S. ; Baland, R.-M. ; Karatekin, Ö. ; Péters, M.-J. ; Rivoldini, A. ; Van Hoolst, T. ; Van Hove, B. ; Yseboodt, M.
LaRa (Lander Radioscience) on the ExoMars 2020 Surface Platform
Proc. EPSC 2019, Geneva, Switzerland, 15-20 September 2019, pp. EPSC2018-891, 2019.

[129] Dehghanian, Maryam ; Ferland, Gary ; Kriss, Gerard ; Peterson, Bradley ; Guzman, Francisco ; Chatzikos, Marios ; van Hoof, Peter A. M.
Uncorrelated behavior of narrow absorption lines in NGC 5548
American Astronomical Society Meeting Abstracts, 233, pp. 243.11, 2019.

[130] Deller J., Vilenius E., Roders O., Karatekin O., Pursiainen S., Wada K., Tortora P., Kohout T., and Bambach P., the the AI3 team
Asteroid In-situ Interior Investigation - 3way: Understanding the formation processes and evolution of small solar system bodies
EPSC-DPS2019, Geneva, Switzerland, 15-20 September 2019, extended abstract, EPSC-DPS2019-1536, 2 pages, 2019.

[131] Deproost M.H., Rivoldini A., Van Hoolst T.
Stratification in the core of Mercury
EPSC-DPS2019, Geneva, Switzerland, poster, 15-20 September 2019, extended abstract, EPSC-DPS2019-1646, 2 pages, 2019.

[132] El Fadhel A., Karatekin Ö., Witasse O., Asmar S., Bergeot N., Van Hove B.
Radio Occultations Using CubeSats to probe the planetary atmospheres
EPSC-DPS2019, Geneva, Switzerland, 15-20 September 2019, extended abstract, EPSC-DPS2019-1832, 2 pages, 2019.

[133] including Elst, E.
Positions of minor planets observed with the Uccle Schmidt telescope
Minor Planet Circulars Supplement, pp. 1091293-1100840, 2019.

[134] Fidalgo, Javier ; Píriz, Ricardo ; Cezón, Anna ; Fernández, A ; Callewaert, K ; Bolchi, M ; Defraigne, Pascale ; Danesi, A ; Jeannot, M ; Boyero, Juan-Pablo
Definition of a European GNSS Timing Service
Proceedings of the ION GNSS, 2019, pp. 827-839, 2019. http://dx.doi.org/10.33012/2019.16940

[135] Folkner, W. ; Le Maistre, S. ; Dehant, V. ; Buccino, D. ; Marty, J.-C. ; Rivoldini, A. ; Yseboodt, M. ; Kahan, D.
Mars precession rate and moment of inertia from InSight/RISE measurements
Proc. EPSC 2019, Geneva, Switzerland, 15-20 September 2019, pp. EPSC2019-1755, 2019.

[136] Galy, C. ; Thizy, C. ; Stockman, Y. ; Galano, D. ; Rougeot, R. ; Melich, R. ; Shestov, S. ; Landini, F. ; Zukhov, A. ; Kirschner, V. ; Horodyska, P. ; Fineschi, S.
Straylight analysis on ASPIICS, PROBA-3 coronagraph
;Proc. SPIE 11180, International Conference on Space Optics — ICSO 2018, 11180 issue 111802H, 2019. http://dx.doi.org/10.1117/12.2536008

[137] Garcia-Moreno, David ; Gupta, Sanjeev ; Collier, Jenny S. ; Oggioni, Francesca ; Vanneste, Kris ; Trentesaux, Alain ; Verbeeck, Koen ; Versteeg, Wim ; Jomard, Hervé ; Camelbeeck, Thierry ; De Batist, Marc
Middle-Late Pleistocene landscape evolution of the Dover Strait inferred from buried and submerged erosional landforms
Quaternary Science Reviews, 203, pp. 209-232, 2019.
http://dx.doi.org/10.1016/j.quascirev.2018.11.011

[138] Ghazoui, Z. ; Bertrand, S. ; Vanneste, Kris ; Yokoyama, Y. ; Nomade, J. ; Gajurel, A.P. ; van der Beek, P.A.
Potentially large post-1505 AD earthquakes in western Nepal revealed by a lake sediment record
Nature Communications, 10, pp. 2258, 2019. http://dx.doi.org/10.1038/s41467-019-10093-4

[139] Gloesener, E. ; Karatekin, Ö. ; Dehant, V.
Stability of clathrate hydrates at low latitude on Mars
Proc. Ninth International Conference on Mars, California Institute of Technology (Caltech), Pasadena, California, 22-25 July 2019.

[140] Gloesener, E. ; Karatekin, Ö. ; Dehant, V.

Advective and diffusive transport of methane from shallow subsurface sources on Mars
Proc. EPSC 2019, Geneva, Switzerland, 15-20 September 2019, pp. EPSC2019-1518, 2019.

[141] Guzman Fulgencio, Francisco ; Chatzikos, Marios ; Balser, Dana ; van Hoof, Peter A. M. ; Dehghanian, Maryam ; Ulrich, Otho ; Ferland, Gary
The impact of inaccurate collisional excitation rates on radio recombination line observations
American Astronomical Society Meeting Abstracts, 233, pp. 412.08, 2019.

[142] Karatekin Ö.,
Equality of opportunities in geosciences: The EGU Awards Committee experience
EPSC-DPS2019, Geneva, Switzerland, 15-20 September 2019, extended abstract, EPSC-DPS2019-1866, 2 pages, 2019.

[143] Karatekin O., Goldberg H., andPrioroc C.
Juventas Cubesat for the HERA mission
EPSC-DPS2019, Geneva, Switzerland, 15-20 September 2019, extended abstract, EPSC-DPS2019-1830, 2 pages, 2019.

[144] Karatekin O., El Fadhel A., Krishnan A., Van Hove B., Witasse O., and Bergeot N.
Analysis of radio-occultation data from Mars Express
EPSC-DPS2019, Geneva, Switzerland, 15-20 September 2019, extended abstract, EPSC-DPS2019-1804, 2019.

[145] Karatekin Ö., Van Hove B., Ferri F., Aboudan A., Colombatti G.
Reconstruction of the Mars atmosphere using the flight data from ExoMars Schiaparelli's instrumented heat shield and radio communications
European Planetary Science Congress, Berlin, 16-21 September 2018, extended abstract, EPSC Abstracts Vol. 12, EPSC2018-1211, 2 pages, 2019.

[146] Lampens, P ; Van Cauteren, P
AGN measurements in 2019
AAVSO AGN Circular issue Feb 6, 2019 to March 8, 2019, pp. 1-2, 2019.

[147] Le Maistre, S. ; Peter, M.J. ; Dehant, V. ; Marty, J.C.
LaRa sensitivity to Mars nutations
Proc. EPSC 2019, Geneva, Switzerland, 15-20 September 2019, pp. EPSC2019-1681, 2019.

[148] Malkin, Z. ; Gross, R. ; Brzezinski, A. ; Capitaine, N. ; Dehant, Veronique ; Huang, C. ; McCarthy, D. ; Schuh, H. ; Vondrak, J. ; Yatskiv, Y.
On the eve of 100-year anniversary of the IAU Commission 19 `Rotation of the Earth´
Proceedings IAU Symposium No. S349 'Under One Sky', 13, pp. 325-331, 2019.
http://dx.doi.org/10.1017/S1743921319000462

[149] Martin, Aurélie ; Fagel, Nathalie ; Lecocq, Thomas ; Camelbeeck, Thierry
Etude des stalagmites cierges dans les grottes belges pour valider l'aléa sismique, présentation du projet
Journée de spéleologie scientifique, 23es Journées de Spéléologie Scientifique - JSS, pp. 12, 2019.
http://hdl.handle.net/2268/243585

[150] Martínez Picar, Antonio ; Marqué, Christophe
Using SPADE for radio meteor observations
Proceedings of the International Meteor Conference, Pezinok-Modra, August 30 — 2 September 2018, pp. 67-69, 2019.

[151] Mathieu, Sophie ; von Sachs, Rainer ; Delouille, Veronique ; Lefèvre, Laure ; Ritter, Christian
Modélisation et estimation du nombre de taches solaires
GRETSI 2019 XXVII Colloque francophone de traitement du signal et des images, 2019.

[152] Middleton, Kevin F. ; Anwand, Heiko ; Bothmer, Volker ; Davies, Jackie A. ; Earle, Andrew ; Ergenzinger, Klaus ; Eyles, Chris J. ; Hardie, Robert ; Hellin, Marie-Laure ; Hinrichs, Johannes ; Huke, Philipp ; Jiggens, Piers ; Kirschner, Volker ; Mazy, Emmanuel ; McCarron, Thomas ; Nicula, Bogdan ; Stopfkuchen, Lars ; Tappin, S. James ; Tosh, Ian A. J. ; Waltham, Nick R ; West, Matthew J.
SCOPE: a coronagraph for operational space weather prediction: phase A/B1 design and breadboarding
Proceedings of the SPIE, 2019.

[153] including Pauwels, T.,
Positions of minor planets observed with the Uccle Schmidt telescope
Minor Planet Circulars Supplement, pp. 1100841-1105550, 2019.

[154] Pevtsov, Alexei ; Griffin, Elizabeth ; Grindlay, Jonathan ; Kafka, Stella ; Bartlett, Jennifer ; Usoskin, Ilya ; Mursula, Kalevi ; Gibson, Sarah ; Pillet, Valentín ; Burkepile, Joan ; Webb, David ; Clette, Frédéric ; Hesser, James ; Stetson, Peter ; Muñoz-Jaramillo, Andres ; Hill, Frank ; Bogart, Rick ; Osborn, Wayne ; Longcope, Dana
Historical astronomical data: urgent need for preservation, digitization enabling scientific exploration
Bulletin of the American Astronomical Society, 51 issue 3, pp. 190, 2019.

[155] Pinat, Elisa ; Bergeot, Nicolas ; Defraigne, Pascale ; Chevalier, Jean-Marie
Seasonal variations of snow height in east antarctica using gnss interferometric reflectometry
Proceedings of the 7th International Colloquium on Scientific and Fundamental Aspects of GNSS, 2019.

[156] Piriz, Ricardo ; Garbin, Esteban ; Diaz, J ; Defraigne, Pascale
Traceable Time for Datacenters Using GNSS and White Rabbit
Inside GNSS, February 7, 2019. https://insidegnss.com/scalable-traceable-time-for-datacenters-using-gnss-and-white-rabbit/

[157] Píriz, Ricardo ; Buendía, F ; Martín, JR ; Fidalgo, Javier ; Defraigne, Pascale ; Danesi, Anna ; Jeannot, M ; Boyero, Juan-Pablo
Safety Analysis for a New GNSS Timing Service via Galileo
Proceedings of the ION GNSS, 2019, pp. 3359-3376, 2019. http://dx.doi.org/10.33012/2019.17105

[158] Rendtel, J. ; Veljković, K. ; Weiland, T. ; Verbeeck, C. ; Knöfel, A.
Tricks of the trade: global analysis of visual meteor observations using VMDB and MetFns
Proceedings of the International Meteor Conference 2018, Pezinok, Slovakia, August 30 - September 2, 2019.

[159] Ritter B., Karatekin O., van Ruymbeke M., Noeker M., Ümit E., Laguerre R., Berkenbosch S., Bonnewijn S., van Ransbeeck E., Neefs E., Wielant F., Tasev E., and Goldberg H.
GRASS: a Gravimeter for the Investigation of Small Solar System Bodies
EPSC-DPS2019, Geneva, Switzerland, 15-20 September 2019, extended abstract, EPSC-DPS2019-1663, 2 pages, 2019.

[160] Rivoldini, A. ; Beuthe, M. ; Van Hoolst, T. ; Wieczorek, M. ; Baland, R.-M. ; Dehant, V. ; Folkner, B. ; Le Maistre, S. ; Péters, M.-J. ; Yseboodt, M.
Non-hydrostatic effects on Mars' nutation
Proc. EPSC 2019, Geneva, Switzerland, 15-20 September 2019, pp. EPSC2019-663, 2019.

[161] Ruiz Lozano, L. ; Karatekin, Ö. ; Dehant, V. ; Vandaele, A.C. ; Caldiero, A. ; Temel, O. ; the NOMAD, team
Use of NOMAD Observations (Trace Gas Orbiter) for Mars surface ice detection
Proc. EPSC 2019, Geneva, Switzerland, 15-20 September 2019, pp. EPSC2019-1781, 2019.

[162] Shimizu, T. ; Imada, S. ; Kawate, T. ; Ichimoto, K. ; Suematsu, Y. ; Hara, H. ; Katsukawa, Y. ; Kubo, M. ; Toriumi, S. ; Watanabe, T. ; Yokoyama, T. ; Korendyke, C. M. ; Warren, H. P. ; Tarbell, T. ; De Pontieu, B. ; Teriaca, L. ; Schühle, U. H. ; Solanki, S. ; Harra, L. K. ; Matthews, S. ; Fludra, A. ; Auchère, F. ; Andretta, V. ; Naletto, G. ; Zhukov, A.
The Solar-C_EUVST mission
Proceedings of SPIE, 11118, pp. 1111807, 2019. http://dx.doi.org/10.1117/12.2528240

[163] Temel O., Karatekin O.
Assessment of meteorological conditions for the formation of liquid brine on Mars using a mesoscale model
EPSC-DPS2019, Geneva, Switzerland, 15-20 September 2019, extended abstract, EPSC-DPS2019-1641, 2019.

[164] Tortora P., Zannoni M., Gai I., Karatekin O., Goldberg H., Prioroc C., Garcia Gutierrez B., Martino P., Carnelli I.
Didymos Gravity Science through Juventas Satellite-to-Satellite Doppler Tracking
EPSC-DPS2019, Geneva, Switzerland, 15-20 September 2019, extended abstract, EPSC-DPS2019-1751, 2 pages, 2019.

[165] Trinh A., Beuthe M., Matsuyama I.
A comparison between physical and classical prescriptions of isostasy
EPSC-DPS2019, Geneva, Switzerland, 15-20 September 2019, extended abstract, EPSC-DPS2019-1784, 2 pages, 2019.

[166] Van Hoolst T., Baland R.-M., Trinh A., Nimmo F.
The rotation of Io
EPSC-DPS2019, Geneva, Switzerland. poster, 15-20 September 2019, extended abstract, EPSC-DPS2019-1334, 2 pages, 2019.

[167] Van Noten, Koen ; Burlet, Christian ; Lecocq, Thomas ; Delaby, Serge ; Soulier, Denise ; Verheyden, Sophie
Polarisation de la Fréquence de Résonance dans la Salle de la Structure à l'aide de Capteurs Sismiques à 3 Composantes
Grotte de Bruniquel (Bruniquel, Tarn-et-Garonne). Rapport Intermédiaire 2019 d'opération archéologique programmée Triennale 2018-20. pp. 67-71 (2019). SRA Occitanie, 2019.

[168] Verbeeck, C. ; Lamy, H. ; Calders, S. ; Tétard, C. ; Martínez Picar, A.
BRAMS radio observations analyzed: activity of some major meteor showers
Proceedings of the International Meteor Conference 2018, Pezinok, Slovakia, August 30 - September 2, 2019.

[169] Yseboodt, M. ; Rivoldini, A. ; Le Maistre, S. ; Dehant, V.
Core radius uncertainty of Mars inferred from nutation estimation for non-hydrostatic interior models
Proc. EPSC 2019, Geneva, Switzerland, 15-20 September 2019, pp. EPSC2019-1223, 2019.

Other publications

[170] Andries, Jesse ; De Patoul, Judith ; Magdalenic, Jasmina ; Marqué, Christophe ; O'Hara, Jennifer ; Berghmans, David ; Rodriguez, Luciano ; Verbeeck, Francis
PECASUS 24h/7d Advisory Production Service for ICAO
Periodical publication. Periodicity: 24h/7d, from 2019. http://pecasus.eu/

[171] Dominique, Marie
Solar flare studies with the LYRA instrument onboard PROBA2
PHD thesis supervised by Lapenta, Giovanni; Zhukov, Andrei (KUL)
http://proba2.oma.be/Presentations/20190226_Dominique_defense/thesis_Dominique_20190215.pdf

[172] Janssens, Jan ; Berghmans, David ; Vanlommel, Petra ; Andries, Jesse
Space Weather: The Impact on Security & Defense
in Handbook of Space Security: Policies, Applications and Programs Space weather (20 pages - Sc. Ed. Schrogl KU. - pp. 1–20). https://doi.org/10.1007/978-3-030-22786-9_94-1

[173] Lobel A., Royer P., Martayan C., Laverick M., van Hoof P.A.M., Merle T., Van der Swaelmen M., David M., Hensberge H., Thienpont E.
BRAIN-be - Belgian Research Action through Interdisciplinary Networks: The Belgian Repository of fundamental Atomic data and Stellar Spectra. Final Report 2014-2019
Brussels: Belgian Science Policy Office - 57 p, 2019. https://www.belspo.be/belspo/brain-be/themes_2_GeoUniClim_nl.stm#BRASS

[174] Pauwels, T., Bruyninx, C. and Roosbeek, F.
Annuaire de l'Observatoire royal de Belgique – Jaarboek van de Koninklijke Sterrenwacht van België 2020
Fedopress, ISSN-0373-4900, 2019. https://www.astro.oma.be/wp-content/uploads/2019/11/yearbook_2020.pdf

[175] Van Noten, Koen ; Sintubin, Manuel
Chapter 9 - Unfolding Veined Fold Limbs to Deduce a Basin's Prefolding Stress State
Developments in Structural Geology and Tectonics, Volume 5, 2019.
http://dx.doi.org/10.1016/B978-0-12-814048-2.00009-0

[176] Verbeeck, Koen
Deterministic seismic hazard assessment in the Belgian Campine basin at the Mol/Dessel site: From seismic source to site effect
PhD thesis supervised by Vandenberghe, Noël; Vanneste, Kris (KULeuven), 2019.

[177] Yseboodt, M. ; Van Hoolst, T. ; Le Maistre, S. ; Dehant, V.
La mission InSight : un atterrisseur pour explorer l'intérieur profond de Mars
Science Connection - Fr, 60, pp. 38-41, 2019.

[178] Yseboodt, M. ; Van Hoolst, T. ; Le Maistre, S. ; Dehant, V.
De InSight-missie: een lander die het diepe binnenste van Mars gaat verkennen
Science Connection - Nl, 60, pp. 38-41, 2019.

Annex 2: Workforce

On 31 December 2019, 171 employees were working at the Royal Observatory of Belgium (including the Planetarium). The staff increased with five employees (166 employees on 31 December 2018) and is close to the 2017 workforce (172 employees on 31 December 2017).

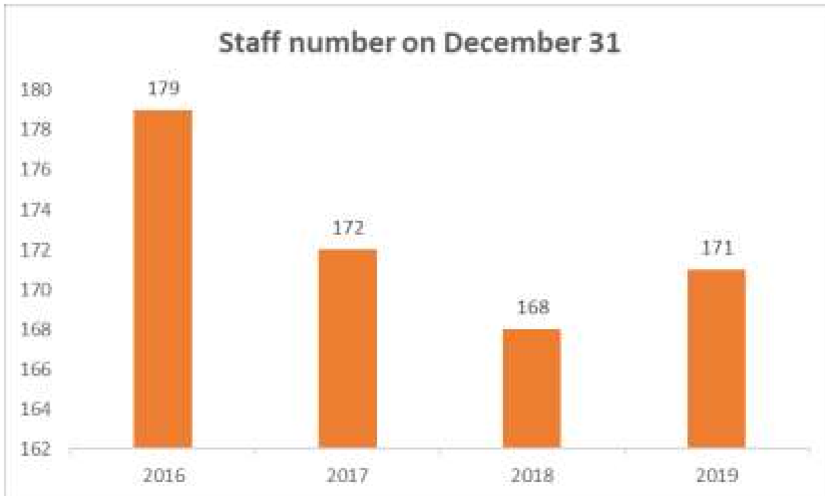

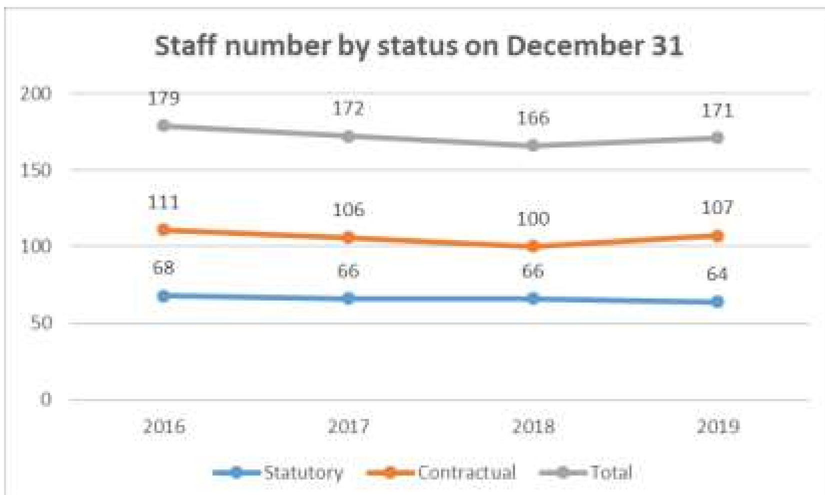

As expected from a research institute, scientists constitute the main part of the personnel (93 people, which constitutes 54% of the staff).

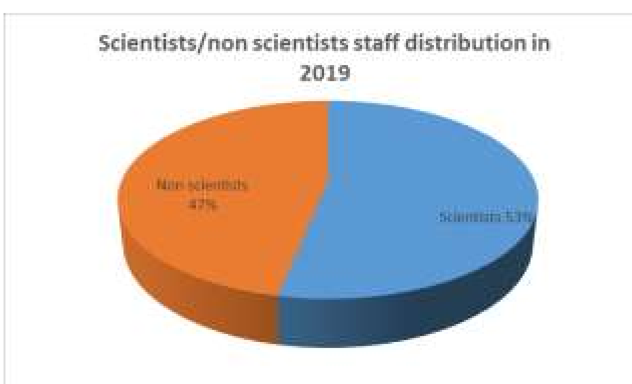

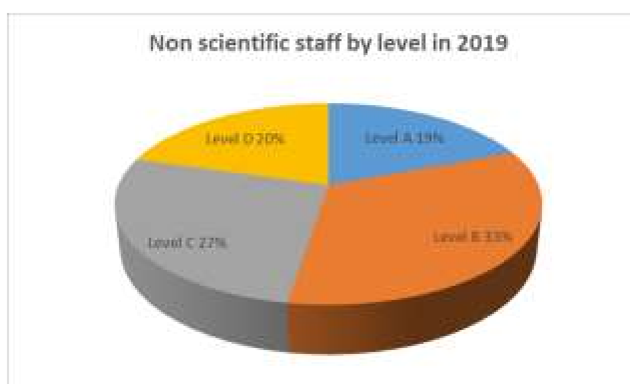

The majority of the personnel (63%) are contractually employed (i.e. non-statutory civil servants). This is particularly true at the scientific level, where contractuals constitute 72% of the scientific staff. This is, a consequence of the fact that scientific research is more and more funded by external projects.

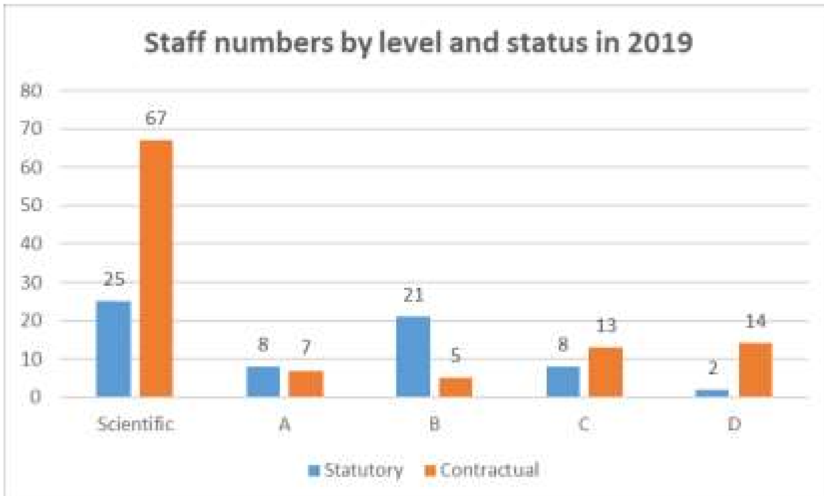

At the gender level, 38% of the employees are women (65 women and 106 men). This proportion has increased compared to the last two years (33% at the end of 2018 and 34% at the end of 2017). This is due to the fact that more contractual women were employed (46 contractual women on 31 December 2019 compared to 36 contractual women on 31 December 2018), while the number of employed contractual men diminished slightly (61 contractual men on 31 December 2019 compared to 65 contractual men on 31 December 2018). This is particularly the case at the scientific level where there are 7 more contractual female scientists hired (25 contractual female scientists in total on 31 December 2019) as compared to 2018.

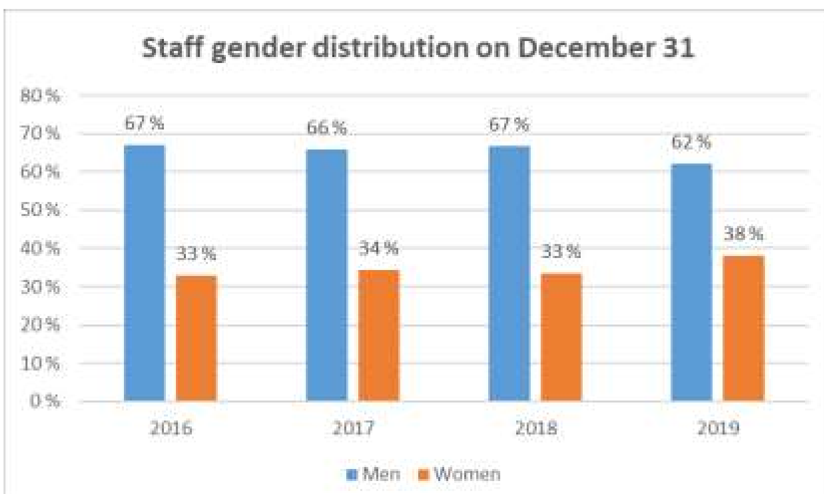

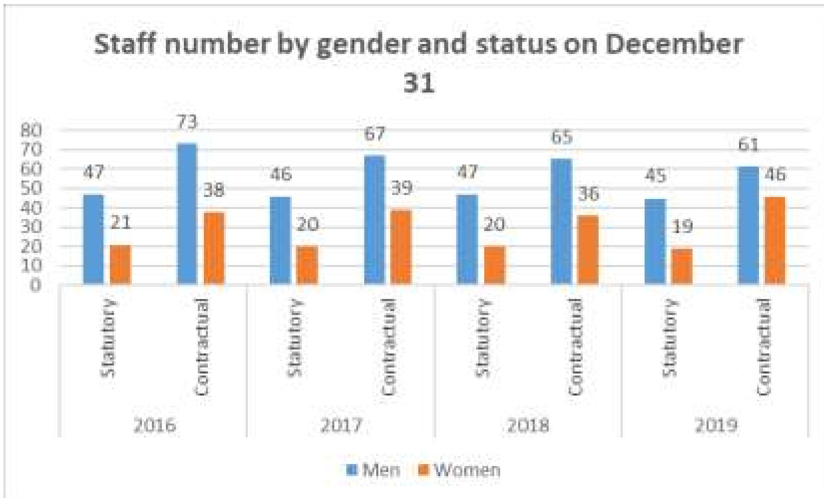
Staff number by gender and status on December 31
80
70
60
50
40
30
20
10
0
47
21
73
38
46
20
67
39
47
20
65
36
45
19
61
46
Statutory
Contractual
Statutory
Contractual
Statutory
Contractual
Statutory
Contractual
2016
2017
2018
2019
Men
Women

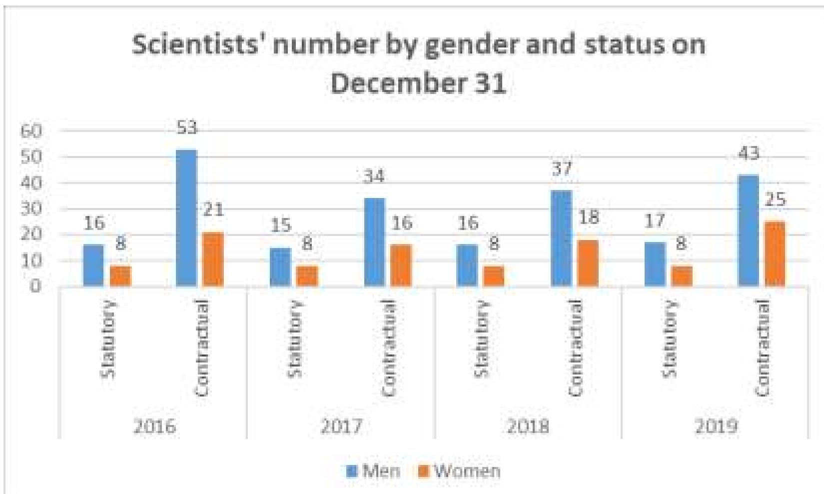
Scientists' number by gender and status on December 31
60
50
40
30
20
10
0
16
8
53
21
15
8
34
16
16
8
37
18
17
8
43
25
Statutory
Contractual
Statutory
Contractual
Statutory
Contractual
Statutory
Contractual
2016
2017
2018
2019
Men
Women

De activiteiten beschreven in dit verslag werden ondersteund door

Les activités décrites dans ce rapport ont été soutenues par

The activities described in this report were supported by

De POD Wetenschapsbeleid

Le SPP Politique Scientifique

The Belgian Science Policy Office

De Nationale Loterij

La Loterie Nationale

The National Lottery

Het Europees Ruimtevaartagentschap

L'Agence Spatiale Européenne

The European Space Agency

De Europese Gemeenschap

La Communauté Européenne

The European Community

Het Fonds voor Wetenschappelijk Onderzoek – Vlaanderen

Le Fonds de la Recherche Scientifique